Chem.

BULLETIN
OF THE
CHEMICAL SOCIETY OF JAPAN

Vol. 32 No. 2 February 1959

OHIO STATE UNIVERSITY
MAR 30 1959
LIBRARY

CONTENTS

General and Physical

M. MURAMATSU: Studies on the Interaction of Surface Films with Solute in Solution. IV. Effect of Congo Red Dissolved in Aqueous Substrate upon the Monolayers of Octadecylamine, Cetyl Alcohol, Ethyl *n*-Hexadecyl Ether, Ethyl Stearate and Cholesterol. 114

Y. TANIZAKI, T. KOBAYASHI and N. ANDO: Absorption Spectra of Dyes. II. On Non-additivity of Absorption Spectra of Binary Mixtures of a Direct Dye and Some Acid Dyes in Aqueous Solution 119

H. OBATA, K. KOGASAKA and M. KOIZUMI: Photochemical Reactions between Methylene Blue and Tri-, Di- and Monomethylamine. III. The Behavior of Methylene Blue in the Presence of Oxygen 125

S. TAKAGI, R. SHINTANI, H. CHIHARA and S. SEKI: Vapor Pressures of Molecular Crystals. XIV. Sulfamide and Diacetylhydrazine 137

H. KURODA and H. AKAMATU: Studies on the Graphitization. II. Sub-structure and Crystallite Growth of Carbon Black 142

K. TAKAHASHI, Y. MATSUKI, T. MASHIKO and G. HAZATO: A Note on the Proton Magnetic Resonance Spectra of Some Thiophene Derivatives 156

Y. SASADA: Crystal and Molecular Structure of 1-Oxa-azulan-2-one. I. X-ray Determination of Crystal Structure 165

Y. SASADA: Crystal and Molecular Structure of 1-Oxa-azulan-2-one. II. A Refinement of the Structure by Low Temperature Technique 171

T. ISEMURA and S. IKEDA: The Roles of Prolyl Residue in Polypeptide Monolayers. I. On the Chain Configurations Deduced from Surface Pressure and Potential Measurements. 178

M. IWASAKI: Electron Diffraction Investigation on the Molecular Structure of 1, 1, 2-Trifluoro-1, 2, 2-trichloroethane 194

Analytical and Inorganic

T. SATA: Phase Relationship in the System $3CaO \cdot P_2O_5$-$CaO \cdot MgO \cdot 2SiO_2$–$SiO_2$ 105

S. MUSHA, M. MUNEMORI and K. OGAWA: Photometric Determination of Indicator End Points in Complexometric Titrations. 132

N. MAKI, Y. SHIMURA and R. TSUCHIDA: Polarographic Studies of Metallic Complexes. IV. Bisethylenediamine Series of Cobalt(III) Complexes 150

(Continued on inside cover)

Published by the Chemical Society of Japan

THE CHEMICAL SOCIETY OF JAPAN

(NIPPON KAGAKUKAI)

Founded in 1948

Successor to the former Chemical Society of Japan founded in 1878 and to the Society of Chemical Industry, Japan founded in 1898.

OFFICERS

Munio KOTAKE, *President*, Osaka University, Osaka
Shin-ichiro FUJISE, *Vice-President*, Tohoku University, Sendai
Taro HAYASHI, *Vice-President*, Ochanomizu Women's University, Tokyo
Tokuichi TSUMAKI, *Vice-President*, Kyushu University, Fukuoka
Kenichi YAMAMOTO, *Vice-President*, Waseda University, Tokyo

BULLETIN OF THE CHEMICAL SOCIETY OF JAPAN

Editor: Yoshiyuki URUSHIBARA, The University of Tokyo, Tokyo
Assistant Editor: Kazuo SAITO, The University of Tokyo, Tokyo
Editorial Board:

Rempei GOTOH	Kei MATSUZAKI	Tadao SHIBA
Hiroshi HAMAGUCHI	Saburo NAGAKURA	Osamu SIMAMURA
Genjiro HAZATO	Hiroshi NOZAKI	Mutsuaki SHINAGAWA
Isao ICHISHIMA	Seizo OKAMURA	Tatsuo TAKESHIMA
Masaji KUBO	Tunetaka SASAKI	Sumio UMEZAWA
Hisao KUROYA	Tetsuro SEIYAMA	

(*Continued from outside cover*)

Organic and Biological

Y. OGATA and I. TABUSHI: Kinetics of the Acid-Catalyzed Peroxide Oxidation of 4-Hydroxybenzaldehyde in Acetic Acid 108

F. SAWADA: The Fundamental Conditions for Countercurrent Distribution Studies of Clupeine 161

T. ARAI: The Electrolytic Reduction of Ketones at a Mercury Cathode—Preparation of Organomercuric Compounds 184

A. TAKAMIZAWA, K. TOKUYAMA and K. TORI: Syntheses of Pyrimidine Derivatives. XVII. On the Reaction Mechanism of Some Pyrimidine Syntheses. 188

Short Communications

S. FUJIWARA, M. KATAYAMA, S. HAYASHI, H. SHIMIZU and S. NISHIMURA: Nuclear Magnetic Resonance Spectra of Dibromothiophene. 201

Y. TAKAKI, Y. SASADA and T. WATANABÉ: Crystal Structure of Pyrazinamide 202

H. KOBAYASHI, S. NAGAHAMA and S AKIYOSHI: Dehydrogenation of the Degradation Products of Thujopsene 202

Y. IKUTANI, T. OKUDA, M. SATO and S. AKABORI: The Reaction of Glycine Cobalt Complex with Acetaldehyde 203

Phase Relationship in the System $3CaO \cdot P_2O_5$—$CaO \cdot MgO \cdot 2SiO_2$—$SiO_2$

By Toshiyuki Sata

(Received August 4, 1958)

According to the present writer's published studies[1,2], slowly cooled specimens of fused phosphatic fertilizer and of bone-ash magnesia porcelain are composed of β-tricalcium phosphate, apatite, diopsidic pyroxene, and silica minerals. The equilibrium study of the system composed of these minerals, therefore, must be of great importance for the industrial manufacture of these products. Henceforth the author constructed the phase diagrams of the ternary system $3CaO \cdot P_2O_5$—$CaO \cdot MgO \cdot 2SiO_2$—$SiO_2$, on which no paper has ever been presented. This investigation is continued from his preceding report on the system $3CaO \cdot P_2O_5$—$MgO \cdot SiO_2$—SiO_2[3].

Experimental

Of the three-component system concerned, data of the two partial systems, $3CaO \cdot P_2O_5$—SiO_2 and $CaO \cdot MgO \cdot 2SiO_2$—$SiO_2$, were given by other authors, the former by Pierre[4] and Wojciechowska[5], and the latter by Bowen[6]. Another partial system $3CaO \cdot P_2O_5$—$CaO \cdot MgO \cdot 2SiO_2$ and the three-component system were investigated by usual quenching method in this study.

Powdered batches of selected compositions, prepared by quenching into glass after being kept at above their melting points, were again held at constant temperatures in a silicon carbide resistor furnace and then quenched in water. Thenceforth the equilibrium phases found therein were determined by the optical and the X-ray examination. For measuring the temperature a thermocouple of platinum-platinum rhodium (10%) was used. Details of experimental

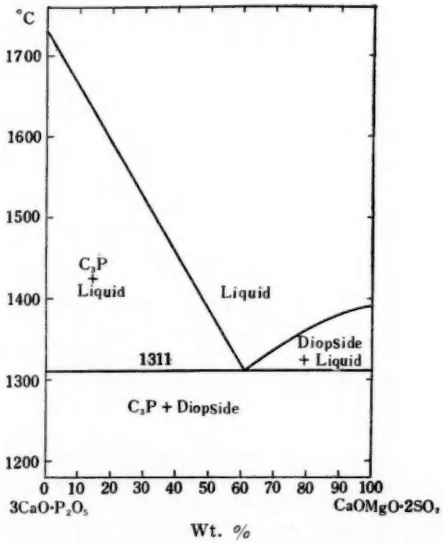

Fig. 1. The system $3CaO \cdot P_2O_5$—$CaO \cdot MgO \cdot 2SiO_2$

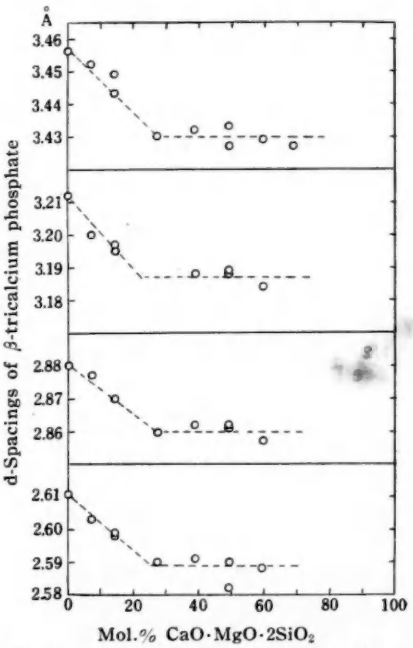

Fig. 2. The change in spacings of β-tricalicium phosphate at 1250~1300°C (pure tricalicium phosphate at 1100°C)

1) T. Sata and R. Kiyoura, *J. Chem. Soc. Japan, Ind. Chem. Sec.* (*Kogyo Kagaku Zasshi*), **62**, 63 (1959).
2) T. Sata and R. Kiyoura, *J. Cer. Assoc., Japan* (*Yogyo Kyokai Shi*), **66**, 294 (1958).
3) T. Sata, This Bulletin, **31**, No. 4 408 (1958).
4) D. D. S. St Pierre, *J. Am. Cer. Soc.*, **37**, (6) 243 (1954), **39**, (4) 147 (1956).
5) J. Wojciechowska et al., *Roczniki Chem.*, **30**, 743 (1956).
6) N. L. Bowen, *Am. J. Sci.*, (4) **38**, 207 (1914), *Z. anorg. allgem. Chem.*, **90**, 1 (1914).

CHEMISTRY HALL LIBRARY

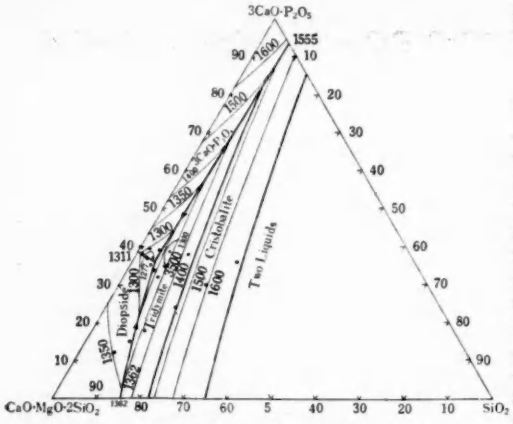

Fig. 3. The system $3CaO \cdot P_2O_5$—$CaO \cdot MgO \cdot 2SiO_2$—$2SiO_2$

procedures are similar to those already described in the author's preceding report[3].

Results

The system $3CaO \cdot P_2O_5$—$CaO \cdot MgO \cdot 2SiO_2$.—Data on the quenching runs for this two-component system are listed in Table I, from which the equilibrium diagram was constructed as shown in Fig. 1. It is found that this system seems to be perfectly described as a binary one, whose eutectic is located at 39% of $3CaO \cdot P_2O_5$ and 61% of $CaO \cdot MgO \cdot 2SiO_2$, melting point at 1311±4°C. In the region rich in $3CaO \cdot P_2O_5$ (over 80%), the following facts were observed. (1) The crystallization of diopside did not take place when samples were kept for about 1 hr. even under the eutectic temperature. (2) The transition temperature of tricalcium phosphate from

TABLE I

QUENCHING DATA IN THE SYSTEM $3CaO \cdot P_2O_5$—$CaO \cdot MgO \cdot 2SiO_2$

No.	Composition wt.% C_3P	Composition wt.% CMS_2*	Holding temp. °C	Holding time min.	Phases present
248	95	5	1500	45	α-C_3P, glass
			1400	120	α-C_3P, β-C_3P, glass
			1292	60	β-C_3P
113	90	10	1500	30	α-C_3P, glass
			1450	60	α-C_3P, small β-C_3P, glass
			1400	60	β-C_3P, glass
			1292	300	β-C_3P, diopside
100	80	20	1600	20	small α-C_3P, glass
			1520	30	α-C_3P, β-C_3P, glass
			1450	60	β-C_3P, glass
			1307	30	β-C_3P
			1272	70	β-C_3P, small diopside
112	70	30	1314	30	β-C_3P, glass
			1302	30	β-C_3P, trace diopside
			1292	50	β-C_3P, diopside
99	60	40	1455	30	glass
			1422	30	very small β-C_3P, glass
			1314	40	small β-C_3P, glass
			1307	40	β-C_3P, diopside, glass
111	50	50	1382	30	very small β-C_3P, glass
			1357	30	small β-C_3P, glass
98	40	60	1324	40	glass
			1314	60	small β-C_3P, glass
			1307	40	β-C_3P, diopside, glass
			1282	40	all crystal
119	35	65	1314	40	small diopside, glass
118	30	70	1340	20	glass
			1324	30	trace diopside, glass
			1314	30	diopside
97	20	80	1364	30	glass
			1358	40	diopside, glass

* Abbreviations: $C_3P = 3CaO \cdot P_2O_5$, $CMS_2 = CaO \cdot MgO \cdot 2SiO_2$

TABLE II

QUENCHING DATA IN THE SYSTEM $3CaO \cdot P_2O_5$—$CaO \cdot MgO \cdot 2SiO_2$—$SiO_2$

No.	Composition wt.%		C_3P	CMS_2 wt.%	S*	Holding Temp. °C	Time min.	Phases present
	CMS_2	No. 23						
195	80	20	12	80	8	1340	30	glass
						1334	30	diopside, glass
						1304	30	almost crystal
200	75	25	15	75	10	1330	60	glass
						1323	40	very small diopside, glass
196	70	30	18	70	12	1354	30	cristbl.,* glass
						1314	60	cristbl., glass
						1304	30	cristbl., diopside, glass
						1237	120	β-C_3P, diopside, cristbl.
197	60	40	24	60	16	1354	30	cristbl., glass
						1294	60	cristbl., glass
						1284	60	cristbl., diopside, glass
						1279	60	cristbl., diopside, small glass
						1274	60	all crystal
198	50	50	30	50	20	1354	30	cristbl., glass
						1284	60	cristbl., glass
						1279	60	all crystal
199	40	60	36	40	24	1292	40	β-C_3P, cristbl., glass
						1277	60	all crystal
						1237	120	β-C_3P, diopside, cristbl., tridymite
	No. 197	No. 98						
203	50	50	32	60	8	1299	40	small cristbl., glass
						1282	50	cristbl., glass
						1273	50	all crystal
204	40	60	33.6	60	6.4	1290	50	diopside, cristbl., glass
						1282	50	almost crystal
205	30	70	35.2	60	4.8	1290	50	glass
						1281	60	diopside, glass
206	19.4	80.6	36.9	60	3.1	1290	50	glass
						1281	60	diopside, glass
	No. 199	No. 98						
202	50	50	38	50	12	1315	40	cristbl., glass
201	30	70	38.8	54	7.2	1315	40	very small cristal., glass
						1299	40	cristbl., glass
						1282	50	cristbl., β-C_3P, glass
						1277	50	all crystal
207	20	80	39.2	56	4.8	1290	50	very small C_3P, glass
						1282	50	diopside, almost crystal
208	10	90	39.6	58	2.4	1290	50	small β-C_3P, glass
						1282	50	diopside, almost crystal

* Abbreviations; S=silica, cristbl.=cristobalite

β to α increased with diopside content, 1350 ~1400°C with 5%, 1450~1450°C with 10%, and 1450~1520°C with 20% of diopside (the transition temperature of pure tricalcium phosphate is 1180°C). (3) The spacings for diffraction lines in β-tricalcium phosphate decreased with diopside contents as indicated in Fig. 2, showing apparent formation of solid solution with some diopside (25±2 mol.% or 19±2 wt.%). These facts occurring in the region rich in tricalcium phosphate will be discussed with more data in the near future.

The system $3CaO \cdot P_2O_5$—$CaO \cdot MgO \cdot 2SiO_2$—$SiO_2$.—This three-component system is a perfect ternary one, and its eutectic was decided from the quenching data of the 14 samples shown in Table II, whose compositions lie along the tie lines connecting No. 23 (C_3P60—SiO_240) with $CaO \cdot MgO \cdot 2SiO_2$ corner and No. 98 (C_3P40—$CaO \cdot MgO \cdot 2SiO_260$) with No. 197 or No. 199, as

plotted in Fig. 3. The ternary eutectic is located at 36±1% C_3P, 59±1% $CaO \cdot MgO \cdot 2SiO_2$, and 5±1% SiO_2, and at 1277±3°C, which is close to the $3CaO \cdot P_2O_5$—$CaO \cdot MgO \cdot 2SiO_2$ join. Accordingly the silica field covers over a very wide area. The isotherms on the liquidus surface were approximately represented in the ternary system.

Summary

The phase relationship in the system $3CaO \cdot P_2O_5$—$CaO \cdot MgO \cdot 2SiO_2$—$SiO_2$ was investigated by the usual quenching method. The two partial systems $3CaO \cdot P_2O_5$—SiO_2 and $CaO \cdot MgO \cdot 2SiO_2$—$SiO_2$ have already been reported by previous investigators. Another partial system $3CaO \cdot P_2O_5$—$CaO \cdot MgO \cdot 2SiO_2$ seems to be approximately binary, whose eutectic is located at 39% of $3CaO \cdot P_2O_5$ and 61% of $CaO \cdot MgO \cdot 2SiO_2$, and at 1311±4°C. In the region rich in $3CaO \cdot P_2O_5$, it was observed that the crystallization velocity of diopside is rather slow under the solidus temperature, that the transition temperature of tricalcium phosphate is considerably increased with diopside content, and that β-tricalicium phosphate apparently makes solid solution with diopside (19 wt.%).

The system $3CaO \cdot P_2O_5$—$CaO \cdot MgO \cdot 2SiO_2$—$SiO_2$ is of a perfect ternary one, whose eutectic is at 36% of $3CaO \cdot P_2O_5$, 59% of $CaO \cdot MgO \cdot 2SiO_2$ and 5% of SiO_2, and at 1277±3°C. Its isotherms of the liquidus surface were approximately represented.

The author acknowledges the constant help and encouragement given by Professor R. Kiyoura, Tokyo Institute of Technology, and also much helpful advice supplied by Professor H. Yamada and Assistant Professor S. Kawakubo, Tokyo Institute of Technology. This work was conducted as a part of a program to investigate the corrosion problems of various refractory bricks in the manufacture of fused phosphatic fertilizer.

Research Laboratory for Ceramics
Tokyo Institute of Technology
Meguro-ku, Tokyo

Kinetics of the Acid-Catalyzed Peroxide Oxidation of 4-Hydroxybenzaldehyde in Acetic Acid

By Yoshiro OGATA and Iwao TABUSHI

(Received July 5, 1958)

It is well known that aromatic ketones and aldehydes give on oxidation with peroxides (e. g., hydrogen peroxides or organic peracids) aryl esters or their hydrolysis products, i. e., phenols and carboxylic acids[1-3].

In general, the reaction is acid-catalyzed. It is of interest to note that *o*- or *p*-hydroxyl, amino or mercapto group facilitates the reaction to such an extent that it takes place at a high pH even in aqueous alkaline media[4], where a mechanism involving an initial attack of hydrogen peroxide to the active hydrogen of these groups was postulated[5]. In contrast, the reaction in acidic media occurs without these activating groups[6,7]. In this case, the mechanism has been suggested to be an addition of peroxide to the carbonyl group followed by a rearrangement[2,3].

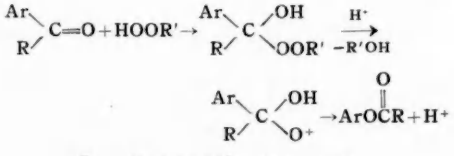

R: alkyl or H[8] Ar: aryl.

1) D. Swern, *Chem. Revs.*, **45**, 1 (1949).
2) J. E. Leffler, ibid., **45**, 385 (1949).
3) C. H. Hasall, *Organic Reactions*, **9**, 73 (1957).
4) a) H. D. Dakin, *Proc. Chem. Soc.*, **25**, 194 (1909).
b) H. D. Dakin, *Am. Chem. J.*, **42**, 477 (1909).
5) a) E. Bamberger, *Ber.*, **36**, 2042 (1903).
b) E. Bamberger and H. O. Eppinger, ibid., **73**, 644 (1940).
6) W. Dilthy, M. Inckel and H. Stephan, *J. prakt. Chem.*, **154**, 219 (1940).
7) W. Dilthy and F. Quint, ibid., **131**, 1 (1931).
8) A. Wacek and A. Bezard, *Ber.*, **74**, 845 (1941).

However, few detailed mechanistic studies from the kinetic standpoint have been reported on the hydrogen peroxide oxidation in acidic media. The present study was undertaken to elucidate the mechanism as well as the true oxidizing agent of the acid-catalyzed hydrogen peroxide oxidation of hydroxybenzaldehyde in aqueous acetic acid by estimating the effects of acidity on the rate.

Experimental

Materials.—*p*-Hydroxybenzaldehyde was purified by recrystallization from water, m. p. 116°.

Kinetic Procedures.—*Procedure A. Simultaneous Addition of the Reactants.*—Hydroxybenzaldehyde, acetic acid, sulfuric acid and water were mixed in a flask in the above order, thermostated at 15° or 20°; then hydrogen peroxide was added to the mixture. To avoid the temperature increase during the addition of hydrogen peroxide, a lower concentration of sulfuric acid and relatively high water content should be used. In the procedure, however, the apparent rate constant usually increases during the reaction except at high acidity.

Procedure B. Addition of Aldehyde to an Equilibrium Mixture of Peroxides.—Hydrogen peroxide was added to a cooled mixture of aqueous acetic acid and sulfuric acid in a brown flask, and the mixtue thermostated at 15±0.1 or 20±0.1° until the equilibrium state between hydrogen peroxide and peracetic acid was attained. Then hydroxybenzaldehyde was added to a known amount of the peroxide solution, the oxidation being started here. The reaction temperature was 15±0.1 or 20±0.1°.

In order to ascertain the establishment of the equilibrium and also to estimate hydrogen peroxide and peracetic acid contents in the preliminary equilibrium mixture, permanganate titration for hydrogen peroxide and iodometry for the peracetic acid were employed. Aliquots were taken out at appropriate intervals from the preliminary mixture before the addition of the aldehyde, run into a cooled mixture of ice and sulfuric acid and titrated rapidly at ca. −5° with potassium permanganate to determine the hydrogen peroxide content. An aqueous solution of potassium iodide was then added to the mixture, warmed and titrated with thiosulfate to estimate the peracid content. In general, the aliquot consumes a slight excess of permanganate because of the obscurity of the end point; it was corrected by a separate determination of total peroxides.

When the ratio a/b (where the equivalent amount of hydrogen peroxide present is a, that of peracetic acid b) becomes constant within experimental error, the equilibrium constant K_1 and the forward and the reverse rate constant of peracetic acid formation (k_1 and k_{-1}, respectively) may be calculated by means of equations:

$$K_1 = k_1/k_{-1}, \qquad k+k_{-1} = \frac{2.303}{t}\log\left(\frac{a_0-a_e}{a-a_e}\right)$$

where a_0 is the initial concentration and a_e is the equilibrium concentration of hydrogen peroxide.

In kinetic runs after the addition of hydroxybenzaldehyde, aliquots were withdrawn and their total peroxide content was determined iodometrically. The rate constants were then calculated by means of the usual second-order rate equation. The spontaneous decomposition of the peroxides in the absence of hydroxybenzaldehydes under these conditions is so small that it may be assumed that the amount of consumed peroxides minus the known amount of the spontaneous decomposition is the amount of peroxides reacted.

Reaction Products Criterion.—The reaction mixture gave, on long standing, a product containing hydroquinone or catechol. As mentioned previously, the formates of these phenols are probably produced at an initial stage, since the conversion percentage is not in accord with those of peroxide, when calculated spectrophotometrically on the assumption that hydroquinone is produced directly. These esters could not be isolated in appreciable quantities presumably because of the rapid hydrolysis during isolation procedures, as the hydrolysis was accelerated in the presence of considerable amounts of water and sulfuric acid.

Results and Discussion

The Equilibrium between Hydrogen Peroxide and Peracetic Acid.—When the rate measurements were carried out by adding hydrogen peroxide to an equilibrium mixture of aqueous acetic acid, sulfuric acid and hydroxybenzaldehyde (Procedure A), an induction period was observed at the initial stage and the apparent second-order rate constants increased rapidly at

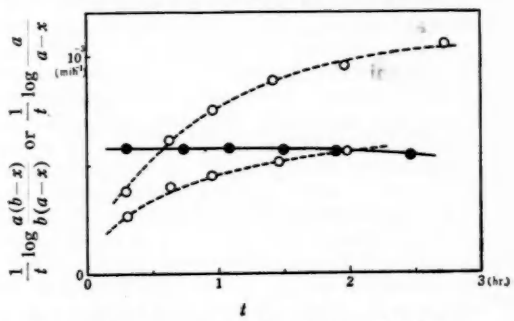

Fig. 1. Comparison of the results with Procedure A and B in the reaction of hydroxybenzaldehyde with peroxide.
dotted line: $\frac{1}{t}\log\left(\frac{a}{a-x}\right)$ vs. t at the early stages of the reaction with Procedure A. (Initial concentration of the aldehyde is considerably higher than that of hydrogen peroxide). solid line: $\frac{1}{t}\log\frac{a(b-x)}{b(a-x)}$ vs. t with Procedure B.

TABLE I

THE APPARENT SECOND-ORDER RATE CONSTANTS OF *p*-HYDROXYBENZALDEHYDE WITH PROCEDURE B

p-HOC_6H_4CHO 10^{-2}M	Total peroxide[a] 10^{-2}M	H_2SO_4 M	H_2O M	$k\times10^3$ [b] l. $mole^{-1}sec^{-1}$	Temp. °C
1.64	2.4	0.392	5.55	4.06±0.02	15
0.984	2.4	0.392	5.55	4.08±0.05	15
1.64	4.8	0.392	5.55	4.07±0.06	15
1.64	2.4	0.392	5.55	5.10±0.05	20
1.64	2.4	0.196	5.55	2.62±0.02	15
1.64	2.4	0.784	5.55	8.70±0.06	15
1.64	2.4	0.784	5.55	10.3 ±0.1	20
1.64	2.4	1.18	5.55	13.9 ±0.1	15
1.64	2.4	0.078	5.55	1.52±0.03	15
1.64	2.4	0.392	3.33	7.44±0.06	20
1.64	2.4	0.392	11.1	2.64±0.05	15
1.64	2.4	0.392	16.7	1.91±0.02	15
1.64	2.4	0.392	16.7	2.27±0.05	20

a) The average value of different initial concentrations of peroxide.
b) Figures following ± show probable errors.

TABLE II

THE APPARENT PSEUDO-FIRST-ORDER RATE CONSTANTS AND APPARENT EQUILIBRIUM CONSTANTS OF THE PERACETIC ACID FORMATION FROM HYDROGEN PEROXIDE AND ACETIC ACID

H_2O M	H_2SO_4 M	H_2O_2 10^{-2} M	K_1	$k_1\times10^4$ sec^{-1}	$k_{-1}\times10^4$ sec^{-1}
5.55	0.392	1.2	3.01	—	—
5.55	0.392	2.4	3.03	1.74	0.58
5.55	0.392	4.8	3.05	1.82	0.60
5.55	0.078	2.4	2.44	0.206	0.084
5.55	0.196	2.4	2.50	0.711	0.284
5.55	0.784	2.4	3.64	4.42	1.20
5.55	1.18	2.4	5.15	—	—
11.1	0.392	2.4	2.75	0.668	0.242
16.7	0.392	2.4	2.33	—	—

first, and then slowly. This trend was remarkable especially with low concentrations of sulfuric acid and with a relatively high initial concentration of hydroxybenzaldehyde compared with that of hydrogen peroxide. Typical examples are shown in Fig. 1.

On the other hand, when hydrogen peroxide is allowed to reach equilibrium with aqueous acetic and sulfric acid before hydroxybenzaldehyde is added to start the reaction (Procedure B), no such initial suppression of apparent rate constant is observed. The rate constant holds a satisfactory constancy during the reaction except near the end of the reaction where a slight decrease of the constant is appreciable. The constant does not, of course, vary with changing initial concentrations of the reactants. Table I shows the apparent second-order constants with Procedure B.

The facts cited above suggest that an active intermediate is formed by the acid-catalyzed interaction of hydrogen peroxide and acetic acid, the rate of its formation being comparable to that of the main reaction of hydroxybenzaldehyde with the intermediate. The facts that the initial suppression of the rate becomes remarkable by reducing the rate of formation of the intermediate and that the apparent rate constant estimated by Procedure A is much lower at an early stage than that by procedure B, agree well with the assumption of such an active intermediate. For example, a "rate constant" with Procedure A at 10% conversion is ca. 1/12.6 of that with Procedure B in the following condition. $[H_2O]=5.55$ M and $[H_2SO_4]=0.0736$ M at 20°.

It is most probable that the intermediate is peracetic acid, the equilibrium constant of its sulfuric acid-catalyzed formation having been estimated by D'Ans[9].

9) J. D'Ans and W. Frey, O; *Z. anog. Chem.* **84**, 145 *Chem. Abstr.*, **8**, 923 (1914).

$$H_2O_2+CH_3COOH \underset{k_{-1}}{\overset{k_1}{\rightleftarrows}} CH_3CO_3H+H_2O \quad (1)$$

$$CH_3CO_3H+\text{hydroxybenzaldehyde} \xrightarrow{k_2} \text{product} \quad (2)$$

In addition to peracetic acid, the formation of Caro's acid may be expected. It seems rational, however, that peracetic acid is the main oxidizing agent, since the acidities used are not very high and the rate of formation of Caro's acid is very low under these conditions, although it may become appreciable at higher acidities[10]. The possibility that the active attacking agent is OH^+(or $H_3O_2^+$) may be eliminated, since the protonation of hydrogen peroxide should be very rapid.

Approximate rate constants and equilibrium constants of the formation of peracetic acid determined under the same conditions as those of the kinetic experiments are shown in Table II. Both constants increase with increasing acidity in accord with the previous observation in such an equilibrium as hydrogen peroxide-performic acid or hydrogen peroxide-monoperoxysulfuric acid[10].

Since the magnitude of k_1 was moderate in these experiments, conditions where v_1 and v_2 (v's are rates of the subscripted steps) are comparable may easily be attained[11].

Our qualitative observation on the initial suppression of the rate agrees with the above discussion and provides another evidence for the justification of eqs. 1 and 2. Furthermore, the oxidation rate measurements in pure aqueous media of the same acidity show that the rate is too slow to measure, thus indicating that no intermediate is produced by the interaction of hydrogen peroxide and sulfuric acid alone.

Effects of Acidity and Water Content.— A study of the effects of sulfuric acid concentration and water content on the apparent second-order rate constant according to Procedure B (k) shows that the results can not be expressed in a simple form, unless corrections for peracetic acid concentration and acidity are made. (see Figs. 2 and 3).

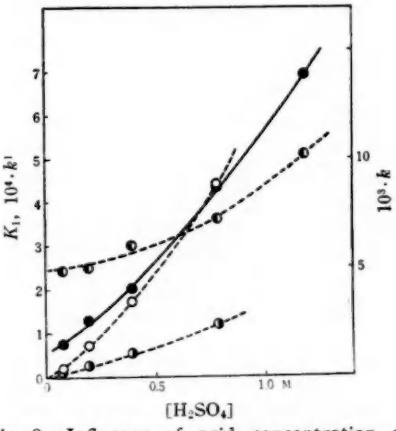

Fig. 2. Influence of acid concentration on the rate and the equilibrium constant for the reaction of peracetic acid formation at 15° and for the oxidation of hydroxybenzaldehyde. $[H_2O]=5.55$ M.
Dotted lines correspond to the peracetic acid formation:
◐, equilibrium constant K_1
○, forward rate constant $k_1 \cdot 10^4$
◑, reverse rate constant $k_{-1} \cdot 10^4$
Solid line correspond to the rate constant of oxidation: $k \cdot 10^3$.

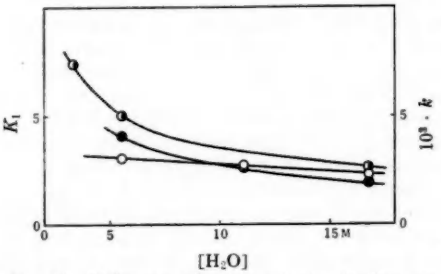

Fig. 3. Influence of water concentration on the rate and the equilibrium constant for peracetic acid formation of 15° and oxidation of *p*-hydroxybenzaldehyde at 15° and 20°.
○, equilibrium constant of peracetic acid formation K_1
◑, for rate constant of the oxidation at 20°
●, at 10°
$[H_2SO_4]=0.392$ M.

10) J. M. Monger and O. Redlich, *J. Phys. Chem.*, **60**, 797 (1956).

11) Under these conditions the observed initial suppression of the rate in Procedure A becomes remarkable. In the following equations (total peroxide is nearly equal to $[H_2O_2]$ in the early stages of the reaction)

$v_1=k_1[H_2O_2][AcOH]$

$v_2=k_2[CH_3CO_3H][\text{hydroxybenzaldehyde}]$
$=k_2'[\text{total peroxide}][\text{hydroxybenzaldehyde}]$

The observed rate constants with *p*-hydroxybenzaldehyde at $[H_2O]=5.55$ M, $[AcOH]=15$ M and $[H_2SO_4]=0.392$ M were found to be

$k_1=1.78\times10^{-4}$ l. mole^{-1}sec.$^{-1}$
$k_2'=4.07\times10^{-3}$ l. mole^{-1}sec^{-1}.

Here, k_2' is the apparent rate contant and k is the rate constant of the subscripted step. Therefore, $v_2/v_1=4.07\times10^{-2}\times[\text{hydroxybenzaldehyde}]/(1.78\times10^{-4}\times15)$

Namely, if the initial concentration of hydroxybenzaldehyde exceeds 10^{-2} M, v_2 appoaches to v_1. This approach should become remarkable as the acidity decreases, since k_1 appreaches to zero with decreasing acidity, while k_2' approaehes to a definite value (see Fig. 2).

The concentration of peracetic acid is obtainable from the concentration of total peroxide [T] as follows.

$$K_1 = \frac{[H_3O]\,[CH_3CO_3H]}{[H_3O_2]\,[CH_3CO_2H]} \quad (3)$$

Here, both $[CH_3CO_2H]$ and $[H_2O]$ may be regarded as constant. Since

$$[T] = [H_2O_2] + [CH_3CO_3H] \quad (4)$$

$$[CH_3CO_3H] = \frac{[CH_3CO_2H]\,K_1}{[CH_3CO_3H]\,K_1 + [H_2O]} \cdot [T] \quad (5)$$

$$[H_2O_2] = \frac{[H_2O]}{[CH_3CO_2H]\,K_1 + H_2O} \cdot [T]$$

$$v = k\,[Hy]\,[T] = k_p\,[Hy]\,[CH_3CO_3H] + k_h\,[Hy]\,[H_2O_2] \quad (6)$$

are obtained, where Hy means hydroxybenzaldehyde, k_p and k_h are rate constants for reactions of peracetic acid and hydrogen peroxide, respectively. Therefore,

$$k = k_p \frac{[CH_3CO_2H]\,K_1}{[CH_3CO_3H]\,K_1 + [H_2O]} + k_h \frac{[H_2O]}{[CH_3CO_2H]\,K_1 + [H_2O]} \quad (7)$$

From the above discussion, it may be concluded that the second term of the right hand side of equation 7 expressing hydrogen peroxide oxidation is far less important than the first term. Hence,

$$k = k_p \frac{[CH_3CO_2H]\,K_1}{[CH_3CO_2H]\,K_1 + [H_2O]} \quad (8)$$

The value of k_p calculated by means of equation 8 holds sufficient constancy as noted later; therefore it is confirmed that the second term participation has little effect on the kinetics. This is supported numerically, comparing k in Procedures A and B at the initial stage of reaction, and the ratio of peracid to hydrogen peroxide in the equilibrium state.

For the expression of the acidity of the solutions, the Hammett's acidity function H_0 was used, the indicators being *o*- and *p*-nitranilines and 4-chloro-2-nitraniline. Plots of H_0 vs. log k_p gave no straight line, but a curve whose slope approaches -1 with increasing acidity, while it approaches zero with decreasing acidity. This fact seems to mean that the rate constant k_p may further be separable into the acid-independent (k_n) terms:

$$k_p = k_n + k_a k_0 \quad (9)$$

where h_0 relates to H_0 in expression $\log h_0 = -H_0$.

Plot of k_p vs. h_0 gives a satisfactory straight line as shown in Fig. 4. A slight decrease of k_a at very high acidity or its change in varying water-sulfuric acid ratio at the same acidity is probably due to the unequality of h_0 and proton activity[12].

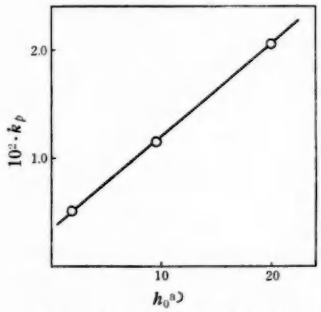

Fig. 4. The plot of k_p vs. h_0 for the reaction of *p*-hydroxybenzaldehyde in moderate acidities at 20°.

Reaction Mechanism.—The above results imply that there is a preliminary, relatively rapid and reversible peracetic acid formation, then acid-catalyzed or uncatalyzed attack of the peracetic acid on the carbonyl group takes place to form an addition complex followed by a rearrangement of the complex to the product. The rearrangement would not perhaps be a rate-determining step, since no stable complex has been isolated, and furthermore, in our preliminary experiments no appreciable difference was observed between the ultraviolet spectrum of the original aldehyde solution and that of the aldehyde solution immediately after mixing it with peracetic acid solution.

On the basis of the observed kinetics, there are two possible mechanisms, i. e., mechanism A involving steps 10, 11, 13, 14 and 16 and mechanism B involving steps 10, 12, 14, 15 and 16.

$$CH_3CO_2H + H_2O_2 + H^+ \rightleftharpoons CH_3CO_3H + H_2O + H^+ \quad (10)$$

$$CH_3CO_3H + H^+ \rightleftharpoons CH_3CO_3H_2^+ \quad (11)$$

$$ArCHO + H^+ \rightleftharpoons ArC^+HOH \quad (12)$$

12) For the ionization and dissociation of sulfuric acid in aqueous acetic acid, see S. Bruckenstein and I. M. Kolthoff, *J. Am. Chem. Soc.*, **78**, 10 (1956).

a) The values of h_0 were calculated from the observed H_0's under these experimental conditions. The values of H_0 were calculated by Hammett's equation $H_0 = pK_a + \log(c_B/c^+_{BH})$ to be -0.28, -0.99 and -1.30 with $[H_2SO_4] = 0.392$ M, 0.784 M and 1.18 M, respectively, where $[H_2O] = 5.55$ M is constant.

$$CH_3CO_3H_2^+ + ArCHO \rightarrow ArCHO\cdot CH_3CO_3H_2^+ \text{(complex, I}\cdot H^+) \quad (13)$$

$$CH_3CO_3H + ArCHO \rightarrow ArCHO\cdot CH_3CO_3H \text{ (complex, I)} \quad (14)$$

$$CH_3CO_3H + ArC^+HOH \rightarrow I\cdot H^+ \quad (15)$$

$$I \text{ (or } I\cdot H^+) \rightarrow ArOCHO + CH_3CO_2H \text{ (or } +H^+) \quad (16)$$

Since the mobile equilibria 11 and 12 probably tend to shift to the left side, step 12 in mechanism A and 11 in B may be neglected except at high acidity. The apparent rate constants k_A and k_B, corresponding to mechanism A and B, respectively, are easily expressed in terms of the equilibrium and rate constants of equations 11—15, where K and k denote equilibrium and rate constants of the subscripted steps, respectively.

$$k_A = k_{13}\cdot\frac{1}{1+K_{12}[H^+]}\cdot\frac{K_{11}[H^+]}{1+K_{11}[H^+]} + k_{14}\cdot\frac{1}{1+K_{11}[H^+]}\cdot\frac{1}{1+K_{12}[H^+]} \quad (17a)$$

$$k_B = k_{15}\cdot\frac{1}{1+K_{11}[H^+]}\cdot\frac{K_{12}[H^+]}{1+K_{12}[H^+]} + k_{14}\cdot\frac{1}{1+K_{11}[H^+]}\cdot\frac{1}{1+K_{12}[H^+]} \quad (17b)$$

Here, k_{13}, k_{14} and k_{15} are acidity-independent constants. At lower acidity, equations 17a and 17b may be simplified in the following way, since both $K_{11}[H^+]$ and $K_{12}[H^+]$ are far smaller than unity.

$$k_A = k_{13}K_{11}[H^+] + k_{14} \quad (18a)$$

$$k_B = k_{15}K_{12}[H^+] + k_{14} \quad (18b)$$

Since both equations 18a and 18b agree with the observed expression 9 and also with the rate-acidity relationship, it seems impossible, on the basis of the kinetics alone, to determine which mechanism is favored in so far as the values of K_{11} and K_{12} are unavailable. However, step 13 is more favorable than step 15, since it involves an attack of a more electrophilic agent $CH_3CO_3H_2^+$.

Summary

The sulfuric acid-catalyzed oxidations of 4-hydroxybenzaldehyde with hydrogen peroxide in aqueous acetic acid were kinetically investigated at 15° and 20° by iodometric estimation of the peroxides. The rates of peroxide consumption were found to be proportional to the product of the concentrations of hydroxybenzaldehyde and peroxide, when the aldehyde was added after the equilibrium between hydrogen peroxide and peracetic acid was attained. The rate constant is a linear function of Hammett acidity function h_0.

Hydrogen peroxide itself reacts slowly with the aldehyde, but it reacts more easily through the formation of peracetic acid. A mechanism involving a ratedetermining attack of protonated and free peracetic acid was postulated and discussed.

Department of Industrial Chemistry
Faculty of Engineering
Kyoto University
Sakyo-ku, Kyoto

Studies on the Interaction of Surface Films with Solute in Solution. IV. Effect of Congo Red Dissolved in Aqueous Substrate upon the Monolayers of Octadecylamine, Cetyl Alcohol, Ethyl n-Hexadecyl Ether, Ethyl Stearate and Cholesterol

By Mitsuo MURAMATSU

(Received August 8, 1958)

In the Part II[1] of this series, the interaction between various dyes in aqueous solutions and stearic acid in the built-up film has been studied. There it was suggested that pH dependence of the amount of dye taken up by the film may be explained by the interaction between dye and stearic acid, involving ionic, dipolar and van der Waals' force. This was generally in agreement with the effect of aqueous dye solution on the monolayer of stearic acid spread on it[2] and has further been supported by the experimental results of a profound effect of aqueous dye on the monolayer of octadecylamine[3]. As has been pointed out in Part II[1], however, there still remained some uncertainty in establishing the mechanism of the interaction between amphoteric dye and the surface film.

Of many amphoteric dyes, Congo red is most familiar to us and the surface-chemical properties of its solution have widely been studied by the measurement of ultrasonic velocity[4], diffusion coefficient[5], viscoelasticity of the adsorbed film[6], and foaming power[7]. Hence Congo red was also adopted in the present work as a representative for the amphoteric dyes and its effect upon the monolayers of several amphipathic compounds has been studied. It may be expected that such a study would also contribute to the understanding of the mechanism of dyeing processes of fibers by so-called direct dyes to which many of the amphoteric dyes belong.

Experimental

Apparatus and procedure were the same as used in the preceding work[3]. The same samples of Congo red[1] and octadecylamine[3] as those which appeared in the preceding reports were used also in of the present experiments. Cetyl alcohol was first grade of Katayama Pure Chemical Co. Ethyl *n*-hexadecyl ether and ethyl stearate were synthesized by the reaction of sodium ethylate with purified hexadecyl bromide and stearyl chloride, respectively. All these amphipathic compounds were purified repeatedly by fractional distillation in vacuo and successive recrystallization from suitable solvents. The highly purified sample of cholesterol was kindly supplied by Dr. E. Kimoto of Kurume Medical College.

Results

Octadecylamine. — It has been suggested[2,8] that the surface pressure, F, of

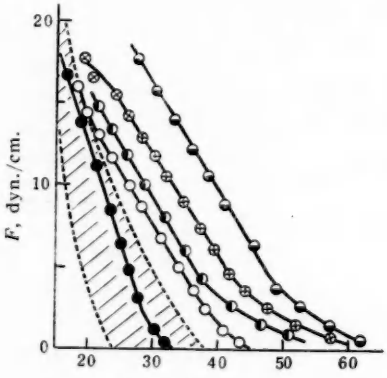

Fig. 1. F~A curves for the monolayers of octadecylamine spread on the solutions of Congo red.
Substrate pH; ◑, 1.0; ⊕, 3.6; ◒, 5.5; ○, 7.3; ●, 9.3: F~A curve for monolayer spread on water lie always in a range of hatched zone.

1) M. Muramatsu, This Bulletin, **31**, 871 (1958).
2) R. Matuura, ibid., **24**, 282 (1951).
3) M. Muramatsu, ibid., **31**, 878 (1958).
4) T. Sasaki and T. Yasunaga, to be published.
5) M. Nakagaki, This Bulletin, **23**, 104 (1950).
6) K. S. G. Doss, *Kolloid-Z.*, **84**, 138 (1938); **86**, 205 (1939); **87**, 272 (1939), etc.; H. Kimizuka, This Bulletin, **26**, 33 (1953).
7) M. Nakagaki, ibid., **23**, 47 (1950); T. Sasaki and H. Kimizuka, ibid., **24**, 230 (1951).
8) T. Sasaki and M. Muramatsu, ibid., **26**, 96 (1953).

this film fluctuated considerably for a given molecular area, A. This came from the effects of ageing of the film, carbon dioxide in the substrate, velocity of compression, etc. This tendency disappeared when Congo red was added to the substrate phase. The effect of dye upon $F\sim A$ curve of the monolayer of octadecylamine is shown in Fig. 1 in which the hatched zone is quoted from the preceding report[3]. It can be seen in this figure that the addition of dye results in a remarkable expansion of the monolayer when pH of the substrate is around 5.5. In Fig. 2 curve

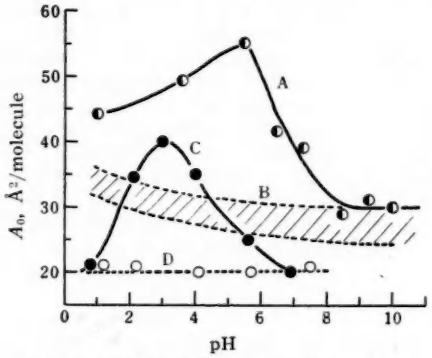

Fig. 2. Effect of Congo red upon A_0 for the monolayer of octadecylamine and cetyl alcohol.
A and B, amine on the substrate with or without dye, respectively; C and D, alcohol on the substrate with or without dye, respectively.

A shows the effect of substrate pH on the area, A_0, of octadecylamine molecule in the monolayer which spread on the solution of dye and is compressed to $F=2$ dyn./cm. In the same figure the hatched zone B expresses the limit of fluctuation of A_0 for a given pH value of the substrate without dye. Maximum expansion of the monolayer was observed at pH 5.5.

Cetyl Alcohol. — No effect of substrate pH was observed upon A_0 for the monolayer spread on the surface of water. When the dye was dissolved in the substrate of pH 2~4, the film expanded considerably. Such an effect of dye is shown in Fig. 2, in which the curve C and D express the pH dependence of A_0 for the monolayer spread on aqueous substrate containing or lacking the dye, respectively. Maximum expansion of the monolayer occurred at pH 3 in this case.

Ethyl *n*-Hexadecyl Ether. — Characteristic kinds of behavior in $F\sim A$ relationship were observed for this film. When the monolayer on the surface of water was compressed, we usually observed an instantaneous rise and subsequent lowering of the surface pressure. A typical example is shown in Fig. 3 (a). The behavior could be reproduced fairly well, though F was determined by means of the vertical plate method which proves to be unsuitable when we measure the decreasing surface pressure. A similar curve was obtained for the film spread on the surface of water of any acidity. The pH dependence of the area, A_0, at $F=2$ dyn./cm. is expressed as curve B in Fig. 4.

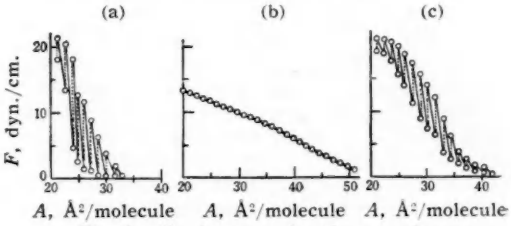

Fig. 3. $F\sim A$ curves for the monolayers of ethyl *n*-hexadecyl ether spread on (a) water of pH 4.0, (b) dye solution of pH 3.8, and (c) dye solution of pH 1.9.

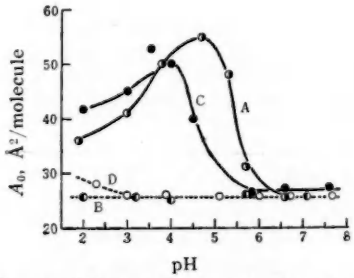

Fig. 4. Effect of Congo red upon A_0 for the monolayer of ethyl *n*-hexadecyl ether and ethyl stearate.
A and B, the ether on the substrate with or without dye, respectively; C and D, the ester on the substrate with or without dye, respectively.

The addition of the dye to the substrate generally resulted in an expansion of the monolayer, as shown in curve A of Fig. 4. The maximum expansion seemed to appear when pH of the dye solution was around 4.4. Precisely speaking, however, there is a difference between the form of $F\sim A$ curve for the region of pH 3.5~5.5 and that for the rest of pH region. In the former region, as illustrated in Fig. 3 (b) for example, dye not only expanded the

monolayer remarkably but also prevented the subsequent lowering of the initial surface pressure. In contrast to this, the effect of surface pressure lowering was evident in the latter region as illustrated in Fig. 3 (c).

Ethyl Stearate.—Effect of substrate pH upon A_0 for the monolayer spread on water is shown by curve D in Fig. 4. Apparently no change in the $F \sim A$ curve was observed throughout pH 3~8. When the monolayer was spread on a substrate water of pH 2.3 and compressed to $F >$ 15 dyn./cm., we usually observed an instantaneous rise and subsequent fall of surface pressure which reached finally an equilibrium value. Such a tendency was most remarkable when the film was compressed fifteen minutes after initial spreading. Any time of elapse longer or shorter than this proved to result in less exaggeration. These phenomena may be due to the hydrolysis of the ester, which was reported for the same film spread on an alkaline substrate[9], and to the change in surface pressure effected by ethanol thereby formed at and ejected from the surface phase. Actually, standing of the monolayer for sixty minutes caused an $F \sim A$ relationship identical with that for stearic acid.

The effect of added dye upon A_0 of the monolayer is shown by curve C in Fig. 4 in which, however, A_0 at pH 1.9 accompanies an inevitable error due to the hydrolysis mentioned above. Even if we took account of this ambiguity, it would be clear that the maximum expansion was observed at pH 3.0.

Cholesterol.—Curve B in Fig. 5 (b) shows pH dependence of A_0 for the monolayer of cholesterol spread on the surface of water. In conforminity with the results appearing in the other reports[10], the monolayer proved to be of low compressibility and of large area when it was spread on distilled water pH of which was less than 7. In more alkaline region, however, A_0 decreased slighty with increasing pH, while the compressibility was scarcely affected at all by the change of the acidity throughout all pH region investigated. This might be ascribed to the dissolution of cholesterol, as predicted by the experimental results on surface evaporation[11].

For the aqueous substrate containing dye, pH dependence of A_0 is shown by the curve A in Fig. 5 (b). Maximum expansion was observed at pH 2 where A_0 was larger by ca. 15 Å²/molecule than that for the control experiment.

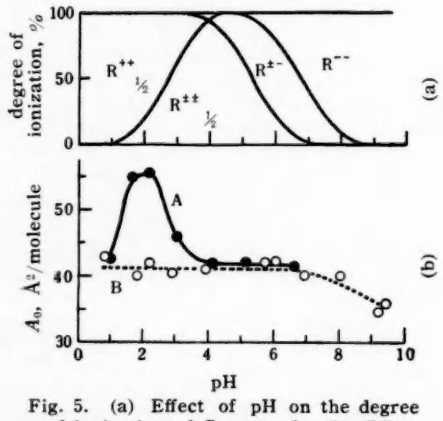

Fig. 5. (a) Effect of pH on the degree of ionization of Congo red. (b) Effect of pH on A_0 for the monolayer of cholesterol spread on the substrate, (A) containing Congo red and (B) lacking it.

Discussion

In Fig. 5 (a) are shown the ionization curves for each ionizable groups in the molecule of Congo red. They are obtained from respective values of the ionization constants which have been reported in Part I[12] of this series. It should be emphasized that the calculations for the dissociation constants were based on the treatment of the dye as a high-polymer electrolyte. When we compare these curves with A_0~pH curves shown in Figs. 2 and 4, it can be seen that the interaction of Congo red with various amphipathic compounds is favored in the isoelectric region, irrespective of the types of their polar heads. In Part II[13] of this series, it has been presumed that the conditions for mutual cohesion of dye molecules among themselves would play simultaneously an important rôle in its interation with film materials. Actually the film materials seem to interact with the colloidal aggregates of dye formed in the solution. Remarkable changes both in the ultrasonic velocity in bulk[4] and in the rheological property of the surface[6] of the solution

9) A. E. Alexander and J. H. Schulman, *Proc. Roy. Soc.*, **A161**, 115 (1937).

10) e. g., J. H. Schulman and E. K. Rideal, *Proc. Roy. Soc.*, **B122**, 29 (1937), etc.

11) E. Sebba and H. V. A. Briscoe, *J. Chem. Soc.*, **1940**, 114.

12) M. Muramatsu, This Bulletin, **31**, 864 (1958).

13) A. Inaba, unpublished.

TABLE I

EFFECT OF CONGO RED UPON A_0 OF VARIOUS MONOLAYERS

Film substance			Area, Å²/molecule			Surface polarity	
Name	Mol. wt.	$pH_{max.}$	$(A_0)_{H_2O}$	$(A_0)_{dye}$	ΔA_0	ΔV, mV	$(A_0)_{H_2O}\cdot\Delta V$ Å²·mV/molecule
Cholesterol	386	2.0	41	56	15	ca. 400[10]	16.1×10^3
Cetyl alcohol	242	3.0	20	40	20	400[14]	$8.0\times$ 〃
Ethyl stearate	312	4.0	25	50	25	370[9]	$9.3\times$ 〃
Ethyl *n*-hexadecyl ether	270	4.4	25	55	30	——	——
Octadecylamine	269	5.5	28	55	27	710[15]	$19.9\times$ 〃

of Congo red being in the same pH range have also been attributed to the formation of colloidal aggregates of dye. Therefore the present results had better be discussed along this line. Additional support for this suggestion was obtained by Matuura[2] who has reported an expanded film of stearic acid spread on a solution of Congo red, pH of which was ca. 3. Inaba[13] has observed that a surface of paraffin was wetted thoroughly by the same solution. All these phenomena emphasize the importance of the rôle of van der Waals' attraction in the interaction. For the other region of pH, ionic repulsion due to the same sign of the charge of dye molecules would suppress the tendency of forming colloidal aggregates in which the molecules of dye interlink each other by the molecular forces other than ionic.

In Table I is summarized the effect of added Congo red on A_0 for various monolayers spread on the substrates, pH values of which are optimum corresponding to the largest expansion. In this table $(A_0)_{H_2O}$ and $(A_0)_{dye}$ represent values of A_0 on pure water and dye solution respectively. Further, the data on surface potential, ΔV, of the monolayer on water are quoted from other literatures. As is seen in the table the amount of increase, ΔA_0, in the area due to the addition of dye seems to depend on the quantity, $(A_0)_{H_2O}\cdot\Delta V$, which may be expressed as the surface polarity, rather than the molecular weight of the monolayer substance. Noticeable deviation from this is observed only for cholesterol which differs in its molecular structure from the other substances. This suggests the distinct contribution to $A\Delta_0$ of the dipolar attraction, in addition to van der Waals' force. It was pointed out[16] that dipolar attraction acting between each other of dye molecules of zwitterion type enhanced the possibility of forming colloidal aggregates of the dye in aqueous medium. A similar explanation was also made for the mechanism of dyeing of fibers[17].

Let us draw attention to the conspicuous nature of the monolayer of ethyl *n*-hexadecyl ether spread on distilled water. As far as the author is aware, the nature of this film has not been studied before. In the case of the monolayer of octadecyl methyl ether, some investigators[18] reported an intramolar rotation of —O—CH_3 bond when the film was compressed to some extent. There the methyl group was considered to orientate itself toward the bulk of substrate, so that the process resulted in a decrease of resultant dipole. It seems to be probable, however, that such a distortion is accompanied by a strong resistance when the end group is ethyl radical as was the case in the present experiment. In Fig. 3 (a) the instantaneous rise and subsequent lowering in surface pressure due to the compression would be an evidence for this effect. In connection with this, it is of interest to note that such an effect disappears whenever Congo red is added to the substrate of pH 3.5~5.5 where the largest expansion of the film is observed. Intramolecular rotation is evidently hindered by Congo red with which the film substance interacts. It should be further noticed that the molecules of dye are almost in the form of $R^{\pm}{}_{1/2}^{\pm}$, as seen in Fig. 5 (a). This increases the possibility of the dipolar attraction between dye and ethyl *n*-hexadecyl ether, if we take account of the hindrance toward reorientation of ethyl group accompanying the change of resultant dipole moment. Presumably both van der Waals' and dipolar force are

14) J. Marsden and J. H. Schulman, *Trans. Faraday Soc.*, **34**, 748 (1938).
15) J. Glazer and M. Z. Dogan, ibid., **49**, 448 (1953).
16) W. Pauli and F. Lang, *Monatsh.* **67**, 159 (1936).
17) e. g., E. L. Valko, "Colloid Chemistry", edited by J. Alexander, Vol. 6, Reinhold Publ. Corp., New York, 1946, p. 594.
18) J. H Schulman and A. H. Hughes, *Proc. Roy. Soc.*, **A138**, 430 (1932); A. E. Alexander, *Trans. Faraday Soc.*, **37**, 426 (1941).

chiefly responsible for the expansion of the monolayer.

Similar kinds of attractive force can also be mentioned to explain the mechanism of the interaction of dye with cetyl alcohol or ethyl stearate. Optimum pH values for the maximum expansion of these films lie in a range of 3~4 where dye molecules are also in the form of zwitterion. On the other hand it is of interest that ΔA_0 for cetyl alcohol is less than that for ethyl *n*-hexadecyl ether. This comes from a decreasing van der Waals' force corresponding to ethyl group. Presumably such a force overwhelms the attraction due to hydrogen bond through the hydroxyl radical of alcohol even if it would be possible. Thus the present result suggests the importance of the rôle of van der Waals' force rather than hydrogen bond in the dyeing process of fibers by the direct dye[17].

Differing from such non-ionic compounds as mentioned above, we may suggest a possibility of ionic interaction in addition to hydrogen bonding, dipole-dipole and van der Waals' force to explain the mechanism of the interaction between Congo red and octadecylamine. The largest expansion of this film is observed when it is spread on the solution of dye of pH 5.5, where a considerable amount of dye molecules are partly ionized, while the molecules of octadecylamine in the film are considered to be perfectly ionized[15]. Therefore we should take account of the additional contribution of ion-ion attraction between dye and octadecylamine to explain the expansion of the monolayer. This is similar to the fact which the present author has pointed out in the case of interaction of basic dye with stearic acid[1] and acid dye with octadecylamine[3]. In connection with this it may be of some values to discuss the effect of dissolved Congo red upon mono- and multilayers of stearic acid and barium stearate. Matuura[2] reported an expansion of the monolayer of stearic acid spread on the dye solution of pH 3. The present author has reported a remarkable increase in thickness of the built-up film of stearic acid and decrease in thickness in the case of barium stearate, when each of them soaks into the dye solution of pH 3.6[1]. In this case both increase have been attributed to the strong interaction. The dye molecules in such a solution are considered to be charged somewhat positively, as shown in Fig. 5 (a). However, no negative charge seems to exist in the molecules of stearic acid in the monolayer spread on pH<6[15,19]. It is probable that the same arguments can also be applied to the case of the multilayers of the same substance. Therefore it would be reasonable to ignore the ion-ion attraction between stearic acid and dye. On the other hand we can not ignore the ion-dipole attraction arising from the positive charge of dye, when dye molecules are allowed to orientate and bind themselves to stearic acid.

Various kinds of behavior of interaction of cholesterol with dye are somewhat erratic. Apparently they are similar to the case of stearic acid rather than cetyl alcohol. This may come from the molecular structure of sterol back-bone being hydrophobic. We can only say at present that the explanation is similar to the case of stearic acid. The detailed discussion may be a future problem.

Summary

Effect of dissolved Congo red upon the monolayers of octadecylamine, cetyl alcohol, ethyl *n*-hexadecyl ether, ethyl stearate and cholesterol spread on the substrate containing the dye has been studied, under varying pH of the solution. It has been observed generally that all monolayers expanded when they were spread on aqueous solution, the pH of which was in such a region that the molecules of dye were almost in zwitterion form. Dipolar and van der Waals' attraction were tentatively postulated to explain the nature of the cohesive force by which the molecules of dye were bond together so that the colloidal aggregates were formed in the solution. The expansion of the monolayer can be accounted for by the binding of the aggregate to film materials. This explanation could successfully be applied to the films of such nonionic substance as cetyl alcohol, ethyl *n*-hexadecyl ether and ethyl stearate.

The largest expansion of the monolayer of octadecylamine was observed when the substrate containing dye showed acidity so that the molecules of dye were partly of negative charge while those of octadecylamine were of positive charge. In this case we had better take account of the possibility of ion-ion attraction between octadecylamine and dye, in addition to the

19) E. Havinga and M. der Hertog-Polak, *Rec. trav. chim.*, **71**, 64 (1952); E. Havinga, ibid., **71**, 72 (1952).

forces which appeared in the cases of nonionic substances.

The author wishes to express his hearty thanks to Professor T. Sasaki for his kind guidance and encouragement in this work. He is also indebted to Professor R. Matuura of Kyūshū University for his helpful discussion, to Professor H. Saikachi of the same university for the elemental analysis of the samples, and to Mr. H. Ōshima of Fukuoka Gakugei University for his assistance on the synthesis and purification of amphipathic compounds. The cost of this research has been defrayed from the Scientific Research Expenditure of the Ministry of Education.

Department of Chemistry, Faculty of Science, Tokyo Metropolitan University Setagaya-ku, Tokyo

---

Absorption Spectra of Dyes. II[1]. *On Non-additivity of Absorption Spectra of Binary Mixtures of a Direct Dye and Some Acid Dyes in Aqueous Solution**

By Yoshié TANIZAKI, Teruaki KOBAYASHI and Noboru ANDO

(Received July 7, 1958)

It has been known that absorption spectra of binary mixtures of dyes in aqueous solution are not always additive[2,3] probably owing to the formation of complexes between dyes in solution, and it is also well known that in dyeing from solutions of mixtures of two dyes, the amounts of dyes adsorbed are frequently non-additive (i. e. a reduction in adsorption)[3]. Moreover in such cases, it seems that there exist some relations between non-additive properties in the amounts of dyes adsorbed and those in absorption spectra. In practical dyeing, mixtures are more frequently used than a single dye in order to produce any desired shade, so that the scientific study on dye mixtures is not only interesting from the physicochemical point of view, but also important practically. For this reason, in our laboratory, the investigation about dye mixtures has been started and the attention is first focused on non-additivity in spectrum.

Hitherto, only a few studies on non-additivity in absorption spectrum of dye mixtures have been carried out[2,3]. Neale and Stringfellow[3] showed that the mixture of Chlorazol Sky Blue FF and an acid dye (*o*-anisidine → H acid) shows non-additive property in absorption spectra, while the mixture of Chlorazol Sky Blue FF and Orange II has an additive spectrum. In this paper, selecting several monoazo acid dyes, the formula of which can be expressed *p*-X-aniline → γ acid with different substituents X, the authors investigated the spectra of pairs of Chlorazol Sky Blue FF and these acid dyes, ranging over the visible and near ultraviolet regions, and found that all of them were more or less different from the sum of the corresponding spectra of their components.

In this paper, a qualitative explanation of non-additivity in spectrum of such mixtures will be given by means of the conventional quantum chemical concept.

Experimental

Materials.—Direct Sky Blue 6B of Mitsubishi-Kasei Co., Ltd. was used as the sample of Chlorazol Sky Blue FF and it was purified by the usual method of Robinson and Mills[4], and the acid dyes made by coupling diazotized *p*-X-aniline with γ acid in acid or alkali solution, were purified by the same method.

Preparation of Samples.—Conductivity water of about 3.5×10^{-7} mho at room temperature was used for the preparation of dye solutions. The

1) Part I of this series, Y. Tanizaki and N. Ando, *J. Chem. Soc. Japan, Pure Chem. Sec.* (*Nippon Kagaku Zasshi*), **78**, 343 (1957).

* Presented at the 11th Annual Meeting of the Chemical Society of Japan, April 1958.

2) D. R. Lemin and T. Vickersraff, *Trans. Faraday Soc.* **43**, 491 (1947); A. N. Derbyshire and R. H. Peters, *J. Soc. Dyers Col.*, **72**, 268 (1956).

3) S. M. Neale and W. A. Stringfellow, ibid., **59**, 241 (1943).

4) C. Robinson and H. A. T. Mills, *Proc. Roy. Soc.* (London), **A131**, 576 (1931).

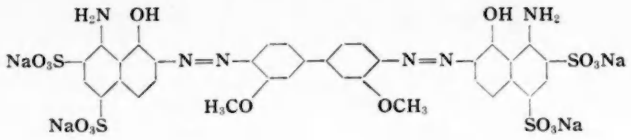

concentrations were 3.59×10^{-6} moles/liter and $1.78\sim1.81\times10^{-5}$ moles/liter for Direct Sky Blue 6B and acid dyes, respectively; these concentrations were determined by the fact that the change in spectrum was the largest when the ratio was about 1 : 5[5].

Dye samples will be conveniently abbreviated in this paper as follows: Direct Sky Blue 6B will be referred to briefly as "Sky Blue". And monoazo acid dyes (p-X-aniline → γ acid)

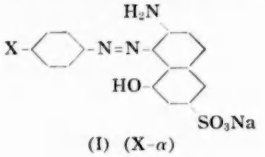

(I) (X-α)

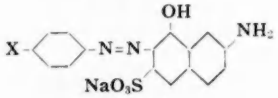

(II) (X-β)

will be represented by substituents X, which means here H, CH_3, OCH_3, Cl and NO_2, of diazotized components and their coupling positions α or β; namely dyes of I will be briefly called X-α, or H-α, CH_3-α, etc. according to their substituents, and similarly those of II will be called X-β or H-β, CH_3-β, etc.

Measurements of Absorption Spectra.—For measurements of absorption spectra of dye solutions, the Shimadzu QB-50 and QR-50 spectrophotometers were used at room temperature (14° to 16°C). Absorption cells were 1 cm. and 2 cm. thick, and optical densities are always reduced to values corresponding to 1 cm. thick.

Results

The most marked non-additivity in absorption spectrum was found for the pair, Sky Blue and the acid dye with substituent NO_2, and in the case of Sky Blue and the acid dye with H for X the least non-additivity was found. As examples, spectra of the combinations of Sky Blue with NO_2-α and NO_2-β, whose non-additivity is the most remarkable, are shown in Figs. 1 and 2, respectively, with those of the components. In each figure curves I and II show the observed absorption curves of Sky Blue and the acid dye, respectively, curve III the sum of them,

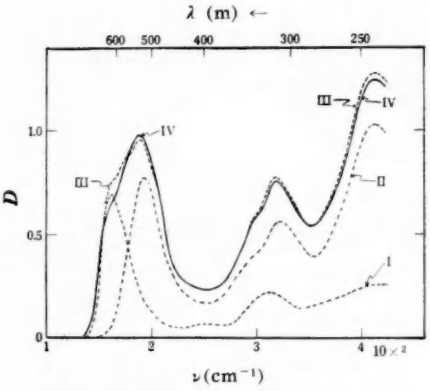

Fig. 1. Absorption spectra of a mixture of Sky Blue and NO_2-α, and its components. Curves I and II show the absorption spectra of Sky Blue and NO_2-α, respectively, curve III shows the resultant of curves I and II, and curve IV observed of the mixture.

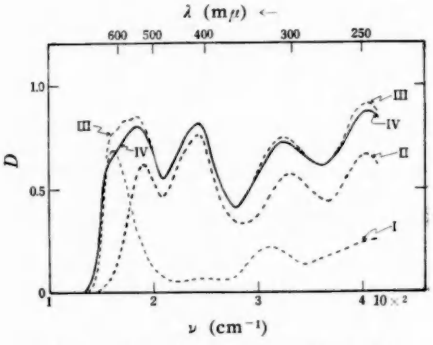

Fig. 2. Absorption spectra of a mixture of Sky Blue and NO_2-β, and its components. Curves show just the same case as in Fig. 1.

and curve IV the observed curve of the mixture. The difference, ΔD, between the sum of optical densities of its components and the observed one of a mixture is the largest in the neighborhood of a wave length of the principal band of Sky Blue (~620 mμ). And here, it is of interest that the bands corresponding to those of NO_2-β in the range of 400~460 mμ ($25\sim22\times10^3$ cm^{-1}) are additive, and that

5) T. Kobayashi, Y. Tanizaki and N. Ando, This Bulletin, to be published.

at the position corresponding to the first band of NO_2-α (~530 mμ) the observed absorption is more intense than the resultant one.

Now, observed wave numbers of absorption maxima of each component are shown in Fig. 3, in which values of difference ΔD between maximum densities of the resultant curve and those of the observed one of a mixture are also shown in round brackets at corresponding positions of absorption bands of acid dyes. Values of ΔD at the principal band of Sky Blue (161×10^2 cm^{-1}), however, are shown in the lowest line corresponding to each acid dye component. Fig. 3 shows distinctive facts to be summarized as follows.

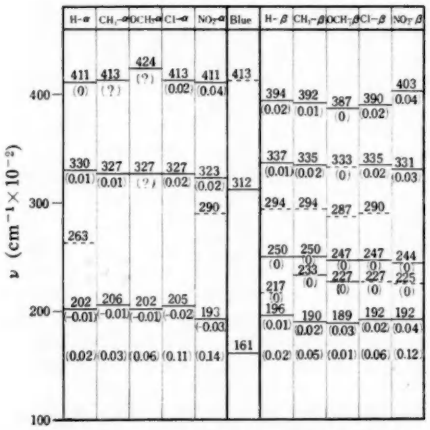

Fig. 3. Observed wave numbers of absorption bands of component dyes. Full and dotted lines mean the maximum positions and shoulders, respectively. Numbers in brackets show the difference between maximum optical densities of the sum of component spectra and observed ones of mixtures.

(1) It can be seen that non-additivity of absorption spectra appears in such positions that the absorption maxima of each component of a mixture are close to each other and there appears such a tendency as that the smaller the difference in wave number between them the larger the difference ΔD.

(2) The observed density near the position corresponding to a wavelength of the first band of each acid dye is smaller than the resultant in the case of Sky Blue and X-β, while it is larger when the acid dye component is X-α, that is to say, ΔD has the negative sign in the latter case.

(3) Absorption bands of the combination with X-β show the additive property in the region of $22\sim25\times10^3$ cm^{-1} (460~400 mμ).

(4) Every mixture shows the largest ΔD at the position corresponding to the wavelength of the principal band of Sky Blue.

Discussion

It may be supposed that such non-additivity in a spectrum comes from the formation of so loose complexes in a solution of dye mixture that the intermolecular charge-transfer does not occur, but some interaction between energy levels of components probably appears provided that their energies are close by. In such a case, for instance, when the excited levels A and B responsible for the absorptions of component dye molecules of a complex interact slightly with each other, it would be assumed that the absorption bands due to the individual transitions change only in wave number, not changing approximately in shape and intensity. Thus, if the spatial configuration of two molecular species were settled, the magnitude of the perturbation would naturally depend upon the difference between energies of A and B, the relative orientation of them in complex or the respective oscillator strength. But if it could be regarded that the effects of the latter two factors were not large and were the same in any complex considered here, the difference between the energies of excited states would become the main factor; namely, the nearer the energies, the larger the perturbation. According to the above consideration, the change in the spectrum of the complex may be approximately discussed by only the difference

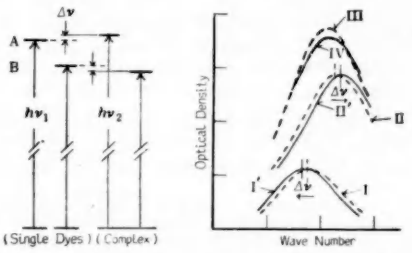

Fig. 4. A schematic illustration of the spectral change in a loose complex. Absorption curves are drawn with a shift of 200 cm^{-1} of each band of the component to the opposite side.

in wave numbers of the corresponding absorption bands of the components. In Fig. 4 the relation between the absorption band of a mixture and those of its components are shown schematically*. In this figure, curves I and II are the absorption bands of the components before interacting, curves I′ and II′ are those after interacting, and curves III and IV are the sums of curves I and II and of curves I′ and II′, respectively. The figure indicates that the intensity of the absorption band composed of those of components after interacting is always smaller than that composed of those before. From studies of dichroism for such dyes as used here, it could be regarded that an apparent single band in the ultraviolet region is the superposition of two, of which the directions of oscillation are orthogonal to each other, originated from the aromatic nucleus of the complicated coupling component[6]. And for this case an explanatory figure also might be given. For example, instead of A mentioned above, $A_{\parallel}$ and $A_{\perp}$ which are orthogonal and close in energy to each other might be considered and the following cases should occur. According to whether $A_{\parallel}$ is directed parallel, normal or inclined to $B_{\parallel}$, the resulting curves will become somewhat different in shape. But practically, the main features of drawn curves for respective cases showed a similar tendency as shown in Fig. 4, indicating a decrease in intensity of the curve after interacting. Anyway, a qualitative and reasonable illustration thus can be obtained for ΔD described in (1) in the foregoing section.

Quite similarly the above consideration will be applied to explain the difference ΔD between the sum of densities of Sky Blue and X-β and the observed one of the mixture at the position corresponding to the first band of X-β. This band is perhaps due to a single absorption and could interact with the first band of Sky Blue in complexes. On the other hand, when a component is X-α the corresponding ΔD has the negative sign. This can be explained, however, if it may be assumed that the first band of X-α consists of two absorption bands, of which one has the same property as the first band of X-β and the other has the different. This assumption is based on the evidence from the dichroic measurement of such dyes in stretched polyvinyl alcohol-sheet[7]. Dichroic properties of some of the dyes used are shown in Fig. 5, in which the curves show absorption spectra when the

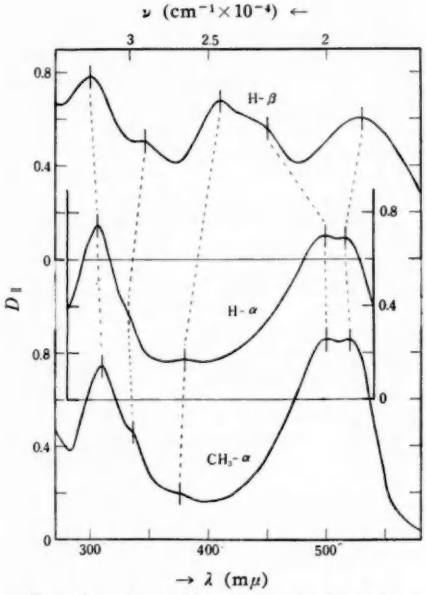

Fig. 5. Absorption spectra for plane polarized light of H-α, CH_3-α and H-β in stretched polyvinyl alcohol sheets when the stretch direction is parallel to the electric vector of incident polarized light.

direction of the electric vector of incident polarized light coincided with the stretch direction. These suggest that respective bands in each curve connected by dotted lines would correspond to each other[7]. It is now possible to assume that the band of the longer wavelength side of two subsidiary bands composing the main band of X-α corresponds to the first band of X-β and is able to interact with the first band of Sky Blue, while the other band of the shorter side has less or no interaction with that of Sky Blue. On the other hand, in Fig. 1 or 2, in which the shoulder of the first band of component Sky Blue (~580 mμ) becomes more distinctive in the

* The polarizability of such a molecule used here may be more responsible for its excited states than the ground state. Therefore, in a complex the interaction between the excited states of the components may be larger than that between the ground states. In Fig. 4, in order to discuss the relative change in levels, all the ground states are indicated on the same line.

6) Y. Tanizaki and N. Ando, *J. Chem. Soc. Japan, Pure Chem. Sec.* (*Nippon Kagaku Zasshi*), **78**, 542 (1957).

7) Y. Tanizaki, presented at the 9th Annual Meeting of the Chemical Society of Japan, April 1956.

resultant curve, it may be presumed that the main absorption band of Sky Blue also consists of such two bands as those just mentioned for X–α. Further the subsidiary band of the longer wavelength side of Sky Blue seems to be more sensitive to the change in external condition than that of the shorter side[8]. Consequently, the correlation shown in Fig. 4 may be able to be diverted by the following method to illustrate the facts described in 2 and 4 in the last section, that is, values of ΔD, near the wavelengths of the first bands of the acid dyes, have the positive sign for pairs of Sky Blue and X–β but the negative sign for those of Sky Blue and X–α, and the largest value is found at the wavelength of the principal band of Sky Blue. If it is supposed schematically that the first absorption band of an X–α consists of two bands shown by curves I′ and II′ in Fig. 4 and is expressed by curve IV, it will be changed to curve III, after being perturbed, with the relative shift of the just-mentioned two bands composing it, while for Sky Blue the reverse is the case; that is, curve III means the principal band of Sky Blue before being perturbed and curve IV that after being perturbed.

Now, supposing that the bands of the shorter wavelength side shown by curves I_b and II_b in Fig. 6, which are constituents of the first bands of Sky Blue (I) and NO_2–α (II), respectively, would remain unchanged, and only the bands of the longer side, curves I_a and II_a, interact with each other, there can be obtained curve IV which, corresponding to the observed absorption, is the resultant of the new component bands coming from the shift just mentioned ($I_a \rightarrow I_a'$, $II_a \rightarrow II_a'$). And curve III shows the sum of curves I and II. The case of the mixture of Sky Blue and NO_2–β is shown in Fig. 7, in which the band of NO_2–β indicated by curve II is assumed to be a single band. In these figures the resolution of the main band into subsidiary bands has been properly made. The curve IV in each figure shows the coincidence in character with those observed (see Figs. 1 and 2). In Fig. 7 it is seen that curve IV is also stronger in intensity near a wave number of 20×10^3 cm^{-1} than curve III; in fact observed results showed, though not very clearly, such a tendency.

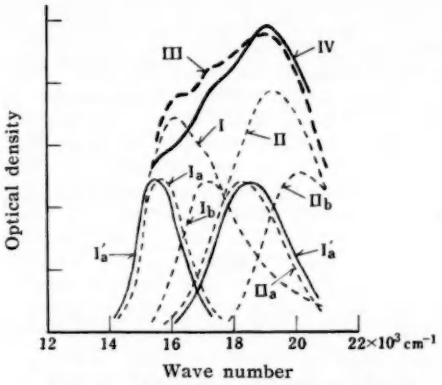

Fig. 6. Absorption curves of a mixture of Sky Blue and NO_2–α, before and after interacting, of the first bands. It is assumed that the interaction occurs only between the bands in the low wave number side, each of which shows a shift of 200 cm^{-1}.

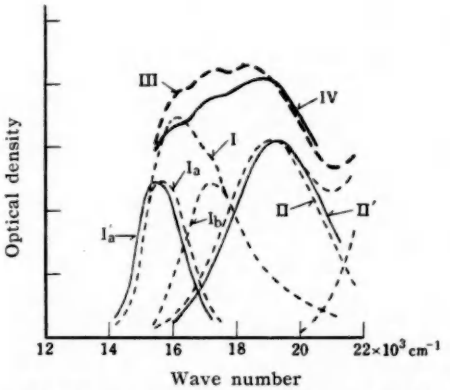

Fig. 7. Absorption curves of a mixture of Sky Blue and NO_2–β, before and after interacting, of the first bands. It is assumed that the interaction occurs between the first band of NO_2–β, which is a single band, and the band of the low wave number side of Sky Blue, each of which shows a shift of 200 cm^{-1}.

It was assumed above that the band of the shorter wavelength side of two constituents of the first band of X–α has less or no interaction with the main band of Sky Blue, corresponding to the second band of X–β (see Fig. 5). If it is true, the second band of X–β should show the

8) Y. Horiki, unpublished. For example, the maximum wavelengths of the first band of Sky Blue in water and in water-pyridine (20% for pyridine) solution were 618 mμ and 630 mμ, respectively, indicating the shift $\Delta\nu$= 310 cm^{-1}. On the other hand, though the determination for the convex parts was not so accurate, it seemed that $\Delta\nu$ was smaller than 290 cm^{-1}, and the shoulder was more distinctive in pyridine solution than in water.

additive spectrum in the combination with Sky Blue. The results observed are indeed in agreement with this expectation. At the same time, the third band also shows the additive property as shown in Figs. 2 and 3. Consequently, it might be considered another reason for the fact described in 3 in the last section that even the band of Sky Blue nearest to the X-β band under consideration lies too far apart for them to interact with each other.

It is well known that the first absorption band of such a dye as used here is quite generally ascribed to the electronic oscillation along the longest conjugated system which includes, as terminal groups, auxochromes characterized by lone-paired electrons in them. That is, the excited state is produced by the migration of an electron on such a terminal group to the inner π-electron system. On the other hand, such frontier electrons may be less protected from the change in the external condition, and are therefore affected easily. It may be, therefore, considered that the first band is more sensitive to the external change than the other bands. Thus, this may be followed by the fact described in (4) in the foregoing section that every mixture shows the largest ΔD at the position corresponding to the principal band of Sky Blue.

Finally, it is interesting to note that ΔD is the largest when X is NO_2 and the smallest when X is H (see Fig. 3). This might be related to the difference in nature of substituents X, but at present there could be found no interpretation for it from these qualitative investigations. As an empirical fact, it can be said that in order to investigate complexes formed in binary mixtures of Sky Blue and the acid dyes used here, NO_2-α or -β will be the most suitable to be selected.

Summary

1. Absorption spectra of mixtures of Direct Sky Blue 6B with *p*-X-aniline→γ acid, in which the substituent X means H, CH_3, OCH_3, Cl or NO_2, and the components in aqueous solution were observed in the visible and near ultraviolet regions.

2. All the absorption bands showed non-additive property, excepting the bands in the region of 400~460 mμ of the mixtures of Sky Blue and X-β shown in Figs. 2 and 3. And optical densities of observed bands of a mixture were generally smaller than sums of the values of each component, but when the acid dyes made by α coupling were used as other components, increases were seen at the positions corresponding to wave lengths of the first bands of them.

3. An explanation for these non-additive properties was given by means of the interaction between the corresponding bands of components.

4. At the same time, in this connection, it is pointed out that the apparent single band of the first of *p*-X-aniline→γ acid in α coupling consists of two bands and similarly the first band of Direct Sky Blue 6B may also consist of two bands.

The authors are indebted to Dr. Ikuzo Tanaka for his useful advice, and they also wish to express their sincere thanks to Mr. Toshiro Iijima for his generous offer of purified acid dyes and to Mitsubishi Kasei Co., Ltd. for the kind contribution of a sample of Direct Sky Blue 6B.

Laboratory of Physical Chemistry
Tokyo Institute of Technology
Meguro-ku, Tokyo

Photochemical Reactions between Methylene Blue and Tri-, Di- and Monomethylamine. III. The Behavior of Methylene Blue in the Presence of Oxygen

By Hiroshi OBATA, Kenichi KOGASAKA and Masao KOIZUMI

(Received August 11, 1958)

In the preceding papers[1], the photochemical reactions between methylene blue and three kinds of amine in vacuo were investigated, and the following scheme was proposed.

$$MB^+ + OH^- + Am \underset{k_2}{\overset{k_1}{\rightleftharpoons}} \text{Intermediate} \xrightarrow{k_3} MBH + AmO \quad (1)$$

Thus, methylene blue when irradiated, reacts with hydroxyl ions and amine and produces a certain type of intermediate with a life time of a few minutes, a part of the intermediate then transforming into leucodye and amine oxide. Now according to a recent paper of Oster[2], methylene blue is photobleached by various kinds of secondary and tertiary amine including ethylenediaminetetraacetic acid, and the reaction which is somewhat similar to ours, was interpreted to take place via the triplet state of dye ion on the ground that the fluorescence of methylene blue is not affected by the added amines. His conclusion will certainly apply to our case, since we have afterwards ascertained that the fluorescence of methylene blue in aqueous solution is practically the same as that of the solution used for the photochemical reaction, both in intensity and in structure.

The objective of the present paper is to elucidate the following three kinetic features which are considered to be important in relation to the above reaction.

(1) *The decision of a species which reacts with oxygen, when the aerobic solution of methylene blue containing amine is irradiated.*—In the studies of photosensitization by methylene blue, Weil[3] observed that amine is oxidized but methylene blue does not practically bleach, and we have also ascertained this fact under our experimental conditions. As to the regeneration of methylene blue in such cases, it seems generally considered especially by biochemists, that the attack of oxygen on leucodye reproduces the original dye. But on the basis of our scheme 1, the possibility of oxygen attack on the intermediate can not be excluded a priori, especially in view of our result that cupric ions react with the intermediate very effectively. The problem must therefore be decided experimentally and for this purpose, a quantitative comparison of the rate of photobleaching in vacuo and that of oxygen absorption by the same solution was undertaken.

(2) *The reactivity of oxygen with a triplet state (T state) of methylene blue.*—Generally, triplet states of dye ions are easily attacked by oxygen[4] as exemplified by the case of eosine studied by Imamura and Koizumi[5]. In the photobleaching of the aqueous solution of eosine under aerobic condition, the reaction takes place chiefly via T state, but most part of the intermediate in the T state is deactivated by oxygen and only a very small fraction of it interacts with oxygen in such an effective way as to lead a bleaching reaction. On this view, the question is raised whether the T state of methylene blue, in the presence of amine, is not attacked altogether by oxygen or alternatively, although attacked by oxygen it is only deprived of its excitation energy, no genuine chemical reaction occurring. This problem is intimately connected with the first one. As a help for the elucidation of this problem, the photobleaching reaction of methylene blue in the aqueous

1) H. Obata and M. Koizumi, This Bulletin, **30**, 136, 142 (1957).
2) G. Oster and N. Wotherspoon, *J. Am. Chem. Soc.*, **79**, 4836 (1957).
3) L. Weil and J. Maher, *Arch. Biochem.*, **29**, 241 (1950).
4) e. g. G. O. Schenck, *Z. Elektrochem.*, **55**, 505 (1951); **56**, 855 (1952); **57**, 675 (1953); *Naturwiss.*, **40**, 205, 229 (1953).
5) M. Imamura and M. Koizumi, This Bulletin, **28**, 117 (1955); **29**, 913 (1956).

solution involving no amine was investigated. It turned out that the rate is somewhat slower than that of eosine under similar conditions, and in relation to the above mentioned question, further investigations were undertaken to make clear of the effect of pH and oxygen pressure on the photobleaching rate.

3) *The behavior of T state of methylene blue in the presence of amine and oxygen.*—A quantitative comparison was made between the rate of photobleaching of methylene blue in vacuo by virtue of trimethylamine and that of oxygen absorption by the same system when irradiated, taking into account of the rate with which the aqueous solution of methylene blue is photobleached by oxygen. A conclusion is that T state of methylene blue is very efficiently deactivated by oxygen in the absence of amine, but such a process is practically suppressed by the presence of amine, oxygen only reacting with leucodye.

Experimental and Results

I. Measurement of the rate of oxygen absorption.—*a) Apparatus and Procedure.*—For our purpose, the rate of oxygen absorption must be compared with that of photobleaching under as much the same condition as possible. This requirement imposes some severe conditions on the apparatus, and as a result of examination of various methods from this viewpoint, it was decided to adopt Tödt's electrochemical method[6].

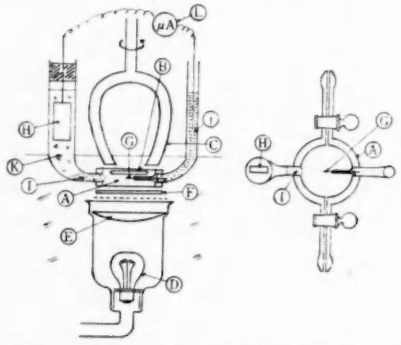

Fig. 1. Apparatus for the measurement of oxygen absorption
A reaction vessel
B magnetic stirrer
C magnet
D light source (automobile head-light lamp 35 w/35 w)
E condensor lens to prepare parallel light
F filter to cut off below 600 mμ
G cathode (platinum wire)
H anode (iron)
I KCl-agar bridge
J mercury
K 0.1 N KCl
L microammeter or galvanometer

The apparatus constructed is shown in Fig. 1. In this figure, A is a reaction vessel with an internal diameter of 28 mm. and a depth of 10 mm., B is a magnetic stirrer, a magnet C being rotated by a phonomotor 80 r. p. m. The cell is irradiated by an automobile head-light lamp 35 w/35 w (D) placed below the cell, E is a condensor lens to prepare parallel light and F is a filter which cuts off below 600 mμ. The intensity of illuminating light is approximately the same as that of the preceding papers[1]. A cathode G., which is polarizable, is a platinum wire 0.3 mm. diameter and 4 mm. length and an anode H, which is unpolarizable, is a piece of iron 30 mm.×10 mm.×4 mm. Tödt's anode contains 2% carbon and 0.6% copper and according to him, the iron rich in carbon and copper generally gives a better stability. Our anode contains 0.18% carbon and 0.98% copper, the specimen being supplied from Osaka Special Steel Ltd. The anode is dipped in 0.1 N potassium (K) solution and is connected to a cell via a potassium chloride-agar bridge I. As shown by Tödt, the amount of current supplied by this cell is determined by the diffusion of oxygen in the neighborhood of platinum electrode, and is given by the following relation after the establishment of a steady state.

$$i = nFDqc/\delta$$

($n=4$, F: Faraday, D: diffusion constant, q: area of the cathode surface, c: oxygen concentration in the bulk solution, δ: thickness of diffusion layer).

In our experiment the speed of rotation of the magnet is slower than that in Tödt's experiment, hence the diffusion current is very dependent on the rotating speed and particular caution must be paid to keep constant the speed of rotation. Another thing to be added is that a platinum electrode needs to be dipped in hydrochloric acid to make its surface clean before use. Perhaps a platinum electrode, when exposed in the air, would have its surface covered with a thin film of oxide or the like, which would reduce the current.

b) Calibration.—Calibration between the diffusion current and the concentration of dissolved oxygen was made using the same solution for the absorption experiment, the composition being 2.0×10^{-5} M methylene blue, 0.1 N potassium chloride and pH 9.2 controlled by borate buffer. Firstly, the air mixed with a certain amount of nitrogen gas was passed through the solution immersed in a thermostat at 40°C, and the cell was filled quickly with this solution without any gaseous phase left behind. The current was measured in 30°C thermostat by a microammeter

6) F. Tödt, *Z. Elektrochem.*, **54**, 485 (1950); F. Tödt et al., *Biochem. Z.*, **323**, 192 (1952); **325**, 210 (1954); F. Tödt, D. Burk and O. Warburg, *Biochim. et Biophys. Acta*, **12**, 347 (1953).

in higher oxygen concentration or a galvanometer in lower oxygen concentration, while the concentration of oxygen was analyzed by Winkler's method[7] using the remaining solution. Winkler's method, however, when applied directly to the above solution did not give correct results owing to some difficulty in iodometry. Hence the dissolved oxygen was excluded by a flow of nitrogen gas and then redissolved in the mixed solution of manganese chloride and sodium hydroxide which was analyzed by the same method. Between the current and the concentration of oxygen, a good linear relationship holds, as shown in Fig. 2.

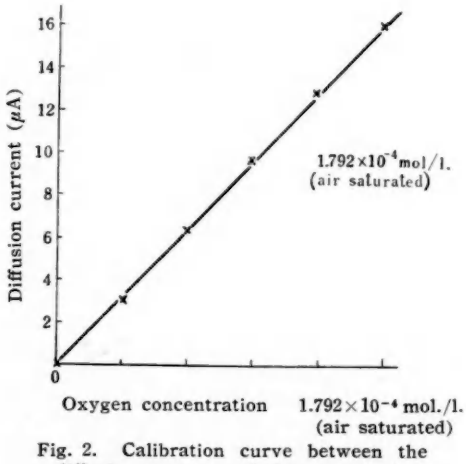

Fig. 2. Calibration curve between the diffusion current and the concentration of oxygen.

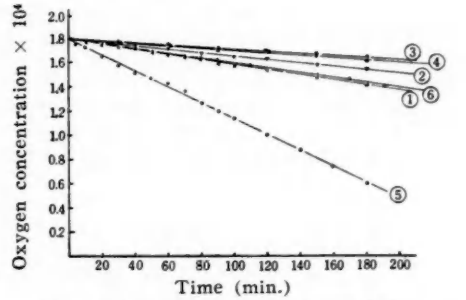

Fig. 3. Oxygen absorption by methylene blue solution containing amines.

①	trimethylamine	2×10^{-3} M
②	〃	1.5×10^{-3} M
③	〃	1.0 〃
④	〃	0.6 〃
⑤	dimethylamine	4×10^{-2} M
⑥	monomethylamine	〃

7) L. W. Winkler, *Ber.*, **21**, 2843 (1888); F.P. Treadwell and W. T. Hall, "Analytical Chemistry", vol 2. John Wiley of Sons, New York (1942) p. 704.

c) Results. — The composition of the solutions employed were usually 2×10^{-5}M methylene blue, 0.1 N potassium chloride pH 9.2 controlled by borate buffer, the amount of trimethylamine being varied from 0.6×10^{-3}M to 2.0×10^{-3}M. In cases of dimethylamine and monomethylamine, the concentration was raised to 4.0×10^{-2}M. A few results obtained for the relation between the concentration of oxygen and time are shown in Fig. 3. As seen from the figure, a linearity holds in all cases. But for a later stage (below about 3×10^{-5}M of oxygen), not shown in the figure, an abnormally rapid decrease of oxygen is observed in cases of trimethyl and monomethylamine, but not in dimethylamine. The origin of the above phenomena is not known at the present stage. It may perhaps be related to the electrode process and different kinds of behavior may partly be due to the mechanism of each reaction in this region. For our present purpose, however, only those regions of the normal behavior were employed and the rate of oxygen absorption was evaluated from its inclination.

The results are summarized in Table I. In this table two kinds of calculated value were obtained as follows.

Calculation A. If one assumes that leucodye, when formed, reacts very rapidly with oxygen according to the following stoichiometric relation

$$MBH+\frac{1}{2}O_2 \longrightarrow MB^+ + OH^-*$$

then, the rate of oxygen consumption will be given by

$$-\frac{d[O_2]}{dt}=\frac{1}{2}\cdot\frac{k_1k_3}{k_1+k_2+k_3}[MB]_0$$

where $[MB]_0$ is the analytical concentration of methylene blue.

Figures given under the heading Cal. A are the values by the above formula.

Calculation B. If one assumes that as soon as the intermediate is produced, it is attacked by oxygen immediately according to the following stoichiometric relation,

$$(MB\cdots HO\cdots Am)+\frac{1}{2}O_2 \longrightarrow MB^+ + OH^- + AmO$$

then the rate of oxygen absorption will be given by

* In view of Weil's results that hydrogen peroxide was not detected by an ordinary method though perceptible by pyruvic acid method, the overall reaction in the main would be such as written above.

TABLE I

Methylene blue (MB) 2.0×10^{-5}M
pH=9.2, Temp. 30°C

[TA]	[TA]/[MB]	k_1	k_2	k_3	$-\frac{d[O_2]}{dt}$ Cal. A	Cal. B	obs.
2.0×10^{-3} M	100	0.109	0.055	0.039	2.07×10^{-7}	1.09×10^{-6}	1.98×10^{-7}
1.5 〃	75	0.057	0.028	0.026	1.373 〃	5.7×10^{-7}	1.42 〃
1.0 〃	50	0.052	0.044	0.027	1.122 〃	5.2 〃	0.9 〃
0.6 〃	30	0.039	0.025	0.024	1.018 〃	3.9 〃	0.96 〃
*1.5 〃	75	0.325	0.216	0.170	7.75 〃	3.25×10^{-6}	5.69 〃
**2.0 〃	100	0.202	0.127	0.071	3.06 〃	1.72 〃	2.73 〃

* pH=10.0
** pH=9.2, temp. 40°C and MB=1.7×10^{-5}

[DA]	[DA]/[MB]	k_1	k_2	k_3	Cal. A	Cal. B	obsd.
4.0×10^{-2}	2000	0.052	0.060	0.041	1.392×10^{-7}	5.2×10^{-7}	5.73×10^{-7}

[MA]	[MA]/[MB]	k_1	k_2	k_3	Cal. A	Cal. B	
4.0×10^{-2}	2000	0.052	0.049	0.035	1.334×10^{-7}	5.2×10^{-7}	2.0×10^{-7}

$$-\frac{d[O_2]}{dt}=\frac{1}{2}k_1[MB]_0$$

Figures given under the heading Cal. B are the values obtained by this formula. k_1, k_2 and k_3 are the constants evaluated from the analysis of the bleaching of the dye ion in vacuo in the same solution used for the oxygen absorption experiment.

II. The photobleaching of the aqueous solution of methylene blue by dint of dissolved oxygen.—*a) Apparatus and procedure.*— The experiment was done in a similar way to that described in Imamura and Koizumi's paper[5]. The concentration of dye was usually 1.6×10^{-5}M. The rate of photobleaching was calculated from the fall of the maximum absorbance. In certain cases the position of maximum absorption showed a slight shift toward a shorter wave length giving rise to some ambiguity to the analysis, although the initial rate generally adopted is quite reliable. The data can be analyzed by Imamura and Koizumi's method and the relation

$$\{\ln(1-e^{-\alpha c_0 d})+\alpha c_0 d)\}-\{\ln(1-e^{-\alpha cd})+\alpha cd\}=k't \qquad (2)$$

can express the experimental results satisfactorily. Thus in almost all cases the plot of $\{\ln(1-e^{-D})+D\}$ (D, optical density) against t gives a straight line and from its inclination the value of k' is evaluated, k' is related with the quantum yield k by the following equation

$$k'=\alpha dI_0 k \qquad (3)$$

in which α is not a genuine extinction coefficient but is to be considered rather a kind of experimental parameter. By an experiment employing a thermopile, k was determined for a certain solution and the proportionality constant between k and k' thus obtained was utilized for calculating k from k' for all the other solutions.

b) Effect of oxygen pressure on the bleaching rate of the aqueous methylene blue solution.—The aqueous solution of methylene blue was found to bleach gradually when irradiated, but if evacuated there occurs no bleaching perceptible. Thereupon, in order to examine the effect of oxygen concentration on the rate, the experiments were done with the solutions which had been previously brought to equilibrium with the air of various pressures. The concentration of the dissolved oxygen was calculated by use of Ostwald's absorption coefficient of oxygen in water neglecting the effect of a small quantity of dye. The results obtained are summarized in Table II and a plot of $1/k$ against the reciprocal of the oxygen concentration is given in Fig. 4, which shows a good straight line.

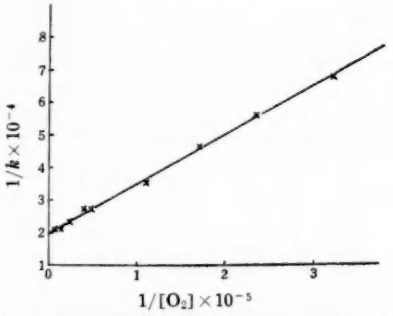

Fig. 4. Plot of $1/k$ against the reciprocal of the oxygen concentration.

TABLE II

Concentration of oxygen mole/l.	k'	k
2.5×10^{-4}	0.0240	4.63×10^{-5}
1.07×10^{-4}	0.0247	4.75×10^{-5}
4.95×10^{-5}	0.0239	4.61×10^{-5}
4.85×10^{-5}	0.0225	4.34×10^{-5}
2.38×10^{-5}	0.0174	3.36×10^{-5}
2.15×10^{-5}	0.0180	3.48×10^{-5}
9.1×10^{-6}	0.0143	2.76×10^{-5}
5.76×10^{-6}	0.0117	2.26×10^{-5}
4.25×10^{-6}	0.00912	1.76×10^{-5}
3.13×10^{-6}	0.00766	1.48×10^{-5}
1.16×10^{-6}	0.00288	5.55×10^{-6}

As the reaction goes via T state, k is to be related with the constants of various steps by the same formula already applied to the case of eosine.

$$k=\varphi_{S\to T}\frac{k^{I}_{O_2}[O_2]}{k^{IS}_{O_2}[O_2]+k^{I}_{H_2O}[H_2O]}\times\frac{k^{II}_{H_2O}}{k^{IIS}_{H_2O}}$$

or $$\frac{1}{k}=\frac{1}{\varphi_{S\to T}}\frac{k^{IS}_{O_2}}{k^{I}_{O_2}}\frac{k^{IIS}_{H_2O}}{k^{II}_{H_2O}}+\frac{1}{\varphi_{S\to T}}\frac{k^{I}_{H_2O}[H_2O]}{k^{I}_{O_2}[O_2]}\frac{k^{IIS}_{H_2O}}{k^{II}_{H_2O}}$$

where $\varphi_{S\to T}$ means transition probability for the suffixes I, II refer respectively to the first and second step and the suffix S means the sum of all the reactions of the related species. Other symbols are evident. From the inclination and the intercept of the plot in Fig. 4,

$$\frac{1}{\varphi_{S\to T}}\times(k^{I}_{H_2O}[H_2O]/k^{I}_{O_2})(k^{IIS}_{H_2O}/k^{II}_{H_2O})=1.55\times10^{-1} \quad (4)$$

$$\frac{1}{\varphi_{S\to T}}\times(k^{IS}_{O_2}/k^{I}_{O_2})(k^{IIS}_{H_2O}/k^{II}_{H_2O})=2.0\times10^{4}$$

or $$\varphi_{S\to T}(k^{I}_{O_2}/k^{IS}_{O_2})(k^{II}_{H_2O}/k^{IIS}_{H_2O})=5\times10^{-5} \quad (5)$$

From 4 and 5

$$k^{I}_{H_2O}[H_2O]/k^{IS}_{O_2}=7.75\times10^{-6} \quad (6)$$

and putting $[H_2O]=55.5$ M

$$k^{I}_{H_2O}/k^{IS}_{O_2}=1.4\times10^{-7}$$

For eosine the above quantities have already been evaluated as follows[8]

$$\varphi_{S\to T}(k^{I}_{O_2}/k^{IS}_{O_2})(k^{II}_{H_2O}/k^{IIS}_{H_2O})=2.8\times10^{-4}$$

$$k^{I}_{H_2O}/k^{IS}_{O_2}=1.3\times10^{-8}$$

Comparing the two sets of values, it may be said that the reactivity (deactivation+genuine reaction) of T state of methylene blue against oxygen is about 1/10 of that of eosine.

c) The effect of pH on the bleaching rate. —The pH effect on the photobleaching was examined only for the solution saturated with air. It is to be noted that absorption spectra of methylene blue change above and below a certain pH value and especially in the strong alkaline region, the dye seems to be quite unstable even in the dark. Hence the effect was examined only in the region where absorption spectra are not affected or affected little. In most experiments the pH values were controlled by the veronal-sodium acetate-hydrochloric acid buffer. All the data could be analyzed by 2, a linearity between $\{\ln(1-e^{-D})+D\}$ and t holding exactly except for a single case of pH 8.59 (the most alkaline solution).

The results are summarized in Table III and are shown in Fig. 5.

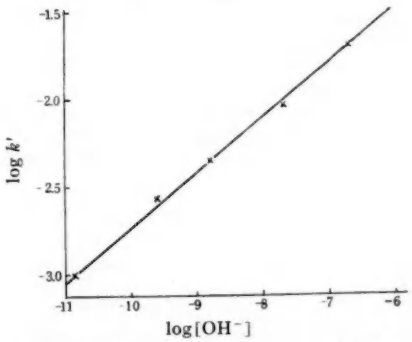

Fig. 5. Relation between $\log k'$ and $\log[OH^-]$.

TABLE III

buffered solution		non-buffered solution	
pH	k'		k'
3.35	0.001	10^{-3}N HCl	0.0019
4.40	0.0027	*pure water	0.024
5.20	0.0043	10^{-3}N NaOH	0.062
6.34	0.0086		
7.30	0.0196		
8.59	0.023		

* pH of the aqueous solution MB 1.6×10^{-5} M was measured by pH meter to be ca. 6.8.

From this figure, it can be said that k is approximately proportional to $[OH^-]^{1/3}$ for the buffered solution and the results for the non-buffered solution are somewhat higher at pH<7.0.

8) M. Imamura, This Bulletin, **30**, 249 (1957).

Discussion

Firstly, the discussion will be given about a species which is attacked by oxygen in the amine added solution of methylene blue. The solution of methylene blue containing trimethylamine does not practically bleach in spite of the presence of oxygen and this fact conforms well with the result that the quantum yield of amine induced photobleaching (reversible photoreduction) in vacuo ($10^{-3}\sim10^{-2}$) is quite larger than that of the oxygen induced photobleaching (irreversible photoöxidation) of the aqueous methylene blue solution ($\sim4.6\times10^{-5}$)***. From the above results the possibility that oxygen attacks T state decomposing methylene blue molecules can be excluded in the amine added solution. And whether oxygen attacks intermediate or leucodye, the rate must be so fast that as soon as the intermediate (or the leucodye) is formed, the consumption of oxygen must immediately take place, because the rate of oxygen absorption is the zeroth order in oxygen concentration. However, there is one thing to be taken into consideration. That is the possibility of deactivation of T state by oxygen. From the results of the irreversible photoöxidation of the aqueous solution, although the value of quantum yield is quite small

$$\varphi_{S\to T}(k^{I}_{O_2}/k^{IS}_{O_2})(k^{II}_{H_2O}/k^{IIS}_{H_2O})=k=5\times10^{-5}$$

the rate constant $k^{IS}_{O_2}$ (for the whole process consisting of deactivation and genuine reaction) is quite larger than $k^{I}_{H_2O}[H_2O]$ ($k^{IS}_{O_2}/k^{I}_{H_2O}[H_2O]=1.3\times10^{5}$). Therefore, there is no reason to deny a priori the posibility of such a deactivation in the solution of methylene blue containing amine. But if this should occur in about the same order as in the aqueous methylene blue solution, the rate of oxygen consumption ought to be exceedingly smaller than the calculated value in Table II. The agreement between the calculated and the observed value in the order of magnitude definitely denies such a possibility, and for the case of trimethylamine, the close agreement between the observed and the calculated value (Cal. A) strongly supports the view that oxygen attacks only on leucodye and not on intermediate. Thus it may be concluded that the behavior of T state toward oxygen is essentially different in two solutions with and without amine. For the solution containing amine, such a view as that competitive reactions of T state with oxygen on the one hand and with amine and OH^- on the other take place, the latter greatly predominating over the former, can not be adopted. Rather, the interpretation that oxygen in the solution containing amine loses the power of deactivating T state or alternatively loses a chance of effective encounter with T state, seems to fit experimental results. This interpretation is further supported from the following argument about the different features of the kinetics already established in the reversible photoreduction and the irreversible photoöxidation. On the basis of a broad outline of the reaction scheme proposed in the previous paper[1], let us asume tentatively a more detailed mechanism which of course must await further studies to confirm it. One plausible scheme would be such as the following

$$\begin{array}{l} MB^+ + h\nu \longrightarrow MB^{+*} \longrightarrow MB^{+\prime} \\ \qquad\qquad \overrightarrow{k}^{I}_{q} \\ MB^{+\prime} \longrightarrow MB^+ \\ \overrightarrow{k}^{I}[OH^-] \downarrow\uparrow \overleftarrow{k}^{II} \qquad \overrightarrow{k}^{II}[Am] \\ MB\cdots OH \longrightarrow MB\cdots HO\cdots Am \\ \qquad\qquad\qquad\qquad \downarrow k_2 \\ \overset{k_3}{\longrightarrow} \text{Product} \end{array}$$

Applying the stationary state condition to T state and MB $\cdots$OH, k_1 in 1 can be expressed as follows in the above scheme

$$k_1\sim\frac{I_{ab}\varphi_{S\to T}\overrightarrow{k}^{I}\overrightarrow{k}^{II}[OH^-][Am]}{\overrightarrow{k}^{I}_{q}\overleftarrow{k}^{II}+\overrightarrow{k}^{I}[OH^-]\overrightarrow{k}^{II}[Am]+\overrightarrow{k}^{I}_{q}\overrightarrow{k}^{II}[Am]}$$

Although somewhat different relations may result from different mechanisms, the essential point would not be affected. It is that the relation experimentally found, $k_1\propto[OH^-][Am]$ requires a far larger magnitude of $\overrightarrow{k}^{I}_{q}\overleftarrow{k}^{II}$ term or the like compared with other terms involved in the denominator. Thus it is a natural expectation that the reaction of T state with OH^- and amine leading to an intermediate is slower than the deactivation or quenching process of T state by water molecules or itself.

The above situations are in sharp contrast with those of the solution without amine, in which T state is deactivated by

*** To avoid confusion let us designate the two reactions as reversible photoreduction and irreversible photooxidation hereafter.

O_2 far more rapidly than water. Thus the different kinds of behavior in two cases are comprehensive only from the viewpoint mentioned above.

Lastly it is to be added that for the case of monomethylamine, the observed rate of oxygen absorption coincides approximately with the values calculated by A method while it lies near to the values calculated by B method for the case of dimethylamine. But in view of few data and their accuracy being not very good, further studies will be necessary for a decisive conclusion except the case of trimethylamine for which the statement that oxygen attacks leucodye may be beyond doubt.

Next the retarding effect of veronal upon the irreversible photoöxidation may be taken up.

A structural formula of veronal

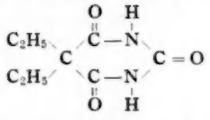

contains two secondary amino nitrogens, and in view of the results reported by Oster[2], it is a natural expectation that another reaction competing with the irreversible photoöxidation takes place between T state of methylene blue and veronal molecule. To ascertain this conjecture, it was examined whether the evacuated buffered solution displays the photobleaching or not. The result as shown in Fig. 6, is that the photobleaching does really take place and moreover the introduction of oxygen into the bleached solution recovers a greater part of the lost color. Such a bleaching process does not occur in the evacuated dye solution containing 10^{-3}M sodium hydroxide.

Thus, there is no doubt that a reversible photoreduction such as the formation of leucodye is taking place in this case. The retardation of the irreversible photoöxidation caused by the addition of veronal, can be attributed to this competitive reductive reaction, the produced leucodye being recovered by the existent oxygen. Veronal can be said to have amino-like action although to a far lesser extent. It may be worthy of adding here that an enough caution must be paid when the buffer solution is used for such experiments as the present one, since the buffer solutions usually employed often involve such a N-containing compound like veronal.

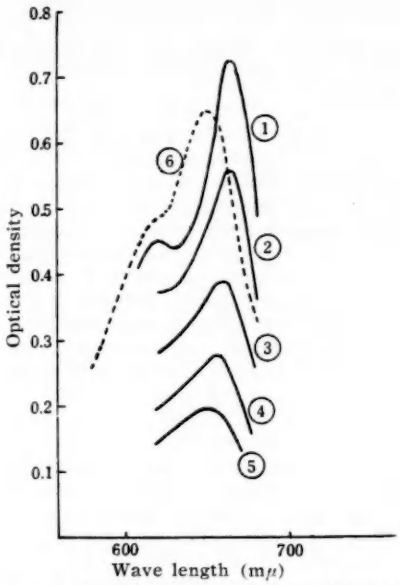

Fig. 6. Photobleaching of the methylene blue solution containing veronal in vacuo.
1 initial
2 after 10 minutes
3 after 20 minutes
4 after 40 minutes
5 after 60 minutes
6 after exposed to the air

Studies on the pH dependence of the rate certainly be essential for the elucidation of a detailed mechanism of the irreversible photoöxidation. But the results obtained in this paper are difficult to interpret because of the complexity introduced by the above circumstances and of the lack of experiments for examining the effect of oxygen concentration upon the rate in various pH solutions. A further more careful and extensive study will be necessary in order to make clear a detailed mechanism of the present reaction.

Summary

In connection with the reversible photoreduction of methylene blue in vacuo published already, the rate of the consumption of oxygen in the irradiated solution of methylene blue containing three kinds of amine was measured. In addition, the irreversible photoöxidation of the aqueous methylene blue solution was

studied, particular attention being paid to the effect of oxygen pressure and pH on the rate. The following conclusions were drawn from the above two series of experiments.

1) In the irradiated aqueous solution of methylene blue containing trimethylamine, oxygen does not affect the T state of dye and attacks only the leuco form, reproducing the dye molecule. Oxygen reacts almost instantaneously with the leucodye as soon as the former is produced.

2) In the aqueous solution of methylene blue (with no amine added) the reactivity of T state against oxygen is about one order less than that of eosine in the analogous condition. The deactivation of T state by oxygen in case of methylene blue is about 10^{-7} times greater than that by water.

3) Comparison of the above results 1 and 2 (taking into account of the result that in the evacuated state the reactivity of T state against OH^- and amine is much less than the deactivation by water) leads to the conclusion that the deactivation of T state by oxygen is almost completely suppressed by the addition of amine.

4) The rate of irreversible photoöxidation increases with the alkalinity of the solution. But in the buffer solution containing N-compound like veronal, a competitive reaction somewhat like that between methylene blue and amine occurs. It is pointed out that enough caution must be taken for such a possibility when the buffer solutions are employed.

A part of this research was done in the Institute of Polytechnics of Osaka City University. The cost of this research has been partially defrayed from the Scientific Research Grant from the Ministry of Education.

Department of Chemistry, Faculty of Science, Tohoku University
Katahira-cho, Sendai

Photometric Determination of Indicator End Points in Complexometric Titrations

By Sôichirô MUSHA, Makoto MUNEMORI and Kin'ya OGAWA

(Received August 13, 1958)

In photometric titrations with an indicator, the color does not develop linearly with the titrant added. This characteristic has been elucidated by a mathematical treatment of complexometric titration with specific indicator for a certain metal[1].

In a previous communication[2], the present authors proposed a graphical method for determining indicator end point in the complexometric titration by a photometric technique and applied it with success to the titration of magnesium with disodium salt of ethylenediaminetetraacetic acid (Complexon III) using Eriochrome Black T (EBT) as indicator. This method is, however, an approximate one and therefore its utility and limitation will be discussed in the present paper.

1) J. M. H. Fortuin, P. Karsten and H. L. Kies, *Anal. Chim. Acta*, **10**, 365 (1954).
2) S. Musha, M. Munemori and K. Ogawa, This Bulletin, **30**, 675 (1957).

Theoretical

List of Principal Symbols.—

m_t, total concentration of metal in titration system
i_t, total concentration of indicator in titration system
c_t, total concentration of titrant in titration system
$\mu = c_t/m_t$, relative concentration of titrant
$\alpha = [I^*]/i_t$, ratio of $[I^*]/([MI] + [I^*])$
$[I^*] = [I] + [HI] + [H_2I] + \cdots\cdots$, sum of the concentrations of metal-free indicator components
$[Y^*] = [Y] + [HY] + [H_2Y] + \cdots\cdots$, sum of the concentrations of metal-free titrant
$K_Y^* = [MY]/[M][Y^*]$, apparent stability constant
$K_I^* = [MI]/[M][I^*]$, apparent indicator constant
A_s, absorbancy during the course of titration

A_{sI}, absorbancy of metal-free indicator
A_{sMI}, absorbancy of metal-indicator complex
V, volume of titrant solution added, in ml.
V_{eq}, volume of titrant solution equivalent to the total concentration of metal, in ml.
V_0, volume of metal ion solution to be titrated, in ml.
C, molarity of titrant

General Expression and Approximate Expression. — In titrating the metal ion with such a reagent as Complexon-III in an aqueous system, there are the following equilibria:

$$M+Y^*=MY \quad \text{and} \quad M+I^*=MI \tag{1}$$

From K_Y^* and K_I^* it follows that:

$$[MY]=K_Y^*[M][Y^*] \tag{2}$$

$$[MI]=K_I^*[M][I^*] \tag{3}$$

On the other hand, m_t, c_t and i_t are expressed by the following equations:

$$m_t=[M]+[MY]+[MI] \tag{4}$$

$$c_t=[MY]+[Y^*] \tag{5}$$

$$i_t=[MI]+[I^*] \tag{6}$$

From Eqs. 2, 3, 4, 5 and 6, the following relationship is derived.

$$c_t=m_t-[MI]\left(1+\frac{1}{K_I^*[I^*]}\right)+[I^*]\frac{K_I^*}{K_Y^*}\left\{\frac{m_t}{[MI]}-\left(1+\frac{1}{K_I^*[I^*]}\right)\right\} \tag{7}$$

By replacing Eq. 7 by the relative values μ and α, comes the following equation:

$$\mu=1-\frac{1}{m_t}(1-\alpha)\left(i_t+\frac{1}{\alpha K_I^*}\right)+\alpha\frac{K_I^*}{K_Y^*}\left\{\frac{1}{1-\alpha}-\frac{1}{m_t}\left(i_t+\frac{1}{\alpha K_I^*}\right)\right\} \tag{8}$$

Eq. 8 is the general expression for the spectrophotometric titration curve and will be called *general equation.*

Now, if $[Y^*]$ and i_t are so small that they can be neglected in the course of titration, Eqs. 4 and 5 are converted into the followings:

$$m_t=[M]+[MY] \tag{9}$$

$$c_t=[MY] \tag{10}$$

From Eqs. 2, 3, 9 and 10 it follows that:

$$c_t=m_t-\frac{1}{K_I^*}\frac{[MI]}{[I^*]} \tag{11}$$

If the dilution of solution by titrant is neglected, Eq. 12 will be obtained by substituting Eq. 11 with V and V_{eq}:

$$V=V_{eq}-\frac{V_0}{C}\frac{1}{K_I^*}\frac{[MI]}{[I^*]} \tag{12}$$

Values of $[MI]/[I^*]$ can be computed from the absorbancy readings by means of the following equation:

$$[MI]/[I^*]=(A_{sI}-A_s)/(A_s-A_{sMI}) \tag{13}$$

If $(A_{sI}-A_s)/(A_s-A_{sMI})$ is plotted against V will result a straight line whose intercept on the V-axis is equal to V_{eq}[2]. By replacing Eq. 11 by μ and α, comes Eq. 14:

$$\mu=1-\frac{1}{m_t}\frac{1}{K_I^*}\frac{1-\alpha}{\alpha} \tag{14}$$

Eq. 14 is the approximate expression for the spectrophotometric titration curve and will be called *approximate equation.*

Discussion

On the basis of general equation, Fortuin et al.[1] discussed the condition to be fulfilled for the accurate determination of indicator end point in complexometric titration by a photometric method. In the present paper, however, we shall discuss the conditions under which the approximate equation is established within experimental errors.

When Eq. 14 is compared with Eq. 8, i_t and K_Y^* are omitted in Eq. 14, and therefore the effects of these variables on the deviation of the approximate equation from the general equation will be mainly examined.

If the magnitudes of m_t, i_t, K_Y^* and K_I^* are assigned in Eq. 8, α and hence $(1-\alpha)/\alpha$ can be evaluated as a function of μ. The curves in Figs. 2 and 4 illustrate the manner in which α changes with μ for the systems defined by Tables I and II, respectively. Corresponding curves in Figs. 1 and 3 illustrate the variation of $(1-\alpha)/\alpha$ with μ. Line A_0 in Fig. 1 and line B_0 in Fig. 3 show the plots obtained by Eq. 14.

1) Effect of i_t.—The effect of the magnitude of i_t was examined when K_I^* is much smaller than K_Y^*. From Fig. 1 it is seen that the deviation of the approximate equation from the general equation becomes greater at higher indicator concentration. Therefore, it may be concluded that in order to estimate μ with precision of 1%, the molarity of the indicator must be ten times smaller than $1/K_I^*$ in numero. Fig. 2, which represents actual behavior of photometric titration curve, shows ambiguous end point at higher indicator concentration.

2) Effect of K_Y^*. — The effect of the magnitude of K_Y^* was examined when the

TABLE I

Curve	$m_t\times10^2$	$i_t\times10^5$	$K_I^*\times10^{-4}$	$K_Y^*\times10^{-12}$
A_1	1/3	3	1/8	4
A_2	1/3	30	1/8	4
A_3	1/3	300	1/8	4

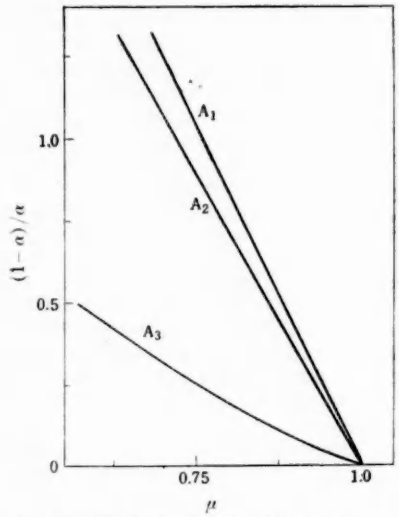

Fig. 1. Variation of $(1-\alpha)/\alpha$ with μ for the systems defined by Table I.

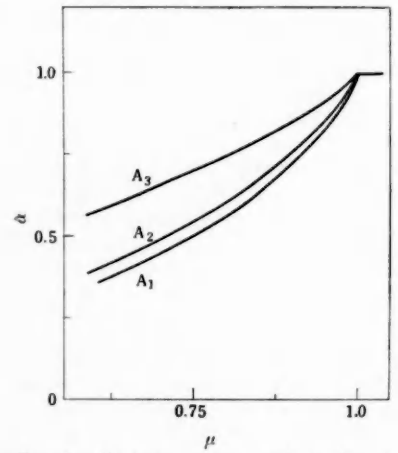

Fig. 2. Variation of α with μ for the systems defined by Table I.

TABLE II

Curve	$m_t\times10^2$	$i_t\times10^5$	$K_I^*\times10^{-4}$	$K_Y^*\times10^{-5}$	$\log\left(\frac{K_Y^*}{K_I^*}\right)$
B_1	1/3	3	1/8	1/8	1
B_2	1/3	3	1/8	10/8	2
B_3	1/3	3	1/8	100/8	3

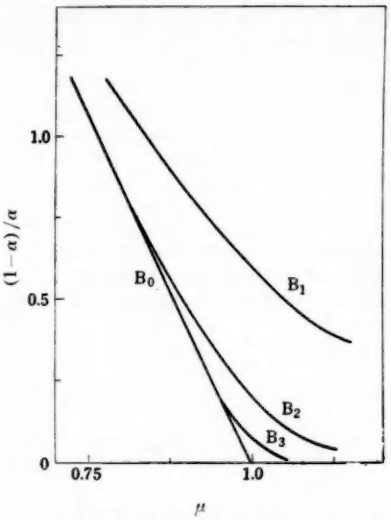

Fig. 3. Variation of $(1-\alpha)/\alpha$ with μ for the systems defined by Table II.

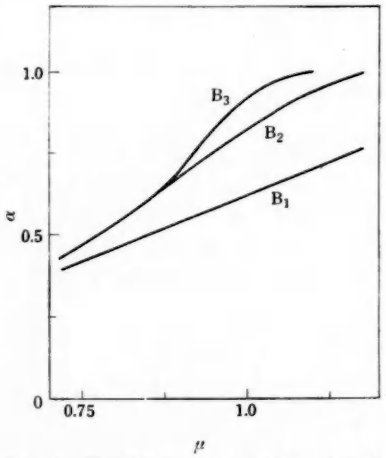

Fig. 4. Variation of α with μ for the systems defined by Table II.

molarity of the indicator was ten times smaller than $1/K_I^*$ in numero. From Fig. 3 it is seen that the deviation of the approximate equation from the general equation becomes larger as the value of $\log(K_Y^*/K_I^*)$ decreases.

In a usual plot of the titration curve (Fig. 4), the end point can be accurately determined only when $\log(K_Y^*/K_I^*)$ is larger than 4. However, if $(1-\alpha)/\alpha$ is plotted against μ (Fig. 3), the end point can be determined through extrapolation even when $\log(K_Y^*/K_I^*)$ is equal to 2 (curve B_2).

3) Slope of the line expressed by the approximate equation.—It is seen from Eq. 14 that the slope of the line expressed by the approximate equation is proportional to the product of m_t and K_I^*. Accordingly, in case of titration where Eq. 12 is well established, the apparent indicator constant can be estimated from the slope of the line expressed by this equation.

Experimental

In order to test the applicability of the linear plot described above, the following titrations were investigated:

1) Micro-titration of calcium at pH 12 using Murexide indicator, as an example of lower concentration of metal ion.

2) Titration of calcium at pH 10 using EBT indicator, as an example of lower value of K_I^*.

3) Titration of magnesium at pH 10 using EBT indicator, as an example of the case where value of log (K_Y^*/K_I^*) is smaller than 3.

Apparatus.—Yanagimoto Photometric Titrator Model PT-1 and Yanagimoto pH meter were used.

Reagents.—All chemicals used were the reagent grade. Standard solution of calcium was prepared by dissolving calcium carbonate (dried at 110°C), in dilute hydrochloric acid and diluting it with distilled water. Standard solution of magnesium was prepared by dissolving magnesium sulfate heptahydrate in distilled water and its concentration was gravimetrically determined with oxine[3]. Standard solution of Complexon-III was prepared by dissolving disodium ethylenediaminetetraacetate dihydrate in distilled water to produce approximately 0.01 M solution. Murexide indicator solution was prepared by shaking 40 mg. of the dye with 10 ml. of distilled water and 2 ml. of its supernatant was used. This solution was prepared daily. EBT indicator solution was prepared by dissolving 0.5 g. of Eriochrome Black T and 4.5 g. of hydroxylamine hydrochloride in 100 ml. of ethanol and its 0.5 ml. was used. This solution was stable for at least 5 months. For the adjustment of pH of the solution to 10 and 12, 1 N ammonium chloride-ammonia buffer solution and 1 N sodium hydroxide solution were used, respectively.

Procedure.—An aliquot of sample solution and a few ml. of buffer solution were placed in the titration cell and diluted to 50 ml. with distilled water. Appropriate wave-length was set and the absorbancy scale was adjusted to zero with slit. The indicator solution was pipetted into the titration cell and then titration was carried out. Absorbancies were recorded at the beginning of titration and at every 0.05 ml. of the titrant added during the titration, until the constant value of absorbancy was obtained.

Results and Discussion. — *Titration of calcium at pH 12 using Murexide indicator.*—Absorbancy measurement was made at 580 mμ. In this titration system, the values of log K_Y^* and log K_I^* are 10.5 and 5.0, respectively[4]. Although the value of log (K_Y^*/K_I^*) is sufficiently large, the photometric titration curve (Fig. 6) is somewhat round near the equivalence point, owing to the lower concentration of the calcium ion in the titration system. The plot of $(As_1-A_s)/(A_s-As_{M1})$ against the volume of the titrant added (Fig. 5) gives a straight line, the intercept of which corresponds to the equivalence point. The

TABLE III

RESULTS OF PHOTOMETRIC TITRATION OF CALCIUM AT pH 12 WITH 0.01 M COMPLEXON-III USING MUREXIDE INDICATOR

Calcium taken, mg.	Titrimetric end point, ml.	Calcium found, mg.	Error %
0.50_7	1.26_6	0.50_7	0
0.50_7	1.26_6	0.50_7	0
1.01_8	2.54_0	1.01_8	0
1.01_8	2.54_0	1.01_8	0
1.28_7	3.16_0	1.26_7	−1.6
1.28_7	3.18_5	1.27_6	−0.7

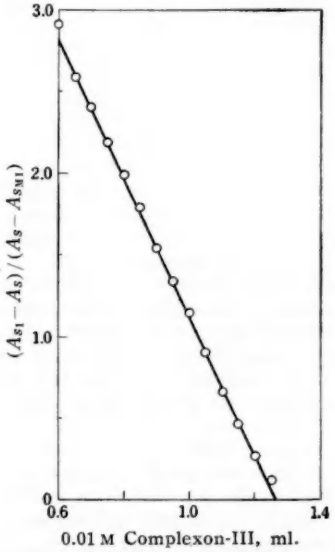

Fig. 5. Plot for titration of 0.50_7 mg. of calcium at pH 12 with Complexon-III using Murexide indicator.

3) F. P. Treadwell and W. T. Hall, "Analytical Chemistry", Vol. II, (9th ed.), John Wiley and Sons, New York, (1942) p. 259.

4) G. Schwarzenbach, "Die komplexometrische Titration", Ferdinand Enke Verlag, Stuttgart, (1956) pp. 7, 31 and 36.

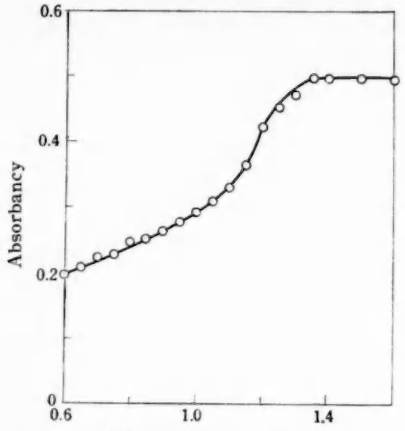

0.01 M Complexon-III, ml.

Fig. 6. Titration curve of the same titration as in Fig. 5.

results given in Table III show that the titration can be carried out with high precision.

Titration of calcium at pH 10 using EBT indicator. — In this titration system, the values of $\log K_Y^*$ and $\log K_I^*$ are 10.2 and 4.03, respectively[4]. Visual titration of this system fails owing to the ambiguous color change at the end point. Even by a photometric technique, the titration curve at 545 mμ (Fig. 8) does not give a sharp end point since the value of $\log K_I^*$ is too small. However, the plot of $(As_I - A_s)/(A_s - As_{MI})$ against the volume of the titrant added (Fig. 7) gives a straight line, the intercept on the V-axis representing the equivalence point. The results given in Table IV show that precisions of the order of a few tenths of one per cent were obtained in most instances.

Titration of magnesium at pH 10 using EBT indicator. — In this titration system, the values of $\log K_Y^*$ and $\log K_I^*$ are 8.5 and 5.44, respectively[4]. The value of $\log (K_Y^*/K_I^*)$ is about 3, so that the photometric titration curve at 545 mμ (Fig. 2 in the previous communication[2]) shows some rounding near the equivalence point. However, the plot of $(As_I - A_s)/(A_s - As_{MI})$ against the volume of the titrant added gives a straight line, the intercept on the V-axis representing the equivalence point (Fig. 1 in the previous communication[2]). The results (Table I in the previous communication[2]) show that the titration was carried out with precision of about 1%.

TABLE IV

RESULTS OF PHOTOMETRIC TITRATION OF CALCIUM AT pH 10 WITH 0.01 M COMPLEXON-III USING EBT INDICATOR

Calcium taken, mg.	Titrimetric end point, ml.	Calcium found, mg.	Error %
1.01_8	2.55_2	1.02_3	+0.5
1.01_8	2.53_0	1.01_4	−0.4
1.01_8	2.55_2	1.02_3	+0.5
1.01_8	2.55_0	1.02_2	+0.4

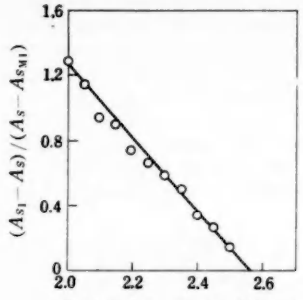

0.01 M Complexon-III, ml.

Fig. 7. Plot for titration of 1.01_8 mg. of calcium at pH 10 with Complexon-III using EBT indicator.

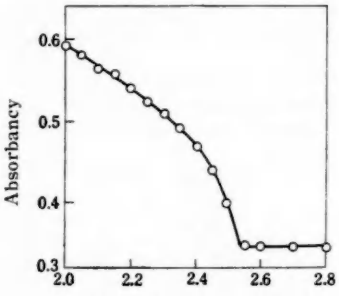

0.01 M Complexon-III, ml.

Fig. 8. Titration curve of the same titration as in Fig. 7.

Apparent indicator constant.—It was previously pointed out that the apparent indicator constant would be estimated from the slope of the linear plot of $(As_I - A_s)/(A_s - As_{MI})$ against the volume of titrant added. The values of $\log K_I^*$ obtained in the above titrations are given in Table V and compared with those described by Schwarzenbach[4](given in the fifth column in Table V). It is seen that there are considerable discrepancies between them. These discrepancies may be due to the differences in ionic strength and temperature and also to some unknown factor such as the influence of buffer components in the equilibria.

TABLE V
VALUES OF LOGARITHM OF APPARENT INDICATOR CONSTANT FOR CALCIUM AND MAGNESIUM

Metal ion	pH	Indicator	$\log K_1^*$ Values obtained	$\log K_1^*$ Values reported
Calcium(II)	12	Murexide	4.3_9	5.0
Calcium(II)	10	EBT	4.0_3	3.84
Magnesium(II)	10	EBT	5.2_8	5.44

Determination of calcium and magnesium in their mixture.—Total amount of calcium and magnesium in their mixture was titrated at pH 10 with standard Complexon-III solution using EBT indicator. Absorbancy measurements were made at 545 mμ. with another aliquot of the sample solution, magnesium was masked by sodium hydroxide and calcium was titrated at pH 12 using Murexide indicator. Absorbancy measurements were made at 580 mμ. The amount of magnesium was calculated by their differences. The linear plots obtained in the titrations of total calcium and magnesium and of calcium give the same pictures as obtained in 3 and 1, respectively. The results are tabulated in Table VI.

TABLE VI
RESULTS OF TITRATION OF CALCIUM AND MAGNESIUM IN THEIR MIXTURE WITH 0.01 M COMPLEXON-III

Calcium, γ			Magnesium, γ		
taken	found[a)]	deviation	taken	found[b)]	deviation
513	507	−2	254	256	+2
203	203	0	254	249	−5
203	203	0	508	507	−1

a) Each value is the average of three separate determinations.
b) Each value was calculated from the difference between the average of the volume of titrant for total and that for calcium in three separate titrations.

Department of Applied Chemistry
College of Engineering
University of Osaka Prefecture
Sakai, Osaka

Vapor Pressures of Molecular Crystals. XIV[1]. *Sulfamide and Diacetylhydrazine*

By Sadao TAKAGI*, Ryuichi SHINTANI, Hideaki CHIHARA and Syûzô SEKI

(Received August 7, 1958)

The energy of the hydrogen bond can be determined by various methods in vapor, liquid, solution, and crystalline solid. All but one method, that have been reported by the authors and other investigators in cases of liquids and crystals, estimate the energy from the temperature variation of the equilibrium constant for the association-dissociation equilibrium due to hydrogen bonding in vapor or in solution state. Those determinations, however, can not be correlated with the so-called hydrogen bond distances with only one exception for the case of gaseous carboxylic acid dimers, the structure of which could be determined by means of the electron diffraction technique. On the other hand when we deal with crystalline solids, it is possible to determine the hydrogen bond distance by the X-ray investigation although we can not obtain the state, in which only the hydrogen bond ceases to act, other forces such as the dispersion forces and the dipolar forces being unchanged. Usually the compromise has been adopted that the contributions other than the hydrogen bond to be subtracted from the total lattice energy may be estimated by one of the following

1) The Report XIII may be found in This Bulletin, **32**, 84 (1959).

* Present address: The Institute of Polytechnics, Osaka City University, Minami-Ogimachi, Osaka.

2) I. Nitta, S. Seki and K. Suzuki, This Bulletin, **24**, 63 (1951).

two methods: (1) the dispersion energy is calculated by using the interatomic distances and the atomic polarizabilities, and the electrostatic energy by assuming the electron density on each atom; (2) the dispersion and the electrostatic energies of the hydrogen-bonded crystal are substituted by the heat of sublimation of the crystal that is isoelectronic with the crystal in question but that possesses no hydrogen bond between molecules[2].

We have here chosen sulfamide and diacetylhydrazine as compounds having NH···O hydrogen bonds in crystals, whose structures were determined[3,4], and we have applied the former method of obtaining the energies of hydrogen bonds.

Experimental

Materials.—Sulfamide $(NH_2)_2SO_2$ was prepared by Goehring's method from liquid ammonia and sulfuryl chloride[5], and purified by fractional sublimation in high vacuum, m. p. 91.9°C (*Anal.* found S 32.84% and N 28.45%.) Diacetylhydrazine $CH_3COHN\text{-}NHCOCH_3$ was supplied by Miss A. Yamaguchi of the University of Tokyo*. This was recrystallized from aqueous solution and dehydrated** and sublimed in high vacuum; m. p. 123°C. The crystal modifications of both substances were checked against the reported crystal structures by X-ray diffractometer.

Apparatus.—The vapor pressures were measured with the apparatus already reported elsewhere[1] except for minor alterations. In the experiments with diacetylhydrazine, it was found that effused vapor condensed on the quartz helical balance which was kept at room temperature, causing a considerable error in the determination of the weight changes. In order to remove this difficulty the balance container was heated with a ribbon heater from outside the glass tubing to maintain the temperature of the balance at about 70°C. The treatment of the quartz balance with dimethyldichlorosilane vapor was also useful in preventing condensation of diacetylhydrazine.

Results and Discussion

The vapor pressures are listed in Table I for both sulfamide and diacetylhydrazine. The experimental values are well reproduced by the equations,

$$\log P = 11.047 - (5300.4/T) \quad \text{(sulfamide)}$$

and

$$\log P = 12.1947 - (5384.4/T) \quad \text{(diacetylhydrazine)}$$

The heat, entropy and free energy changes of sublimation computed by these equations are given in Table II.

TABLE I

VAPOR PRESSURES OF SULFAMIDE CRYSTAL

T°K	P(mmHg)$\times 10^5$	T°K	P(mmHg)$\times 10^5$
347.8_9	6.370	352.7_5	10.43
348.7_0	7.017	354.7_8	12.81
349.7_4	7.960	357.7_9	17.04
350.7_8	8.671		

VAPOR PRESSURES OF DIACETYLHYDRAZINE CRYSTAL (ANHYDROUS)

T°K	P(mmHg)$\times 10^4$	T°K	P(mmHg)$\times 10^4$
342.3_9	2.876	349.6_2	6.100
343.4_8	3.269	350.6_8	6.913
344.9_4	3.946	352.2_5	8.046
347.3_6			

TABLE II

HEATS, ENTROPIES AND FREE ENERGIES OF SUBLIMATION

	ΔH (kcal./mole)	ΔS (cal./deg. mole)	ΔG at 298.16°K (kcal./mole)
Sulfamide	24.25±0.24	37.26±0.68	13.11±0.31
Diacetylhydrazine	24.63±0.39	42.60±1.13	11.93±0.51

The heat of sublimation here obtained may be safely regarded as the lattice energy of the crystal*.

Calculation of the energies of the NH···O hydrogen bonds.—*a) Sulfamide.*—The calculation of the dispersion energy was made by the same procedure as was reported earlier[2]. The summation of r^{-6} (r: interatomic distance) for nonbonded pairs of atoms or atomic groups within 10 Å from a 'central atom' is shown in Table III, which was obtained on the basis of the atomic

TABLE III

SUMMATION FOR SULFAMIDE

Non-bonded pairs	$\sum(1/r^6)\times 10^6$ in Å^{-6}
S∼S	906.63
NH_2∼NH_2	7367.64
O∼O	5962.20
S∼NH_2	6006.26
S∼O	5002.95
NH_2∼O	14792.97*

* The hydrogen-bonded pairs were excluded.

3) K. N. Trueblood and S. W. Mayer, *Acta Cryst.*, **9**, 628 (1956) (sulfamide).

4) R. Shintani and I. Nitta, read before the 4th International Congress of Crystallography, July 1957 (Montreal, Canada); A full paper will be published in *Acta Cryst.* or elsewhere (diacetylhydrazine).

5) M. Goehring, J. Heinke, H. Malz and G. Ross, *Z. anorg. u. allgem. Chem.*, **273**, 200 (1953).

* The authors are indebted to her for her kindness.

** The monohydrate of diacetylhydrazine is more stable than the anhydrous form at room temperature and humidity.

* Association in vapor can be ignored as the vapor pressure is very low.

parameters determined by Trueblood and Mayer[3]. The atomic polarizabilities were calculated from the molecular refractions R_D for O (in a carbonyl), NH_2 (in a primary amine) and SO_2 (in dialkyl sulfate) compiled by Vogel[6]. The static polarizabilities given in Table IV have been corrected for the dispersion effect by subtracting 3% from the values for the NaD light[7]. The dispersion energy was then computed by using the Slater-Kirkwood formula[8] by summation within the 10 Å sphere and by integration outside that sphere. The summation part contributed 13.71 kcal and the integration part contributed 0.014 kcal. to the dispersion energy. The number of terms included in the summation was 1128. The dipolar interaction energy in sulfamide was obtained by summing up the contribution from each pair of molecules in the crystal by using the value of the dipole moment 3.9 D[9]. The dipolar energy contribution within the 10 Å sphere amounted only to 2.87 kcal. and this was taken as the total electrostatic energy as the integration diverges. The hydrogen bond energy was set equal to the difference between the observed lattice energy and the sum of the dispersion and electrostatic energies; $24.25-(12.08+2.9)=9.30$ kcal./mole. There are two NH···O hydrogen bonds per molecule of sulfamide and therefore the energy of a hydrogen bond is 4.6_5 kcal./mole. Omission of the repulsive potential energy in the calculation may be partly justified by the fact that in many molecular crystals the Margenau potential of r^{-8} factor nearly cancels out the repulsive contribution[10].

TABLE IV

STATIC POLARIZABILITIES

	No. of outer shell electrons	Static polarizability
S	6	1.382×10^{-24} cc.
O	6	0.8162 〃
NH_2	7	1.707 〃

b) Diacetylhydrazine. — The summation of r^{-6} and the static polarizabilities are given in Tables V and VI. The dispersion energy is 19.30 kcal./mole for summation within the 10 Å sphere (1064 terms) from "central atoms" and 0.39 kcal./mole for integration outside the sphere. The electrostatic contribtion to the total lattice energy was calculated by point charge model with unbalanced charges on C and O atoms, $\pm2.002\times10^{-10}$ c. g. s. e. s. u., estimated from the bond moment of C=O 2.50 D and the bond length 1.249 Å. The resultant energy was 1.15 kcal./mole, being repulsive. The total hydrogen bond energy is then about 6.06 kcal./mole or 3.03 kcal./mole for each bond.

TABLE V

SUMMATION FOR DIACETYLHYDRAZINE

Non-bonded pairs	$\Sigma(1/r^6)\times10^6$ in Å^{-6}
NH∼NH	4286.9
C∼C	3674.0
O∼O	5361.7
CH_3∼CH_3	4126.3
C∼O	11359.2
CH_3∼O	8470.5
NH∼O	9038.3*
C∼CH_3	5110.5
C∼NH	6778.2
CH_3∼NH	3455.5

* H-bond pairs were excluded.

TABLE VI

STATIC POLARIZABILITIES

	No. of outer shell electrons	Polarizability
O	6	$0.816_2\times10^{-24}$ cc.
C	4	1.60 〃
CH_3	7	1.89 〃
NH	6	1.61 〃

Comparison of the energy of NH···O hydrogen bond.—In Table VII are summarized the energies of NH···O hydrogen bonds in crystals hitherto reported. In general the NH···O energies fall in a range of values between 3 and 6 kcal. and are in comparable magnitude with the energies of OH···O bands. However, from the point of view that the energy should decrease with increasing length of the bond, it seems hopeless to correlate the energies with the bond lengths in Table VII. This is partly due to the difference of the method of evaluation of the energy and partly due to relatively small contribution of hydrogen bonding forces to the total lattice forces. The situation is in a sense analogous to the evaluation of the resonance energy of conjugated molecules from the experimental heat of formation and the energy of a Kekulé structure.

6) A. I. Vogel, *J. Chem. Soc.*, **1948**, 1833; see also J. R. Partington, "An Advanced Treatise of Physical Chemistry", Vol. IV, Longmans, London (1953), p. 50.

7) S. Seki and H. Chihara, *Sci. Papers Osaka University*, No. 1 (1949).

8) J. C. Slater and J. G. Kirkwood, *Phys. Rev.*, **87**, 684 (1931).

9) G. Devoto and R. D. Nola, *Gazz. chim. ital.*, **63**, 495 (1953); The gaseous dipole moment of $SO_2(CH_3)_2$ is 4.41D and thus it was assumed that the effect of association of sulfamide in dioxane solution would be small.

10) I. Nitta and S. Seki, *J. Chem. Soc. Japan, Pure Chem. Sec.* (*Nippon Kagaku Zasshi*), **64**, 475 (1943).

TABLE VII
ENERGY OF HYDROGEN BONDS

Crystal	N···O length	Energy in kcal./bond	Method	Reference
Diketopiperazine	2.88	5.3	**a**	i
Diformylhydrazine	2.788	6.1	**a**	ii
δ-Valerolactam	—	(7.2)*	**a**	ii
ε-Caprolactam	—	(7.0)*	**a**	ii
Oxamide	—	(4.2)*	**a**	ii
Acetamide	2.89, 2.99	3.0	**a**	ii
Urea	2.99, 3.04	3.5	**a**	ii
Sulfamide	3.02	4.7	**b**	iii
Diacetylhydrazine	2.875	3.0	**c**	iii

i: S. Seki, K. Suzuki and T. Koide, *J. Chem. Soc. Japan, Pure Chem. Sec.* (*Nippon Kagaku Zasshi*), **77**, 346 (1956).
ii: K. Suzuki, S. Onishi, T. Koide and S. Seki, This Bulletin, **29**, 127 (1956).
iii: Present study.
a: Subtraction of the heat of sublimation of the isoelectronic compound possessing no dipole moment.
b: Calculation of the dispersion and the electrostatic energies by use of theoretical formulae (point dipole model).
c: Calculation of the dispersion and electrostatic energies by use of theoretical formulae (point charge model).
* It is uncertain how many bonds there are per molecule.

The method **a** gives the hydrogen bond energy in which the energy required for the rearrangement of molecules from the structure of the isoelectronic crystal to the hydrogen-bonded structure is included. This rearrangement energy is quite analogous to the compression energy[11] and should differ from compound to compound. Thus this type of hydrogen bond energy does not represent the energy localized in the hydrogen bond but includes all the contributions to the change in the lattice energy that would be needed if the hydrogen-bonded structure were transformed into a non-bonded structure, i.e. the energy localized at the hydrogen bonds, the energy of electronic rearrangement within a molecule to make it non-polar within the crystal lattice and the energy for the change of crystal structure[12]. In other words, such "hydrogen bond energy" is a measure of how much gain in stability would result in a crystal as a whole by forming the hydrogen bonds compared with a hypothetical non-bonded structure.

The methods **b** and **c** are less unambiguous than the method **a** in that the former give the energy values in the approximation, the origin of which is less obscure. The estimation of the electrostatic energy is always a hard thing to do correctly; the point dipole model would be a very rough approximation in short-range interaction as in crystals and the charge distribution in crystal is rarely known except in cases of fully refined analysis of the crystal structures. Although the resultant contribution of the electrostatic energy to the total lattice energy is usually small, it is still so large as to affect the hydrogen bond energy value significantly.

The precision with which the dispersion energy is estimated by use of the Slater-Kirkwood formula depends primarily on the choice of the values for the static polarizability of atoms or atomic groups. We have some ground for believing that the calculated dispersion energy is a good measure to the actual interaction energy because we obtained relatively good agreement with the experimental heats of sublimation of nonpolar compounds as is shown in Table VIII. The difference between the calculated and the observed energies still amounts to a few kcal./mole which can not be ignored in comparison with the energy of a hydrogen bond. It may be concluded that the method of evaluating the energy of hydrogen bonds by subtracting contributions of other sources than the hydrogen bonds from the total lattice energy may be applied only to those crystals in which the hydrogen bonding plays an overwhelmingly important role in determining the crystal structure such as ice.

11) C. A. Coulson, "Valence", Clarendon Press, Oxford (1953), p. 236.
12) H. Chihara, *J. Japanese Chem.* (*Kagaku no Ryoiki*), **10**, 31 (1956).

TABLE VIII

CALCULATED AND OBSERVED LATTICE ENERGIES OF NONPOLAR COMPOUNDS (kcal./mole)

	Calculated	Observed	Reference
Tin tetraiodide SnI_4	20.6	18.1	(10)
Titanium tetraiodide TiI_4	16.4	14.9	(10)
Iodine, I_2	15.5	14.8	(10)
Benzene, C_6H_6	10.7	9.2	(13)
Naphthalene, $C_{10}H_8$	18.2	15.9	(10)
Anthracene, $C_{14}H_{10}$	27.2	22.8	(10)
Hexamethylbenzene $C_6(CH_3)_6$	19.4	19.3	(7)

The lattice forces in relation to the crystal structure.—Only one of two hydrogen atoms in each NH_2 group participates in hydrogen bonding in sulfamide crystal. The closest approach between molecules is through the hydrogen bonds but their distance is longer than in diformlyhydrazine. Diformylhydrazine is probably the crystal possessing the shortest NH···O hydrogen bonds (2.788Å) ever known* and its closest approach in the crystal is through hydrogen bonds and not at the contact CH ···O between neighboring molecules (the non-bonded closest distance CH···O is 3.69 Å, which is longer than the sum of the van der Waals radii 3.4 Å). Therefore the equilibrium distance in the system NH···O would be 2.788 Å**. In sulfamide also, there is nothing hindering the neighboring molecules from approaching nearer and nevertheless its hydrogen bond is longer than in diformlyhydrazine. This may be explained by the difference in electronic configuration in these two compounds. In fact the infrared absorption spectrum of sulfamide, recorded with Hilgar Model H800 spectrometer, showed NH stretching absorptions at 3338 and 3248 cm^{-1} by the Daifloil mull method in comparison with about 3100 cm^{-1} in diformylhydrazine[14].

Sulfamide is a polar crystal with parallel orientation of molecular dipoles in the direction of the *c* axis. This may plausibly give rise to the spontaneous polarization of the crystal unless twinning masks the effect. An estimation of the spontaneous polarization gives about 44226 e. s. u. by using the dipole moment 3.9 D. This is surprisingly large polarization being in comparable magnitude with the case of ferroelectric barium titanate $BaTiO_3$ (the saturation polarization 48000 e. s. u.). The measurement of the polarization should give the value of the dipole moment of a molecule in the crystal, and a study along this line is now going on.

The heat of sublimation of diacetylhydrazine is by about one kcal./mole smaller than would be predicted by the additivity of lattice energies; the heat of sublimation of diformylhydrazine is 24.1 kcal./mole and an increment of about one kcal./mole may be predicted for the addition of a CH_2 unit*. The melting point 132°C and the density 1.35 are lower than 158°C and 1.59 of diformylhydrazine. Diacetylhydrazine is very hygroscopic and changes to the monohydrate in air under ordinary condition within an hour. Such properties are reflected on relatively weak hydrogen bonds in diacetylhydrazine. The fact that the electrostatic interaction is acting as repulsive** is somewhat surprising result

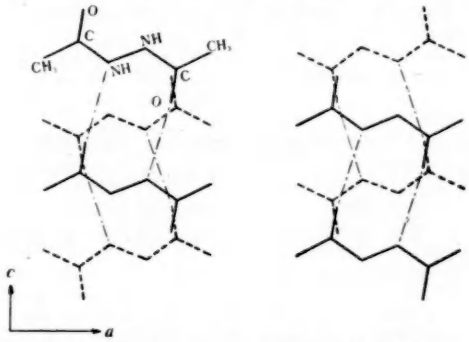

Fig. 1. The arrangement of diacetylhydrazine molecules projected along the *b* axis. Full line shows the molecules lying on *c* plane and dotted line shows molecules displaced halfway in *b*-direction. Hydrogen bonds are represented by chain lines.

13) J. H. de Boer, *Trans. Faraday Soc.*, **32**, 10 (1936).

* 2.75Å for NH···O bond was reported for amino acids or peptides (cf. H. L. Yakel and E. W. Hughes, *Acta Cryst.*, **7**, 291 (1954); R. A. Pasternak, L. Katz and R. B. Corey, ibid., **7**, 225 (1954)) but these are the bonds, N^+H···O^-, between zwitterions.

** In ice and in solid and gaseous hydrogen fluoride there is nothing that hinders the molecules from getting nearer excepthe inherent potential energy along the hydrogen bonds, so that the actual distances found 2.76Å and 2.55Å would correspond to the shortest approach in linear OH···O and FH···F systems, respectively, if other effects like conjugation do not greatly modify the electronic structure of the molecules. In other words the single minimum OH···O bond will not exist unless the hydrogen bond is very strongly conjugated with the molecular network.

14) T. Miyazawa, *J. Chem. Soc. Japan, Pure Chem. Sec.*, (*Nippon Kagaku Zasshi*), **76**, 341 (1955).

* Mr. Hiroshi Suga of our laboratory has found a lambda-type phase transition of diacetylhydrazine at about 50°C with the heat of transition of probably less than one kcal./mole. In comparing the heats of sublimation of these two compounds the heat of transition must be considered and then the discrepancy would be much smaller. This transition, however, does not affect much the discussion on the hydrogen bond energy.

** Solid carbon dioxide is another example of repulsive electrostatic energy.

in view that the molecules are packed in layers so that C=O bonds are directing antiparallel, one over another (see Fig. 1). This is only a deceptive appearance in the arrangement and actually the lattice is mainly constructed by the dispersion forces.

Summary

The vapor pressures of crystalline sulfamide and diacetylhydrazine were measured between 347°K and 358°K and between 342°K and 353°K, with the results, $\log P = 11.047 - (5300/T)$ and $\log P = 12.195 - (5384/T)$, respectively. The heats of sublimation were found to be 24.25±0.24 kcal./mole and 24.63±0.39 kcal./mole, respectively. The hydrogen bond (NH···O) energies were evaluated by subtracting from the observed heat of sublimation the contribution of the dispersion energy (by Slater-Kirkwood formula) and the contribution of the electrostatic interaction energy. The latter contribution was obtained by adopting the point dipole model with the dipole moment 3.9 D (for sulfamide) and by adopting the point charge model with the charges ±2.002 e.s.u. at C and O atoms diacetylhydrazine). The NH···O energies were 4.7 kcal. and 3.0 kcal., respectively. The electrostatic interaction in diacetylhydrazine is repulsive. Critical discussions are given on the significance of the hydrogen bond energy values obtained by various methods. The inter-relation between the lattice forces and the packing of molecules in the crystals is discussed on the basis of the calculation of separated contributions to the lattice energy and it is shown that the principal forces, acting between diacetylhydrazine molecules are the dispersion forces and the antiparallel arrangement of C=O dipoles in crystal is only a deceptive appearance. It is suggested that the nearest approaches in the linear systems OH···O and FH···F are 2.76 Å and 2.55 Å, respectively, unless very strong conjugation with the molecular network occurs. The NH stretching modes of vibration in sulfamide absorb at 3338 and 3248 cm^{-1}.

The authors wish to express their sincere thanks to Professor I. Nitta for his interest and encouragement during the present series of works. The cost of the research was partly defrayed by the financial support of the Ministry of Education to which their thanks are also due.

Department of Chemistry
Faculty of Science
Osaka University
Kita-ku, Osaka

Studies on the Graphitization II. Sub-structure and Crystallite Growth of Carbon Black

By Haruo KURODA and Hideo AKAMATU

(Received August 29, 1958)

The Graphitization is a process of crystallite growth and continuous improvement of the crystal structure of carbon to graphite with heat-treatment. The most powerful method of investigation is the X-ray diffraction by which not only the crystallite growth but also the ordering of crystal structure can be well defined[1].

In the previous paper[2], we have examined the graphitization of several kinds of carbon and found that petroleum-coke as well as coal-tar-coke are well graphitized, but carbon blacks are less graphitized with heat-treatment even in the same conditions. With heat-treatment up to 3000°C, the crystallites grow up to 444Å (L_a) for petroleum-coke and their lattice layers are stacked in graphitic orientation, while for Kosmos Carbon Black, for example, the crystallites grow to only

1) R. E. Franklin, *Acta Cryst.*, **3**, 107 (1950); **4**, 253 (1951); *Proc. Roy. Soc.*, **A209**, 196 (1951).
C. R. Houska and B. E. Warren, *J. Appl. Phys.*, **25**, 1503 (1954).
B. E. Warren, "Proceeding of 1st. and 2nd. Conference on Carbon", University of Buffalo, p. 49 (1956).

2) H. Akamatu, H. Inokuchi, H. Takahashi and Y. Matsunaga, This Bulletin, **29**, 574 (1956).

129Å and about 89 per cent of their layers still remains in disordered stacking. The strongest characteristic for carbon blacks is the fact that the crystallite growth does stop. L_a as well as L_c attain to a limited size respectively at about 2500°C, and these values depend on the original particle size of raw carbon blacks. It is widely known that the maximum value of layer diameter, L_a, is about one-third of the original particle size.

The results with both these cases of soft-cokes and carbon blacks, with violanthrone-coke and polyvinyl chloride-coke, show that there is a wide variety in graphitizability, and this should be attributed to the difference in micro-structures or sub-structures of these original cokes or carbons. In this paper, the sub-structures of carbon blacks and their change with heat-treatment will be discussed, from the results of investigation by means of X-ray small-angle scattering and electron microscopy. The sub-structures of soft-cokes will be discussed in the following paper.

Materials and Heat-Treatment.—Three kinds of commercial carbon black were used in the present investigation; Kosmos-15A (LFT, United Carbon Co.), Tokyo Gas Carbon (Tokyo Gas Co.) and Thermax (MT. Thermatomic Co.). The average particle size of Kosmos-15A is 400Å, that of Tokyo Gas Carbon 350Å, and that of Thermax 3000Å. The heat-treatment has been made in vacuo at several temperatures from 1000 to 3000°C. The data for crystallite size, by X-ray diffraction method, are summerized in Table I.

TABLE I

GROWTH OF CRYSTALLITE DIMENSION WITH HEAT-TREATMENT

	Temperature of H.T. (°C)	L_a(Å)	L_c(Å)
Kosmos-15A	original	33.6	15.9
	1570	50.4	19.1
	1750	56.3	27.8
	1960	68.8	34.0
	2500	124	44.6
	3000	129	44.7
Tokyo Gas	original	30.6	13.3
	1350	38.0	15.9
	1750	51.3	24.0
	2040	77.5	32.3
	2500	113	36.6
	3000	118	39.4
Thermax	original	38.5	17.0
	1500	47.5	20.2
	1900	78	73
	2500	326	152
	3000	320	177

The crystallite sizes are similar to one another in these original carbon blacks. This is the case even after being heat-treated below 2000°C. However, after being heated over 2000°C, where generally crystallite growth proceeds rapidly, the crystallite size of Thermax becomes much greater than that of the other blacks. The diffractometer records show that, for Kosmos and Tokyo Gas Carbon, (10) and (11)-diffraction still maintain the wedge-like profiles characteristic of the random orientation of layers even after heated to 3000°C, while for Thermax a remarkable modulation of the diffraction profile can be observed after being heated to 3000°C, and the ordering parameter shows that 50 per cent of layers are in the graphitic orientation.

X-Ray Small-Angle Scattering.—*Experimental.*—A X-ray small-angle scattering camera is designed[3] which consists of collimation system, specimen holder and camera body. The collimation system is made of metal tube with two apertures separated by 500 mm.. Several sizes of aperture are prepared; the smallest one is 0.09 mm. in width and 0.1 mm. in length. Each aperture is fixed on a holder which can be fitted to the collimator tube and is easily exchangeable with others without a rearrangement of setting. Thus we can use a selected pair of apertures. The specimen is packed into a circular cavity of 10 mm. diameter in a flat metal plate of 0.5 mm. thickness, and placed immediately behind the second aperture. The camera body is made of a metal tube with a film cassette at one end. The distance from specimen to film is 549 mm.. A beam stopper is placed in front of the film, the thickness of which is controlled so that the image of the direct beam can be registered faintly on the film. The apparatus is evacuated except for the specimen. Cu-K_α radiation filtered with a nickel foil is used.

About twenty diagrams are usually registered for each specimen, with various exposure times from 5 minutes to 20 hours and with different aperture sizes. Of a microphotometer trace, only a restricted range of the photographic density is used for an intensity curve, so that a linear relation can be assumed between the incident energy of X-rays and the corresponding photographic density. A series of intensity curves for each specimen are combined by graphical matching to a complete scattering angle.

Results.—The results for the heat-treated samples of Kosmos and Tokyo Gas Carbon are shown in Fig. 1 and Fig. 2, where the scattering intensity in logarithmic scale is plotted against the scattering angle.

The geometrical condition of our camera, using filtered X-rays, is not applicable to the correct investigation of a very small angle part. We omitted Thermax, since its particle size is too large and the

3) H. Kuroda, *J. Chem. Soc. Japan Pure Chem. Sec.* (*Nippon Kagaku Zasshi*), **77**, 1298 (1956).

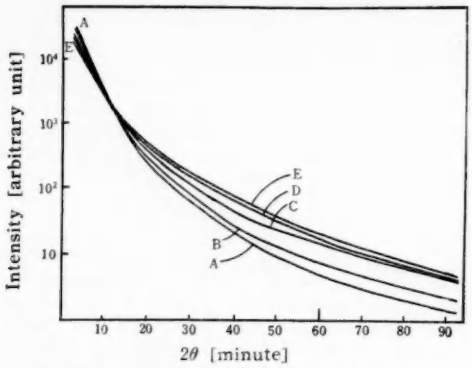

Fig. 1. Intensity curves of small-angle scattering by heat-treated Kosmos-15A Carbon Black.
(A) original, (B) 1325°C, (C) 1570°C, (D) 1950°C, (E) 2500°C.

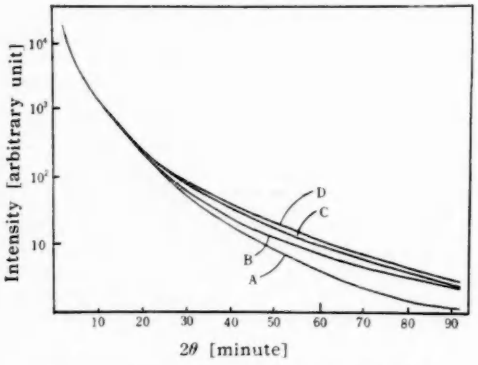

Fig. 2. Intensity curves of small-angle scattering by heat-treated Tokyo Gas Carbon Black.
(A) original, (B) 1350°C, (C) 2100°C, (D) 3000°C.

important part of scattering is presumed to be in such a very small angle part.

It can be seen in Fig. 1 and Fig. 2 that the intensity increases in higher angle part as the heat treatment temperature is higher, while in the lower angle part no remarkable change or slight decrease in intensity is observed. It can be assumed qualitatively that the scattering at a higher angle is due to smaller particles or heterogeneity of smaller dimension, and at lower angle due to larger particles or heterogeneity of larger dimension.

The X-ray small-angle scattering by raw carbon blacks has been discussed in a previous paper[4], where it has been reasonablly interpreted by Porod's theory[5]. According to this theory, a parameter called the distance of heterogeneity, l_c, can be known from the observed intensity curve by means of the following integration,

$$l_c = \pi \int_0^\infty h \cdot I(h) \cdot \mathrm{d}h \Big/ \int_0^\infty h^2 \cdot I(h) \cdot \mathrm{d}h$$

where $h = 4\pi \sin\theta/\lambda$ at scattering angle of 2θ, with X-ray wave length λ, and $I(h)$ is the intensity at h. There is the following relation between the distance of heterogeneity and the average diameter of particle,

$$D = \frac{4}{3} l_c$$

when the system consists of spherical particles and the inter-particle interference is absent.

It has been revealed that in the case of raw carbon blacks, the average diameter of particles estimated from the above relation is in good agreement with the particle size observed by electron microscope. This is the case also for untreated samples of Kosmos and Tokyo Gas Carbon. Therefore, in raw carbon blacks, the structural unit which is responsible for the greater part of the observed scattering is an individual carbon black particle which is observed directly by electron microscope. In consequence, one can assume that each particle is made of homogeneous material density. This is true, however, in the first approximation. According to the theory, the scattering intensity is expected to be proportional to h^{-4} in the higher angle region, when a system consists of particles of homogeneous density. In the case of raw carbon blacks, the region in which $h^4 I(h)$ is nearly constant is observed as seen on curve a in Fig. 3. However, this is realized only in a limited region below a certain scattering angle, and beyond this angle the intensity deviates from the prediction of the theory. This deviation in the higher angle region is presumablly due to the heterogeneity of electron density in a particle.

The change in the parameter l_c with heat-treated temperature is illustrated in Table II. The value of this parameter decreases as heat treated temperature increases. However, the geometrical significance of this parameter is not so simply

4) H. Kuroda, *J. Colloid Sci.*, **12**, 496 (1957).

5) G. Porod, *Kolloid-Z.*, **124**, 83 (1951); **125**, 51 (1952).

TABLE II
CHANGE IN DISTANCE OF HETEROGENEITY WITH HEAT-TREATMENT.

	Temperature of H.T. (°C)	l_c (Å)
Kosmos-15A	original	289
	1325	281
	1570	243
	1950	230
	2500	215
Tokyo Gas	original	261
	1350	232
	2100	216
	3000	208

interpreted as in the case of raw carbon blacks. The decrease in the size parameter can not be attributed to the shrinkage of carbon black particles, since their shape and size do not change appreciably, by electron microscope, below 2000°C, and so also the density even after being heated up to 3000°C.

In Fig. 3 the plot of $h^4I(h)$ versus h is shown. Although a horizontal part is realized for the untreated sample, the deviation from the constancy of $h^4I(h)$ becomes more and more serious as heat treated temperature is higher. This is presumably due to the advancement of heterogeneity in a particle. Thus, after being heated, the structure unit responsible for the observed scattering is not the individual particle, but the sub-structures which developed in the particle; the sub-structure made of crystallites which grow in the particle.

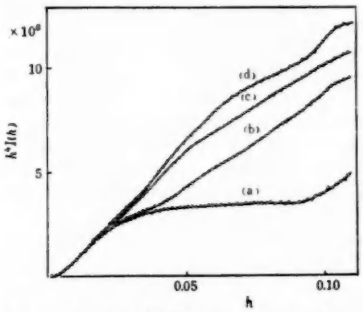

Fig. 3. Plot of $h^4I(h)$ versus h. Tokyo Gas Carbon Black.
(a) original, (b) 1325°C, (c) 2100°C, (d) 3000°C.

The distance of heterogeneity decreases as heat trated temperature is higher, while the crystallite size increases. Thus, at an extreme both these dimensions might approach each other. Neverthless, in reality they do not coincide with each other, since strong interference is likely to be present between crystallites.

In Fig. 4, $\log I(h)$ is plotted against $\log h$. On this curve, the inclination of the curve is illustrated, the value of which is around 2 or 3. This value indicates that the intensity of scattering by heated sample to above 2500°C is nearly proportional to the inverse of the second power of the scattering angle. It can be expected, when a system consists of plate-like particles, that the intensity will be proportional to the inverse of the second power of the scattering angle in a wide

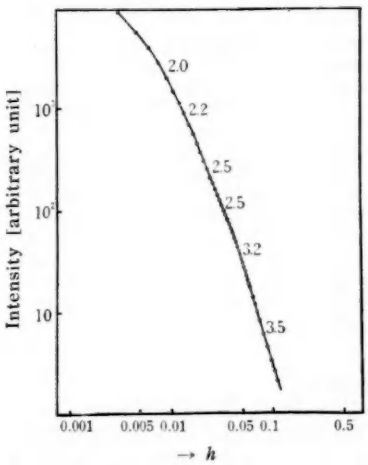

Fig. 4. Log $I(h)$ vs. Log h. Kosmos-15A heat-treated to 2500°C.

range[6]. One can conclude that the most part of the observed scattering for a heated sample above 2500°C is caused by crystallites which have a plate-like shape.

The results from X-ray small-angle scattering leads to the following conclusion. A particle of raw carbon black is made of nearly homogeneous density. With heat-treatment, sub-structures develop to plate-like crystallites; at an extreme, however, the carbon black particle does not grow to a large crystalline unit but splits into smaller crystalline units. These small crystallites are quite independent of each other, as each of them can be the center of scattering, but they are still in aggregation so tightly that interference between them is sure to be strong.

6) A. Guinier and G. Fournet, "Small-Angle Scattering of X-Rays" John Wiley, Chapt. 2, New York (1955).

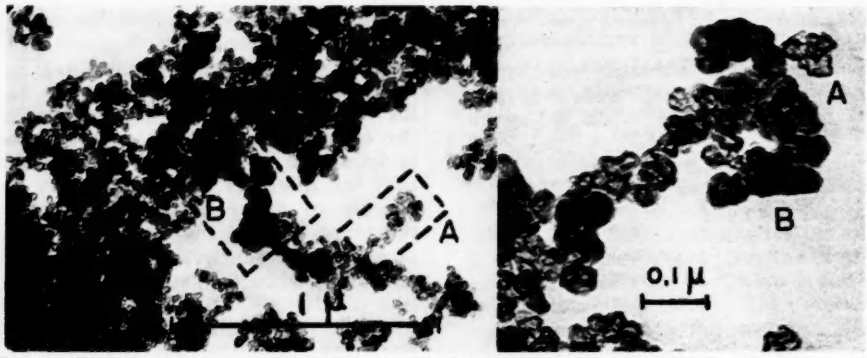

Fig. 5. Electron Micrograph of Tokyo Gas Carbon Black, heated to 3000°C. (Unshadowed).

Electron Microscopic Observation.— *Experimental.* — Electron micrographs were made with Hitachi Electron Microscope, Model-10-A. Special precautions are required to observe the details of structure, with high resolution as well as contrast, of such a minute particle as carbon black. Recently, Sakata[7] in our laboratory has developed a technique of making a collodion grid, whose pore size is one micron or less. This is called micro-grid. One can spread over a micro-grid a very thin collodion film, less than 50A in thickness. The specimen is mounted on this thin film. Thus, the undesirable effects from mounting the film is avoidable to a great extent. Experimental procedures were conducted so as to reduce the effects of contamination[8] to the minimum.

Results.—The electron micrographs show that the appearance of particles does not change appreciably when the heat treated temperature is lower than 2000°C; particles keep their spherical shape, the average size being similar to those of untreated carbon black. Only a slight change of contrast is seen in the inner part of images of particles. However, after being heated up to 2500°C, the particles suddenly show a completely different appearance. This will be seen in Fig. 5. In these figures, one can see two modes of particle shape. Some particles have very irregular contours and are transparent to an electron beam. These are shown in the region lettered A. Other particles have rather round outlines and are less transparent to an electron beam. These can be seen in the region lettered B. The particles of mode-A have plate-like shape with sharp edges. The particle size is nearly 100 A, which is comparable to the crystallite size determined from X-ray diffraction pattern. Each of these minute particles might be a crystallite. The particles of mode-B show a heterogeneity of density; the inner part is more transparent than the peripheral part, which suggests a hollow structure of particle. They consist of minute grains whose size is also comparable to the crystallite size. These facts indicate that a particle of mode-B is a shell-like cluster of crystallites, with a loose packing in the inner part. Such a structure is presumably not different from the structure of heat-treated Thermax. It can be easily presumed that particles of mode-A are produced by disintegration from particles of mode-B.

Thermax is most advantageous for electron microscopic observation, for the particle size is very large. The electron micrographs of heat-treated Thermax have been presented by Ragoss, Hoffman and Holst[9], and by Kmetko[10]. Kmetko has given a polyhedron model of graphitized carbon black particles, based on electron microscopic observation by replica technique. In the present investigation, we used a high accelerating potential, 10 kV, in operating the electron microscope. This gives a clear internal structure of particles. Some typical micrographs are illustrated in Fig. 6, 7 and 8.

Below 1500°C of heat treated temperature, no appreciable change can be seen. However, at this temperature, fine contrast is seen in the images. This fine contrast develops to dark radiated strips along the periphery of particle as heat treated temperature is higher. Finally, above 2500°C, the dark strips grow up to trigonal or trapezoidal dark patterns. The

7) S. Sakata, *J. Electronmicroscopy*, **6**, 75 (1958).
8) J. H. L. Watson, *J. Appl. Phys.*, **18**, 153 (1947).
9) A. Ragoss, U. Hoffman and R. Holst, *Kollod-Z.*, **105**, 118 (1943).
10) E. A. Kmetko, "Proceeding of 1st. and 2nd. Conference on Carbon," University of Buffalo, 21 (1956).

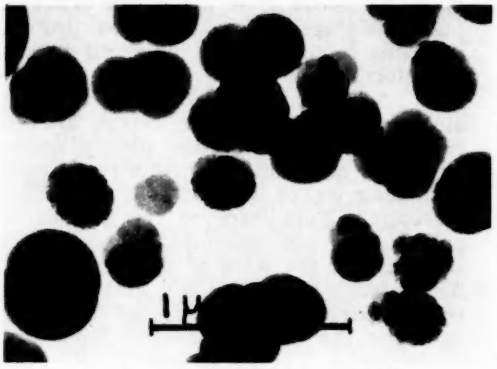

Fig. 6. Thermax heated at 1540°C.

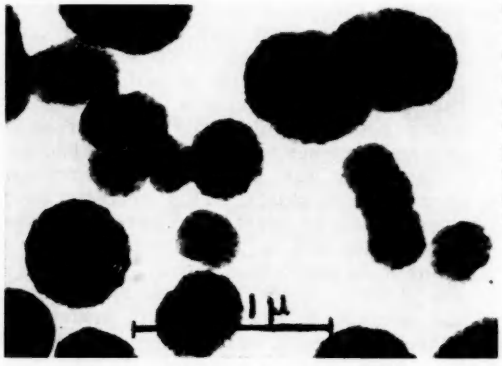

Fig. 7. Thermax heated at 1900°C.

bases of trigons or trapezoids coincide with the edges of the polygonal outlines of the particles. These dark patterns are not due to the difference in thickness of material, but are produced by the diffraction effect. This is illustrated in two micrographs (a) and (b) of Fig. 8. Both the micrographs were made from the same field, but made with different inclination to incident beam by 12°. The dark patterns in each particle change the shape, or disappear, depending sensitively on the direction of incident beam. This is indicated by arrows. It can be easily presumed that these dark patterns are due to (002)-diffractions by the graphite-like crystals. This leads to the conclusion that crystallites are orientated with their c-axes being in the direction normal to the particle surface. The length of edges of the polygonal outlines is in the order of 1000Å, which is only a few times that of L_a-dimension determined by X-ray diffraction. Therefore, the area corresponding to each dark pattern might be a single crystal or a cluster made of a few crystallites with a common direction of their c-axes.

Discussion

Carbon black is deposited from a gas phase in the process of incomplete combustion or thermal decomposition of hydrocarbon gas or vapor. The resulting solid

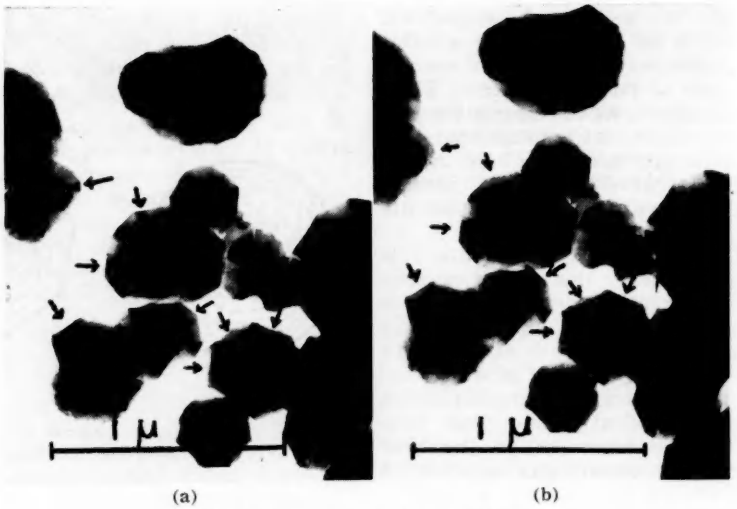

(a) (b)

Fig. 8. Thermax heated at 3000°C.
(a) and (b) were made from the same field with different directon to incident beam by 12°. The dark patterns in each images are slightly different in (a) and (b).

particles consist mainly of turbostratic carbon crystallites. However, the spheroidal shape suggests that the particles are in a fluid-state when they are produced at a higher temperature. The X-ray small-angle scattering by raw carbon black indicates that the material density is nearly homogeneous in the particle. The minute turbostratic crystallites may be imbedded among heavy hydrocarbon molecules or cross-linkages of disorganized carbon atoms. However, alignment of minute crystallites would not be at random, but may be in a preferential orientation. As this is due to the effective action of surface tension, which is responsible for the spheroidal shape, the preferential orientation should be most effectively conducted along the surface of the particle, with the basal planes of crystallites being tangent to the surface. Hall[11] found indications of such a preferential orientation at the surface of a raw carbon black. The schematic diagram of such a model is illustrated in Fig. 9, A.

In the process of heat-treatment, minute crystallites grow by the condensation process at the expense of the disorganized carbon atoms with liberating hydrogen. Meanwhile, the alignment of crystallites will be further improved. The crystallite growth proceeds mainly in such a way in an early stage of heat-treatment, presumablly below 1500°C. The rate of growth is not different between smaller particles and larger ones. No appreciable change can be seen in the particle shape nor size in electron micrographs, excepting a fine structure which can be seen in images of large particles of Thermax, which indicate rather clearly the preferential orientation of crystallites. The X-ray small-angle scattering can reveal the continuous development of heterogeneity which results from the crystallite growth.

When the heat treated temperature is over 2000°C, suddenly the rate of crystallite growth is greatly advanced. This is so, when the particle size is greater, while in small particles the growth attains very rapidly to a limited size. It is widely experienced that the degree of graphitization is primarily dependent on the peak temperature, but less dependent on the time of soaking. The remarkably accelerated rate of crystallite growth at the higher temperature demands an explanation other than the mechangism mentioned above.

At this stage, the condensation process has been completed, leaving slight defects or distortions between neighboring crystallites. As the crystallites are in such an alignment in that their c-axes are in nearly the same direction among neighbors, they can easily be further rearranged with their c-axes in completely the same direction. This leads to the growth of crystallites, not accompanied by mass transfer nor the work of breaking bonds. The intermediate state is a cluster. The rearrangement would be forced thermally to relax the stresses caused from the distortions.

At a temperature higher than 2000°C, a plastic deformation or creep is known for carbons, therefore, the thermal relaxation would be advanced only at a higher temperature. Mrozowski[12] proposed a driving force of the crystallite growth, which is the anisotropic expansion of crystallites along c-axes. This leads to the creation of local stresses which lead to and become relieved by the growth and rearrangement of crystallites. This process, however, would be practically effective if the crystallites are in alignment in such a manner as mentioned above. The crystallite growth would be accelerated along the surface of the particle in preference to the inner part, as the alignment would be found primarily along the surface. This is what we observed. Thus, the polyhedral particle will result from the preferential orientation of crystallites, which developed with their c-axes being in the direction of normal to the surface. The schematic diagram is given in Fig. 9, B.

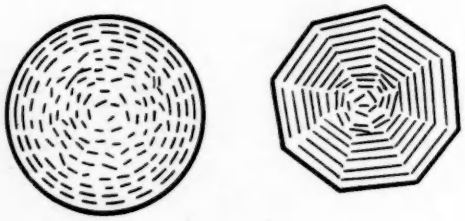

A B

Fig. 9. Schematic diagram of alignment of crystallites in a carbon black particle. (A) before heat-treatment, (B) after heat-treatment.

11) C. E. Hall, *J. Appl. Phys.*, **19**, 271 (1948).

12) S. Mrozowski, "Proceeding of 1st. and 2nd. Conferences on Carbon", University of Buffalo, 31 (1956).

As the crystallite growth proceeds in this way, however, the mutual relation between the neighbors becomes different from the alignment mentioned above. This is easily seen when one compares the diagram (A) with (B). Moreover, great stresses would be stored up between crystallites, especially when the anisotropic expansion of crystallites are made at a higher temperature. We observed, for Tokyo Gas Carbon heated to 3000°C, a remarkably asymmetrical profile of (002)-diffraction, which suggests the presence of a large distorsion in lattice.

In this stage, the scheme proposed by Mrozowski must be modified, but becomes rather more important. When the stresses become too great, they are not likely to be relieved practically and the rearrangements of crystallites are not likely to be realized. There is no place for the energy dissipation within the particle, and this is the characteristic for carbon blacks which differ from soft-cokes. This would be so, as the size or the mass of a particle is smaller. Thus, the limited size of crystallite growth would be proportional to the original particle size. The result which would be expected from the further heattreatment is disintegration or rather bursting into individual crystallites, as this is the only way to relieve the stored stresses. This is the case we observed in the case of the small particles of Kosmos-15A and Tokyo Gas Carbon Black.

As the crystallites grow by the mechanism discussed, the turbostratic structures still remain unimproved. It is believed that the crystallite growth proceeds in advance of ordering of crystal structure. The crystal structure will be improved by the rearrangement of layers as pairs of the nearest neighboring layers take on graphitic orientation. The mechanism would not be far from that discussed above. However, this process begins when the layer diameter, L_a reaches a value of about 150Å. For small particles, the growth of crystallites stops for the reason discussed above, even when less than 150Å. In consequence, the crystal structure can not be improved. This is the reason why one can not make graphitization of carbon blacks with small particle size. A similar argument can be extended to hard carbons. The graphitization is primarily dependent on the sub-structures of raw materials.

Summary

The sub-structures of carbon black and its change with heat-treatment have been investigated by means of X-ray small-angle scattering and electron microscopy.

With heat-treatment, the X-ray small-angle scattering intensity increases in the higher angle region, indicating the development of heterogeneous sub-structures to minute crystallites. Above 2000°C, the crystallite growth is rapidly accelerated, and at an extreme, a carbon black particle disintegrated to smaller crystalline units. Electron microscopic observations, especially for Thermax which has a large particle size, revealed that the crystallites are in alignment with their c-axes being in the direction of normal to the particle surface. This alignment leads to the polyhedral shape of the heat-treated particles. From these observations, the sub-structures and the mechanism of crystallite growth in carbon black particles have been discussed.

This investigation is a part of the research project for carbons, which is supported by Committee 117 in Nippon Gakujutsu Shinkokai, and the expense has been defrayed in part from a grant given by the Ministry of Education, for which the authors' thanks are due.

Department of Chemistry
Faculty of Science
University of Tokyo
Hongo, Tokyo

Polarographic Studies of Metallic Complexes. IV.[1] *Bisethylenediamine Series of Cobalt(III) Complexes*[2]

By Nobufumi MAKI, Yoichi SHIMURA and Ryutaro TSUCHIDA

(Received August 13, 1958)

There have been reported, heretofore, some polarographic studies on the ethylenediaminecobalt(III) complexes[3-10]. Holtzclaw et al.[3-5] studied several kinds of *cis*- and *trans*-bisethylenediaminecobalt (III) complex and found that the *trans*-isomer having two negative ligands in its coordination sphere exhibits a little more negative half-wave potential than the corresponding *cis*-isomer. This fact was explained as being due to the stabilization of the complex compound by the trans effect of the two negative ligands. On the other hand the *trans*-isomer containing one or two neutral ligands in its coordination sphere showed almost the same half-wave potential as the corresponding *cis*-isomer.

As regards the reduction wave of tris-ethylenediaminecobalt(III) ion, Kivalo[8] and Laitinen et al.[7] obtained the following results. The ion, $[Co\ en_3]^{3+}$, is reduced reversibly to $[Co\ en_3]^{2+}$ ion in the presence of an excess of 0.1~0.5 F ethylenediamine. ($E_{1/2} = -0.456$ V. vs. S.C.E) However, in the absence of an excess of ethylenediamine the irreversible wave of $[Co\ en_3]^{3+}$ was given. This fact was considered to be due to the following reason. The apparent irreversibility of the reduction is due to the aquation of the reduction product, or to the decrease in the coordination number of cobalt(II) complex ion, though the electron transfer reaction for $[Co\ en_3]^{3+} + e^- \rightarrow [Co\ en_3]^{2+}$ is fast enough to be reversible. While the reversible electrode reaction in the presence of excessive ethylenediamine was explained as being due to the existence of the stable ion, $[Co\ en_3]^{2+}$, which is in equilibrium with an excess of ethylenediamine, being different from the reduction product of hexamminecobalt(III) ion. The latter ion gave an irreversible wave, even if an excess of ammonia was present in solution.

However, Doležal[9] obtained a somewhat different result recently. Namely, his polarographic and oscillopolarographic studies showed that the redox system, $[Co\ en_3]^{3+}/[Co\ en_3]^{2+}$, is not perfectly reversible. It was found that the difference of the half-wave potentials between the anodic and the cathodic wave was 30 mV. under equal conditions. The dependence of the cathodic wave on the pH value of the solution and on the concentration of ethylenediamine and of gelatin was also different from that of the anodic wave. The anodic wave approaches reversibility more perfectly than the cathodic wave.

In the previous work of this series[1] the present authors determined the order of the polarographic stability for the cobalt (III) complexes of pentammine series, $[Co(NH_3)_5X]$. For the same purpose, a comparison of the half-wave potentials of the first waves has been carried out for the cobalt(III) complexes of bis-ethylenediamine series, $[Co\ en_2X_2]$ or $[Co\ en_2Y]$. The polarographic behavior of these complexes has also been dealt with in the present paper.

Experimental

Apparatus.—A Yanagimoto model 104 polarograph with the sensitivity of galvanometer of 2×10^{-9} A/mm./m. was used. For the accurate evaluation of curves and half-wave potentials the method described previously was used[10]. As an electrolysis cell an H-type vessel with a saturated calomel electrode was employed. The capillary used had a rate of flow of mercury, 0.615 mg./sec. and a drop time of 7.42~6.98 sec./drop in the solution of 0.5 F potassium sulfate and of 0.1 F potassium chloride at an open circuit with a mercury head of 65.5 cm.. The capillary was

1) Part III of this series; N. Maki, Y. Shimura and R. Tsuchida, This Bulletin, **32**, 23 (1959).
2) Presented in part at the Eleventh Annual Meeting of the Chemical Society of Japan, Tokyo, April 6, 1958.
3) H. F. Holtzclaw, Jr., *J. Am. Chem. Soc.*, **73**, 1821 (1951).
4) H. F. Holtzclaw, Jr. and D. P. Sheetz, ibid., **75**, 3053 (1953).
5) H. F. Holtzclaw, Jr., *J. Phys. Chem.*, **59**, 300 (1955).
6) J. B. Willis, J. A. Friend and D. P. Mellor, *J. Am. Chem. Soc.*, **67**, 1680 (1945).
7) H. A. Laitinen and M. W. Grieb, ibid., **77**, 5201 (1955).
8) P. Kivalo, ibid., **77**, 2678 (1955).
9) J. Doležal, *Coll. Czech. Chem. Communs.*, **21**, 113 (1956).
10) N. Maki, Y. Shimura and R. Tsuchida, This Bulletin, **30**, 909 (1957).

connected to the mercury reservoir by a tube of polyvinylchloride. All the measurements were made at 25±0.1°C, the temperature being maintained by a water thermostat. The reversibility of the electrode reaction was examined by determining the slope of $\log i/(i_d-i)$ vs. potential. Slopes of the log plots indicated irreversible reaction throughout.

Material.—The complex compounds studied were prepared by the method described in literature[11-27,30]. (The references are given in Tables I, II and III.) Each solution for the electrolysis was made freshly from the dry crystalline cobalt(III) complexes before use and the polarographic measurements were made as soon as possible after the removal of oxygen. The concentration of the solution was 0.001 gram complex ion per liter.

In order to remove the dissolved oxygen, a vigorous stream of nitrogen which was purified from oxygen by means of an alkaline solution of pyrogallol, was passed through the cell solution for an hour prior to each electrolysis, preventing the evaporation.

In order to compare the half-wave potentials with each other, no maximum suppressor was used, because its presence at the concentration which is enough to suppress the maxima of the second waves of bisethylenediaminecobalt(III) complxes, causes lowering of the diffusion current, shift of the half-wave potential of the first wave towards negative direction, and sometimes deformation of the wave. The supporting electrolytes used are 0.5 F potassium sulfate and 0.1 F potassium chloride.

Results and Discussion

In Tables I and II are shown the half-wave potentials of the cobalt(III) complexes of bisethylenediamine series.

All the compounds are reduced irreversibly in two steps at the dropping mercury electrode in the solution of 0.1 F potassium chloride or 0.5 F potassium sulfate except the case of the complexes which aquate easily in solution. The complex ions such as $[Co\ en_2S_2O_3]^+$, $[Co\ en_2gly]^{2+}$*, $[Co\ en_2leuc]^{2+}$* show two waves in 0.5 F potassium sulfate at the potential corresponding to the reduction of cobalt(III) → cobalt(II). The height of the second wave was very close to twice that of the first wave in the presence of Tween-80**, a maximum suppressor. The height of the first wave was proportional to the concentration of the complex ion in the range of the concentration $1\times10^{-2}\sim5\times10^{-4}$ F. In the case of the mixed solution of a complex ion and its aquated species, the total height of the waves of the original ion and of the aquated species was roughly proportional to the original concentration of the cobalt(III) complex. Hence, the first wave, corresponding to a gain of one electron, represents the reduction of cobalt(III) to cobalt(II) and the second, corresponding to two electrons, represents the reduction of cobalt(II) to metallic state.

In the solution of a non-complexing supporting electrolyte such as potassium chloride or potassium sulfate, the reduction processes of bisethylenediaminecobalt(III) complexes are considered to be in the following:

$$[Co\ en_2X_2]^{(3-2n)+}+e^-\rightarrow[Co\ en_2X_2]^{(2-2n)+}$$

$$[Co\ en_2X_2]^{(2-2n)+}+mH_2O\rightarrow$$

$$[Co\ en_2(OH_2)_2]^{2+}+2X^{n-}$$

$$[Co\ en_2(OH_2)X]^{(2-n)+}+X^{n-}$$

$$[Co\ en(OH_2)_4]^{2+}+2X^{n-}+en$$

etc., etc.

$$[Co\ en_2(OH_2)_2]^{2+}+2e^-\rightarrow Co+2H_2O+2en$$

$$[Co\ en_2(OH_2)X]^{(2-n)+}+2e^-\rightarrow Co+H_2O+X^{n-}+2en$$

$$[Co\ en(OH_2)_4]^{2+}+2e^-\rightarrow Co+4H_2O+en\ \text{etc.}$$

From the scheme of the reduction processes, it may be seen that the first step in the polarographic reduction of these cobalt(III) complexes corresponds to the disruption of the cobalt(III) complexes, resulting in the formation of aquo-ethylenediaminecobalt(II) ions such as $[Co\ en_2(OH_2)_2]^{2+}$, $[Co\ en_2(OH_2)X]^{(2-n)+}$ and $[Co\ en(OH_2)_4]^{2+}$, so its half-wave potential may be regarded as a measure of the stability toward polarographic reduction.

* The following abbreviations are used: gly, $NH_2CH_2COO^-$; leuc, $NH_2CH(COO^-)CH_2CH(CH_3)_2$; ox, $(COO^-)_2$.

** Polyoxyethylene sorbitan mono-oleate (Atlas Powder Co. in U. S. A.).

11) P. Ray and B. Sarma, *J. Indian Chem. Soc.*, **28**, 59 (1951).
12) A. Werner and K. R. Lange, *Ann.*, **386**, 88 (1912).
13) A. Werner, ibid., **386**, 1 (1912).
14) Y. Shimura and R. Tsuchida, This Bulletin, **29**, 311 (1956).
15) A. Werner and E. Humphrey, *Ber.*, **34**, 1728 (1901).
16) A. Werner, ibid., **44**, 2453 (1911).
17) A. Werner, H. Müller, R. Klien and F. Bräunlich, *Z. anorg. Chem.*, **22**, 91 (1900).
18) W. C. Fernelius et al., "*Inorganic Synthesis*", vol 2, McGraw-Hill Co., New York (1946) p. 222.
19) S. M. Jörgensen, *J. prakt. Chem.*, **39**, 1 (1889).
20) A. Werner, *Ann.*, **386**, 1 (1912).
21) M. Linhard, *Z. Elektrochem.*, **50**, 224 (1944).
22) P. Pfeiffer and O. Angern, *Ber.*, **60**, 305 (1927).
23) A. Werner and M. Pokrowska, *Ann.*, **386**, 1 (1912).
24) J. C. Duff, *J. Chem. Soc.*, **1922**, 450.
25) J. Meisenheimer, L. Angerman and H. Holsten, *Ann.*, **438**, 261 (1924).
26) A. Werner and A. Vilmos, *Z. anorg. Chem.*, **21**, 145 (1899).
27) Y. Shimura, This Bulletin, **31**, 315 (1958).

TABLE I

HALF-WAVE POTENTIALS OF COBALT(III) COMPLEXES OF [Co en$_2$X$_2$] TYPE

Compound	Supporting electrolyte; 0.5 F K_2SO_4		Supporting electrolyte; 0.1 F KCl	
	$E_{1/2}$ of 1st wave [Co(III)→Co(II)]	$E_{1/2}$ of wave of aquated complexes [Co(III)→Co(II)]	$E_{1/2}$ of 1st wave [Co(III)→Co(II)]	$E_{1/2}$ of wave of aquated complexes [Co(III)→Co(II)]
[Co en$_2$(CN)$_2$]Cl[11]	−0.85	—	−0.80	−0.61
cis-[Co en$_2$(OH$_2$)$_2$] (NO$_3$)$_3$[12]	−0.50	—	−0.42	—
trans-[Co en$_2$(NH$_3$)$_2$]Cl$_3$·H$_2$O[13]	−0.45	—	−0.31	—
cis-[Co en$_2$(NH$_3$)$_2$] (ClO$_4$)$_3$[14]	−0.45	—	−0.31	—
trans-[Co en$_2$(NO$_2$)$_2$]Cl[15]	−0.26	−0.5	−0.27***	−0.40***
cis-[Co en$_2$(NO$_2$)$_2$]ClO$_4$[16]	−0.25	−0.5	−0.24***	−0.41***
trans-[Co en$_2$(NCS)$_2$]Cl·H$_2$O[17]	+	−0.51**	+	*
cis-[Co en$_2$(NCS)$_2$]Cl·H$_2$O[17]	+	−0.51**	+	*
trans-[Co en$_2$Cl$_2$]Cl[18]	+	*	+	*
cis-[Co en$_2$Cl$_2$]Cl[19]	+	*	+	*
trans-[Co en$_2$Br$_2$]Br[20]	+	*	+	*
cis-[Co en$_2$Br$_2$]Br[20]	+	*	+	*

1) The concentration of the complex ion; 0.001 F.
2) The characteristics of capillary used; m = 0.615 mg./sec., t = 7.42~6.98 sec./drop.
3) Potential unit; V. vs. S. C. E.
4) Temp., 25°C.
* Maximum wave.
** The data obtained in the presence of 0.0016% Tween-80.
*** The data adopted from H. F. Holtzclaw, Jr. and D. P. Sheetz, *J. Am. Chem. Soc.*, **75**, 3053 (1953).

TABLE II

HALF-WAVE POTENTIALS OF COBALT(III) COMPLEXES OF [Co en$_2$Y] TYPE

Compound	Supporting electrolyte; 0.5 F K_2SO_4		0.1 F KCl	
	$E_{1/2}$ of 1st wave Co(III)→Co(II)	$E_{1/2}$ of wave of aquated complexes Co(III)→Co(II)	$E_{1/2}$ of 1st wave Co(III)→Co(II)	$E_{1/2}$ of wave of aquated complexes Co(III)→Co(II)
[Co en$_3$] (ClO$_4$)$_3$[21]	−0.51	—	−0.41	—
[Co en$_2$CO$_3$]Cl·H$_2$O[22]	−0.45$_5$	—	−0.40	—
[Co en$_2$SO$_3$]Cl·3H$_2$O[23]	−0.43	*	*	*
[Co en$_2$S$_2$O$_3$]Br·3H$_2$O[24]	—	−0.49$_5$	—	**
[Co en$_2$gly]Cl$_2$·H$_2$O[25]	−0.41	−0.5	−0.36	—
[Co en$_2$ox]Cl[26]	−0.31	−0.5	−0.32****	—
[Co en$_2$leuc] (ClO$_4$)$_2$[27]	−0.30$_5$	−0.5	−0.33$_5$***	—

1) The experimental conditions are the same as mentioned in Table I.
2) Potential unit; V. vs. S. C. E.
* The waves of the original complex ion and of the aquated species are so near located that both the waves cannot be discriminated one another. However, it was noticed that the half-wave potential shifted towards negative direction with the decreasing concentration due to the aquation of the complex ion.
** Maximum wave.
*** The data obtained in the presence of 0.0016% Tween-80.
**** The data obtained in the solution of 1 F $(NH_4)_2C_2O_4$.

The polarographic stability of the cobalt (III) complexes of [Co en$_2$X$_2$] type increases in the following order of the ligand X;

$$Br^-, Cl^- < NCS^- < NO_2^- < NH_3 < OH_2 < CN^-$$

(Supporting electrolyte; 0.5 F K_2SO_4)

The same order was also obtained in 0.1 F potassium chloride. For the complexes of [Co en$_2$X$_2$] type the difference of the half-wave potentials between *cis*- and *trans*-isomer is far smaller than that among the other kinds of the complex of this series, hence the difference between *cis*- and *trans*-isomer need not be taken

into consideration in this case.

The order of stability of [Co en_2Y] type complexes was in the following order of the ligands;

$$leuc^- < ox^{2-} < gly^- < SO_3^{2-} < CO_3^{2-} < en$$

(0.5 F K_2SO_4 or 0.1 F KCl as supporting electrolyte)

No relation between the above orders of the polarographic stability and that of the spectrochemical series[28] could be found in accordance with the result obtained in the previous paper[1].

Polarographic Behavior of Individual Complexes.—The second waves of all the bisethylenediaminecobalt(III) complexes indicated the maxima which could be suppressed by the maximum suppressor, Tween-80, except the case of dicyanobis-

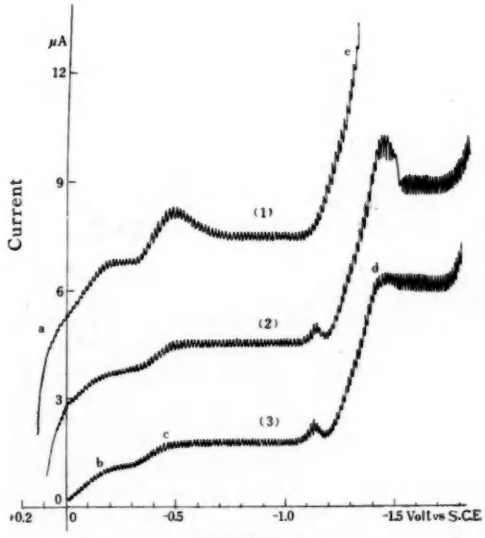

Fig. 1. The polarograms of *trans*-[Co $en_2(NCS)_2$]Cl·H_2O obtained at the concentration of 0.001 F in the solution of 0.1 F KCl.
1) In the absence of maximum suppressor
2) In the presence of 0.0016% Tween-80
3) In the presence of 0.0032% Tween-80
a Anodic wave
b The first wave of *trans*-[Co $en_2(NCS)_2$]$^+$
c The reduction wave of the aquated complexes
d The second wave of *trans*-[Co en_2 $(NCS)_2$]$^+$
e Maximum wave
Sensitivity; 0.06 μA/mm., Damping; 200

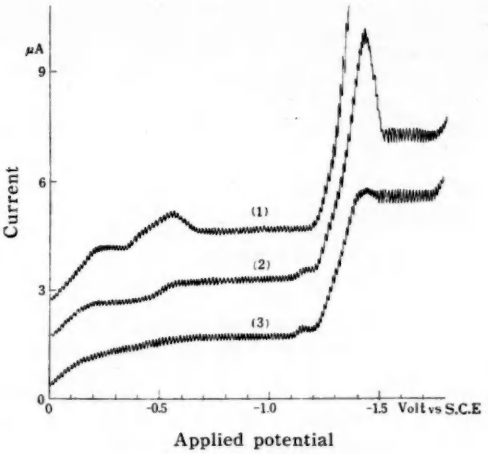

Fig. 2. The polarograms of *cis*-[Co $en_2(NCS)_2$]Cl·H_2O obtained at the concentration of 0.001 F in the solution of 0.5 F K_2SO_4.
1) In the absence of maximum suppressor
2) In the presence of 0.0016% Tween-80
3) In the presence of 0.0032% Tween-80
Sensitivity; 0.06 μA/mm., Damping; 200

ethylenediaminecobalt(III) ion, [Co en_2 $(CN)_2]^+$. Trisethylenediaminecobalt(III) and monoethylenediamine-tetramminecobalt(III) ions have also the maxima in the second step of the reduction, which was reported briefly in an earlier communication[10]. Therefore, it can be said that all the cobalt(III) complexes containing one or more ethylenediamine in their coordination sphere show the maxima at the second wave corresponding to the reduction for Co(II)→Co(0).

Figs. 1 and 2 show the polarograms of *cis*- and *trans*-diisothiocyanato-bisethylenediaminecobalt(III) ions, [Co $en_2(NCS)_2]^+$, respectively. It is expected that these ions aquate to some extent in solution. In fact, for *trans*-[Co $en_2(NCS)_2]^+$ ion, the small maximum wave was given at around −0.4 V. (vs. S. C. E.), which could be suppressed in the presence of 0.0016% Tween-80. The half-wave potential of this small wave is near to that of diaquobisethylenediamine-cobalt(III) ion, [Co $en_2(OH_2)_2]^{3+}$. ($E_{1/2}$ = −0.44 V. vs. S. C. E. in 0.1 F KCl) Therefore, this small wave is considered to correspond to the reduction wave of the aquated species such as [Co $en_2(NCS)OH_2]^{2+}$ and [Co $en_2(OH_2)_2]^{3+}$. Similarly, for *cis*-[Co $en_2(NCS)_2]^+$ ion, the small wave of the aquated cobalt(III) ions was given at around −0.51 V. (vs. S. C. E.)

28) Y. Shimura and R. Tsuchida, ibid., **29**, 311 (1956).

in a solution of 0.5 F potassium sulfate. The half-wave potential of $[Co\ en_2(OH_2)_2]^{3+}$ ion is -0.50 V. in 0.5 F potassium sulfate.

In a dilute supporting electrolyte, a similar wave of the aquated cobalt(III) complex ions was found for the following ions;

$[Co\ en_2Cl_2]^+$, $[Co\ en_2Br_2]^+$

$[Co\ en_2(NCS)_2]^+$, $[Co\ en_2ox]^+$

$[Co\ en_2gly]^{2+}$, $[Co\ en_2S_2O_3]^+$

$[Co\ en_2(CN)_2]^+$

Among these ions it was noticed that the height of the wave of the aquated species increases gradually with time for some complex ions, but does not for the others. This is considered to be due to the variety of the rate of the aquation. Namely, the aquation of some ions is comparatively slow, compared with the time of the polarographic measurement, while for the others, the aquation is so rapid that the usual polarographic method can not detect and trace the change of the height of the wave. The ions, $[Co\ en_2(CN)_2]^+$, $[Co\ en_2SO_3]^+$ belong to the former and the ions, $[Co\ en_2Cl_2]^+$, $[Co\ en_2Br_2]^+$ to the latter.

In a solution of 0.1 F potassium chloride dicyano-bisethylenediaminecobalt(III) ion, $[Co\ en_2(CN)_2]^+$ showed the wave of the aquated complexes at around -0.80 V., but did not show anything in 0.5 F potassium sulfate. It seemed that the wave of the aquated species was probably covered by the wave of the original ion in the solution of potassium sulfate, because the waves of the original and the aquated ions were located very near to each other. The reduction potential of the aquated ions of $[Co\ en_2(CN)_2]^+$ did not coincide with that of $[Co\ en_2(OH_2)_2]^{3+}$ ion, so it is considered that the main species of the aquated ions is a partly aquated complex ion, $[Co\ en_2(CN)OH_2]^{2+}$. (Fig. 3)

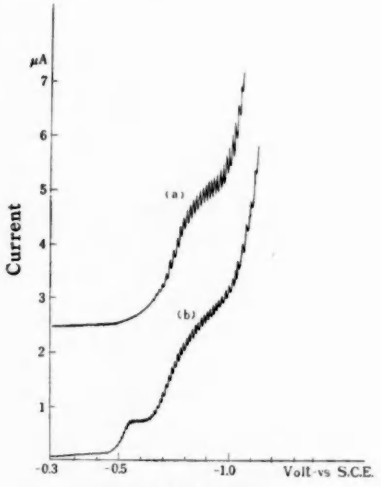

Fig. 3. The polarograms of $[Co\ en_2(CN)_2]Cl$ obtained at the concentration of 0.001 F.
a) In the solution of 0.5 F K_2SO_4
b) In the solution of 0.1 F KCl
Sensitivity; 0.04 μA/mm., Damping; 100

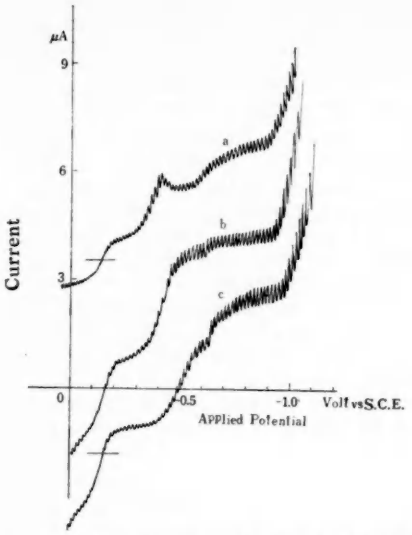

Fig. 4. The polarograms $[Co\ en_2S_2O_3]Br \cdot 3H_2O$.
a) obtained at the concentration of 0.001 F complex ion in the solution of 0.1 F KCl
b) obtained at the concentration of 0.005 F complex ion in the solution of 0.1 F KCl
c) obtained at the concentration of 0.005 F complex ion in the solution of 0.5 F K_2SO_4
Sensitivity; 0.06 μA/mm., Damping; 200

In 0.1 F potassium chloride, thiosulfato-bisethylenediaminecobalt(III) ion, $[Co\ en_2S_2O_3]^+$ has the small maximum wave which could be suppressed in the presence of 0.0016% Tween-80. (Fig. 4) The half-wave potential of the first wave of this ion could not be determined owing to the interference of the anodic wave of the thiosulfate ion liberated from the original complex by the aquation.

Fig. 5 shows the polarogram of the first wave of *cis*-diaquo-bisethylenediaminecobalt(III) ion, $[Co\ en_2(OH_2)_2]^{3+}$ in 0.5 F potassium sulfate. The wave has always

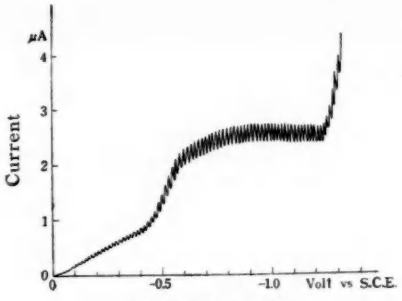

Fig. 5. The polarogram of *cis*-$[Co\ en_2(OH_2)_2]^{3+}$ obtained in the solution of 0.5 F K_2SO_4 at the concentration of 0.001 F complex ion.
Sensitivity; 0.04 μA/mm., Damping; 200

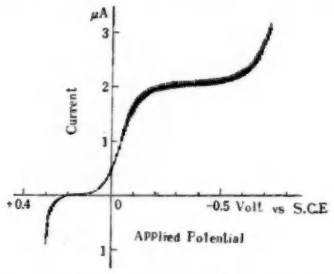

Fig. 6. The polarogram of *cis*-$[Co\ en_2(OH_2)_2]^{3+}$ obtained in 1 F $HClO_4$ at the concentration of 0.001 F complex ion.
Sensitivity; 0.04 μA/mm., Damping; 200
$E_{1/2} = -0.01$ V. (vs. S. C. E.)
$i_d = 2.09$ μA.

a slower slope at the half-wave potential than that of the other complex ions of bisethylenediamine series. A gradually rising current near the zero potential was observed. However, it can not necessarily be said that this current is a residual current, since the diffussion current reaches a plateau parallel to the axis of the potential. (Usually, the diffusion current, runs parallel to the residual current, not to the axis of the potential.) Moreover in 1 F perchloric acid, a well-defined wave is obtained, which has a steep slope at the half-wave potential. (Fig. 6) One of the reasons for this is the presence of an equilibrium between the aquo-bisethylenediaminecobalt(III) ion and hydroxo-bisethylenediaminecobalt(III) ion.

$$[Co\ en_2(OH_2)_2]^{3+} \rightleftarrows [Co\ en_2(OH_2)OH]^{2+} + H^+$$

$$[Co\ en_2(OH_2)OH]^{2+} \rightleftarrows [Co\ en_2(OH)_2]^{+} + H^+$$

In perchloric acid the above equilibrium is markedly shifted to the left hand. Consequently, the steep wave of diaquo-bisethylenediaminecobalt(III) ion could be obtained.

Another reason for this is the polymerization of diaquo-bisethylenediaminecobalt (III) ion in neutral solution. Namely, as verified by the spectrochemical studies of Rasmussen et al.[29], various kinds of polynuclear cobalt(III) complex are formed in solution. For instance,

2 *cis*-$[Co\ en_2(OH_2)OH]^{2+} \rightarrow$

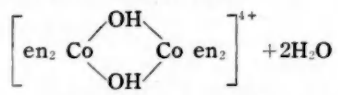

$+2H_2O$

It is also considered that in perchloric acid, the polymerization is inhibited due to the presence of an overwhelming

TABLE III
HALF-WAVE POTENTIALS OF AQUO-AMMINE AND DIAQUO-BISETHYLENEDIAMINE COBALT(III) COMPLEXES

Complex	Supporting electrolyte; 0.5 F K_2SO_4 $E_{1/2}$ of 1st wave [Co(III)→Co(II)]	1 F $HClO_4$ $E_{1/2}$ of 1st wave [Co(III)→Co(II)]
$[Co(NH_3)_6](ClO_4)_3$	-0.43_9	—
$[Co(NH_3)_5OH_2]_2(SO_4)_3 \cdot 2H_2O$[30]	-0.47_5	−0.06
cis-$[Co(NH_3)_4(OH_2)_2]_2(SO_4)_3 \cdot 3H_2O$[30]	-0.48_5	+0.14
$[Co(NH_3)_3(OH_2)_3]^{3+}$	-0.24_9*	—
cis-$[Co\ en_2(OH_2)_2](NO_3)_3 \cdot H_2O$[12]	−0.50	−0.01

1) The concentration of the complex ion; 0.001 gram complex ion per liter.
2) Potential unit; V. vs. S. C. E.
3) Temp., 25°C.
* The data adopted from J. B. Willis, J. A. Friend and D. P. Mellor, *J. Am. Chem. Soc.*, **67**, 1680 (1945).

29) S. E. Rasmussen and J. Bjerrum, *Acta Chem. Scand.*, **9**, 735 (1955).

30) S. M. Jörgensen, *Z. anorg. Chem.*, **17**, 461 (1898).

hydrogen ion. Consequently, only the original ion is present in solution. Therefore, the steep well-defined wave of this ion was obtained in perchloric acid.

A similar behavior was observed for the aquo-ammine cobalt(III) complexes, which were shown in Table III.

Summary

1. Most of the cobalt(III) complex ions of bisethylenediamine series, $[Co\ en_2X_2]^{(3-2n)+}$ or $[Co\ en_2Y]^{(3-m)+}$ are reduced irreversibly in two steps at the dropping mercury electrode. The first diffusion current corresponds to the reduction, Co(III)→Co(II) and the second to the reduction, Co(II)→Co(0). The second step always exhibits the maximum wave.

2. The polarographic stability of $[Co\ en_2X_2]$ type complexes increases in the following order of the ligands;

$Br^-, Cl^- < NCS^- < NO_2^- < NH_3 < OH_2 < CN^-$

(Supporting electrolyte; 0.5 F K_2SO_4)

Similarly, the order of the stability of $[Co\ en_2Y]$ type complexes is as follows;

$leuc^- < ox^{2-} < gly^- < SO_3^{2-} < CO_3^{2-} < en$

(Supporting electrolyte; 0.5 F K_2SO_4)

These orders are independent of the kind of supporting electrolyte such as potassium chloride or potassium sulfate. The orders of the polarographic stability did not agree with that of the spectrochemical series.

3. In perchloric acid the well-defined wave of steep slope was obtained for diaquo-bisethylenediaminecobalt(III) ion, $[Co\ en_2(OH_2)_2]^{3+}$, while the ion gave a modified wave in the neutral solution of 0.1 F potassium chloride and of 0.5 F potassium sulfate. This phenomena was explained as being due to the inhibition of the dissociation and polymerization of the complex in the presence of an overwhelming hydrogen ion. A similar behavior was observed in the aquo-ammine cobalt (III) complexes.

Department of Chemistry
Faculty of Science
Osaka University
Kita-ku, Osaka

---

*A Note on the Proton Magnetic Resonance Spectra of Some Thiophene Derivatives**

By Kensuke TAKAHASHI, Yasuo MATSUKI, Tatsuo MASHIKO and Genjiro HAZATO

(Received August 19, 1958)

High resolution magnetic resonance spectra of the aromatic ring protons for a large number of substituted benzenes have at times been studied by several authors[1], but no available data were obtained for substituted thiophenes except for 2-bromo-5-chlorothiophene[2]. Here we present the experimental results and preliminary discussions on the proton magnetic resonance spectra of several thiophene derivatives. With respect to the number of the ring protons, they are less by two than the corresponding benzene derivatives, and so the spectra of mono-, di- and tri-substituted thiophenes are generally expected to show the structure of three quartets, two doublets and one singlet respectively. The analyses are simple for the ring protons of di- and tri-substituted thiophenes but more complicated for mono-substituted ones, and they will be discussed here qualitatively.

Experimental

The basic theory and experimental details of n-m-r measurements have been described by several authors in excellent articles, so they will not be given here.

* Presented partly at the 11th Annual Meeting of the Chemical Society of Japan, held on April 4, 1958, at Tokyo.

1) P. L. Corio and B. P. Dailey, *J. Am. Chem. Soc.*, **78**, 3043 (1956); H. S. Gutowsky, D. W. McCall, B. R. McGarvey and H. L. Meyer, ibid., **74**, 4809 (1952); H. S. Gutowsky, C. H. Holm, A. Saika and G. A. Williams, ibid., **79**, 4596 (1957).

2) W. A. Anderson, *Phys. Rev.*, **102**, 151 (1956).

TABLE I

Substituent	b. p. (°C)	Measured condition (Weight per cent)		
		Sample	CCl_4	C_6H_{12}
—		70.5		29.5
2-CH_3	107~112	95.9		4.1
3-CH_3	114~115	95		5
2, 3-$(CH_3)_2$	139~140	96.2		3.8
2, 4-$(CH_3)_2$	139~142	94.8		5.2
2-Cl		77.8		22.2
2-Br	148~151	81.0		19.0
2-I	72~74/15	82.5		17.5
2, 5-Cl_2		80.9		19.1
2, 5-Br_2		80.2		19.8
2, 5-I_2		26.5	67.2	6.3
2-Br, 3-CH_3	34.5~35.0/4.8	80.1		19.9
2-$COCH_3$	88/8	74.3		25.7
2-NO_2	m. p. 45~46	97		3
2-CHO	76/12	81.1		18.9
2-SO_2Cl	m. p. 32~33	93.2		6.8
2, 4-$(SO_2Cl)_2$	m. p. 76~77	8.3	89.9	1.8
2, 5-$(SO_2Cl)_2$	m. p. 44~45	28.8	68.3	2.9
2, 5-$(NO_2)_2$				
2-SO_2Cl, 3-CH_3	98~100/3	98.9		1.1
2-SO_2Cl, 5-CH_3		78.4		21.6
2, 4-$(SO_2Cl)_2$, 3-CH_3	m. p. 96	36.7	62.0	1.3
2, 5-$(SO_2Cl)_2$, 3-CH_3				

Materials.—All thiophene derivatives used in the present observations were synthesized by Y. M. and T. M., the details of the procedure will soon be published in the Journal of the Chemical Society of Japan, Ind. Chem. Sec..

Procedure and Apparatus. — The apparatus used in this research is a Bloch-type high resolution n-m-r spectrometer (Model V-4300B), purchased from Varian Associates, Palo Alto, California. Proton resonances were observed at a fixed frequency of 40 mc./sec. and the corresponding magnetic fields in the neighborhood of 9400 gauss.

The chemical shifts were read from the signals recorded with a Sanborn Model 127 Recorder, comparing with the shift of 227 cps for benzene-cyclohexane mixture, 1 : 1 by volume, as a reference, and the values given here are the averages, usually from about three recordings, and the small values were calibrated by running acetaldehyde, with its known splitting of 2.85 cps.

The values of chemical shift will not be sensitive to the presence of small amounts of impurities, especially in the case of C-H bonds, so that the samples were used after several times distillations or recrystallizations without any other special procedures of purification.

Samples which are solid at room temperature were measured in the super-cooled conditions after being heated above their melting points or dissolved in carbon tetrachloride. In such a case, it should be kept in mind that the occurrence of the additional shift due to the concentration effect or the molecular interaction is possible, so that the measured conditions are given in Table I.

Additional errors do not result from neglecting the bulk diamagnetic susceptibility corrections by using cyclohexane as a internal reference. Another error results from the difference of the reference concentration, but it is assumed that this error is small[3]. In some compounds, especially in 2-bromothiophene and in thiophene itself, it was observed that the line shapes were slightly changed with the variation of the concentration of the reference compound.

The results were reproducible within the deviation of about 4 cps.

Results and Discussion

Table of Chemical Shifts.—The chemical shifts of the ring protons obtained from the twenty-two compounds are given in Table II, in cps, indicating the separations from the cyclohexane signal, the larger value showing the lower field side. In the case where the signal is split by the indirect spin-spin interaction, the shift given here is that for the center of the resonance pattern. As for 2-methyl-, 3-methyl- and 2-bromothiophene, the assignments of their spectra are not given in Table II and they will be discussed in the latter paragraph of monosubstituted thiophenes.

3) P. L. Corio and B. P. Dailey, *J. Am. Chem. Soc.*, **78**, 3043 (1956); *J. Chem. Phys.*, **25**, 1291 (1956).

TABLE II

THE MAGNETIC RESONANCE DATA FOR THE RING PROTONS IN SUBSTITUTED THIOPHENES, REFERRED TO CYCLOHEXANE IN CPS, AT 40 mc./sec.

Substituent	Assignment				Mean shift	Mean shift from thiophene
	2-H	3-H	4-H	5-H		
——					220	0
2-CH_3	—				210	−10
3-CH_3		—			211	− 9
2,3-$(CH_3)_2$	—	—	203	211	207	−13
2,4-$(CH_3)_2$	—	197	—	197	197	−23
2-Cl	—	209	209	209	209	−11
2-Br	—				214	− 6
2-I	—	224	204	224	218	− 2
2,5-Cl_2	—	204	204	—	204	−16
2,5-Br_2	—	207	207	—	207	−13
2,5-I_2	—	214	214	—	214	− 6
2-Br, 3-CH_3	—	—	204	219	211	− 9
2-$COCH_3$	—	248	223	248	239	19
2-NO_2	—	252	227	252	244	24
2-CHO	—	255	229	255	246	26
2-SO_2Cl	—	257	230	257	248	28
2,4-$(SO_2Cl)_2$	—	266	—	281	273	53
2,5-$(SO_2Cl)_2$	—	258	258	—	258	38
2,5-$(NO_2)_2$	—	277	277	—	277	57
2-SO_2Cl, 3-CH_3	—	—	224	252	238	18
2-SO_2Cl, 5-CH_3	—	246	215	—	230	10
2,4-$(SO_2Cl)_2$, 3-CH_3	—	—	—	288	288	68
2,5-$(SO_2Cl)_2$, 3-CH_3	—	—	257	—	257	37

Indirect Spin-Spin Coupling Constants.—The indirect spin-spin coupling constants (J) for disubstituted thiophenes are given in Table III in cps, obtained by reading the scales of their spectra. In monosubstituted thiophenes, however, there are three independent coupling constants, the reasonable values of which can not be determined without theoretical calculations referring to the multiplet structure.

TABLE III

THE COUPLING CONSTANT (J) AND THE CHEMICAL SHIFT (δ) OF TWO RING PROTONS IN DISUBSTITUTED THIOPHENES IN CPS AT 40 mc./sec.

Substituent	J	δ
2,3-$(CH_3)_2$	5.2	5.9
2-Br, 3-CH_3	5.6	14
2-SO_2Cl, 3-CH_3	5.5	27
2-SO_2Cl, 5-CH_3	4.1	31
2-Br, 5-Cl*	3.9	6.2
2,4-$(SO_2Cl)_2$		15
2,4-$(CH_3)_2$		≃0
2,5-Cl_2		0
2,5-Br_2		0
2,5-I_2		0
2,5-$(NO_2)_2$		0
2,5-$(SO_2Cl)_2$		0

* from Anderson's value[2].

The mean value (5.4 cps) of the indirect coupling constants between the 4- and 5-positioned protons (J_{45}) for three compounds, i.e. 2,3-dimethyl-, 2-bromo-3-methylthiophene and 3-methylthiophene-2-sulfonylchloride, is greater than the mean value of J_{34} (4.0 cps) for two compounds, 5-methylthiophene-2-sulfonylchloride and 2-bromo-5-chlorothiophene. The values of J_{35} can not be determined from the spectra of 2,4-dimethylthiophene and 2,4-thiophenedisulfonylchloride, for the signals of 3- and 5-positioned protons of these compounds are broad; perhaps they will have the unresolved multiplet structures.

With our results and the help of the values analyzed in detail for selenophene and furan[4], it can be assumed that $J_{45} \simeq J_{23} > J_{34} > J_{25} > J_{24} \simeq J_{35}$ in thiophene derivatives.

And also the methyl resonances for methylthiophenes have the fine structure due to spin-spin coupling with adjacent ring protons, having the approximate coupling constants of 1.0 cps, the signals of which are shown in b and d in Fig. 1.

Monosubstituted Thiophenes.—Nine compounds were measured and the spectra of

4) T. Isobe, Presented at the Symposium on the Structural Chemistry, held on Nov. 21, 1957, at Fukuoka.

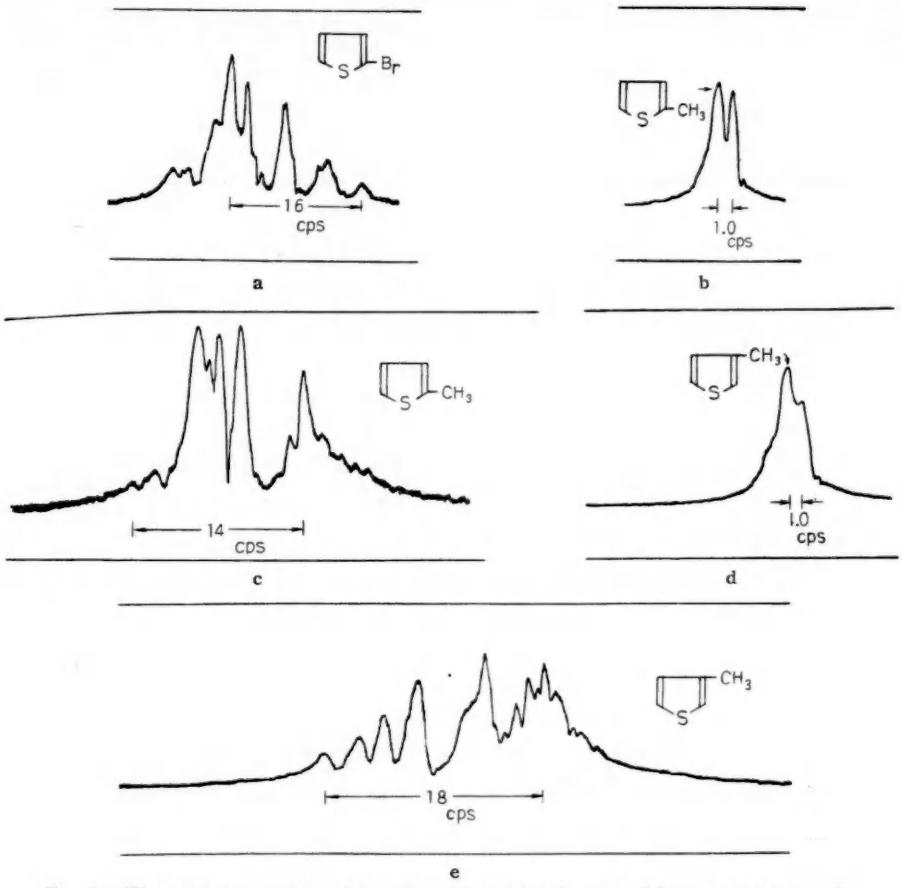

Fig. 1. The proton magnetic resonance spectra showing (a), 2-bromothiophene; (b), methyl group in 2-methylthiophene; (c), ring protons in 2-methylthiophene; (d), methyl group in 3-methylthiophene; (e) ring protons in 3-methylthiophene. Applied magnetic field increasing from left to right.

their ring protons can be classified into three types. The spectrum of 2-chlorothiophene is in the first type; it has a broad single line, so that the three protons in the ring are almost magnetically equivalent. The spectra of 2-bromo-, 2-methyl- and 3-methylthiophene are in the second type and they have the most complicated spectra as shown in a, c and e in Fig. 1, but their analyses are difficult for the present, so that they are not given in Table II. As for the others, 2-acetyl-, 2-iodo-, 2-nitrothiophene, 2-thiophenesulfonylchloride and 2-thiophenealdehyde, the spectra are in the third type and they are shown in a, b, c, d and e in Fig. 2. Their signals consist of two main parts separated approximately 20 cps or more. The intensity ratio of the high-field part to the low-field one is 1 : 2, corresponding to one proton and to two protons respectively. At the high-field side of the signal, there are three or four sub-lines. Therefore these sub-lines can be considered as the lines coming from the 4-positioned proton. At the low field side of their signal, there are two sub-lines and they can be assumed to be the lines coming from the 3- and 5-positioned protons, and that both protons have almost the same chemical shifts.

In the spectra of the ring protons in the third group, we can assume that J_{34} and J_{45} have approximately the same value of

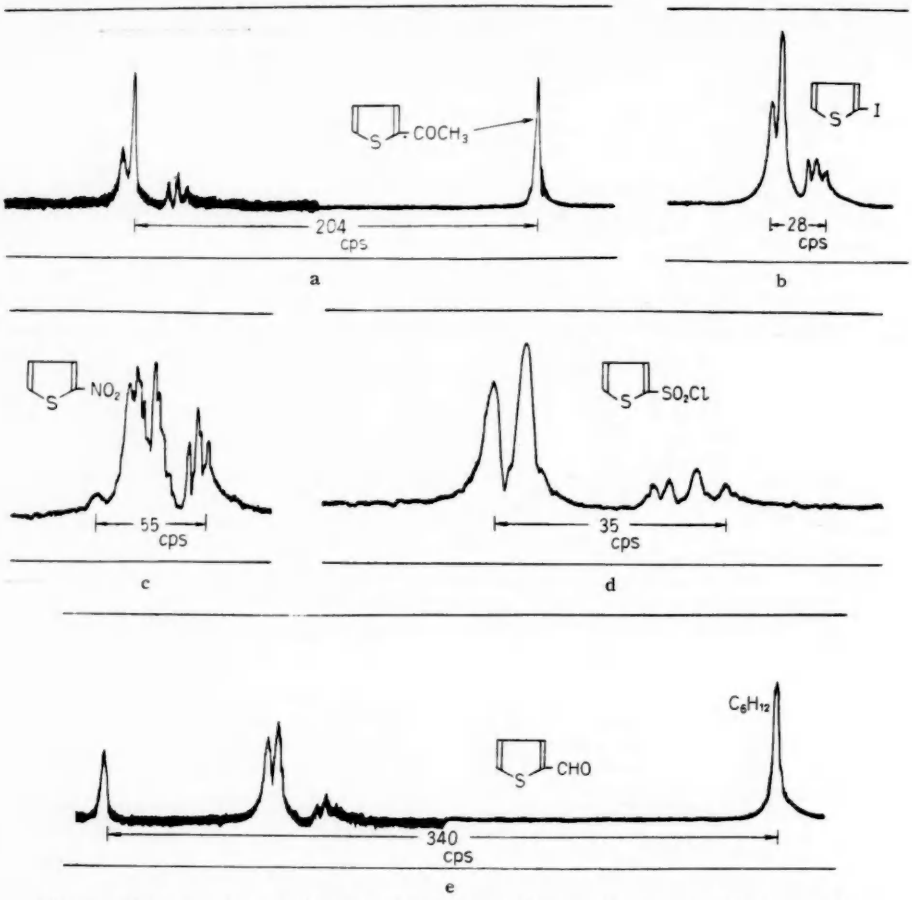

Fig. 2. The proton magnetic resonance spectra showing (a), 2-acetylthiophene; (b), 2-iodothiophene; (c), 2-nitrothiophene; (d), 2-thiophenesulfonylchloride; and (e), 2-thiophenealdehyde. Applied magnetic field increasing from left to right in all figures.

5 cps, closely consistent with the values shown in the preceding paragraph. The spectra of 2-nitrothiophene are more complicated than the others (Fig. 2 c), and in this figure, a signal which appeared at the lowest field side is assumed as coming from 2,5-dinitrothiophene by which the sample is contaminated.

In general, the multiplet structure of the n-m-r spectrum depends upon the ratio of the coupling constant to the chemical shift (J to δ). In monosubstituted thiophenes, it can be supposed that the chemical shifts are small as compared with the coupling constants in the first type, approximately the same in the second type and large in the third type.

Disubstituted Thiophenes. — The disubstituted thiophenes are the typical model of the two-proton system and there are four isomers as follows:

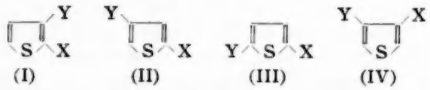

Their spectra consist of two doublets, but if X and Y are the same, the spectra for III and IV should have the single line.

The chemical shifts and coupling constants between the two ring protons are given in Table III; the samples in type IV were not measured. In the near future, we hope to obtain the measurements of this type for the determination of J_{25}, the coupling constant between the two protons

by way of the sulfur atom.

Trisubstituted Thiophenes. — Two compounds were measured and they have a single line.

Substituent Effects to Thiophene Ring. —The nitro, sulfonylchloro, aldehyde and acetyl groups have the strong electron withdrawing power. The introductions of these substituents to the thiophene nuclei should have lessened the electron density of the ring protons, we can see these aspects in the experimental results shown in the seventh column of Table II. In the case of 2-nitrothiophene, the magnitudes of the shifts are large in 3- and 5-H but small in 4-H toward lower field. On the contrary, the shift of the ring proton to the lower frequency in the spectra of methylthiophenes is consistent with the effect of higher electron density in the ring due to methyl substitution.

Also in the halogeno-substituted thiophenes, the similar shifts toward the higher field were observed as shown in Table II. The I-effect of the halogen-substituent withdraws charge from the ring, while the E-effect donated charge to the ring. Therefore, the situation here shows probably a predominance of the E-effect over the I-effect.

It is hoped that the present results will be usefull in determining the structure of unknown thiophene derivatives and in analyzing the spectrum for thiophene in detail.

Summary

1) The chemical shifts of the ring protons for twenty-two kinds of thiophene derivative were measured, and the qualitative discussions on the substituent effects were also given.

2) The coupling constants between the ring protons for thiophene derivatives can be generally assumed to be $J_{45} \simeq J_{23} > J_{34} > J_{25} > J_{24} \simeq J_{35}$.

The Chemical Research Institute of Non-aqueous Solutions
Tohoku University
Katahira-cho, Sendai

*The Fundamental Conditions for Countercurrent Distribution Studies of Clupeine**

By Fumio SAWADA

(Received September 5, 1958)

The heterogeneity of some protamines, protein moieties in sperm nuclei of fishes, namely clupeine[1-9] from herring, salmine[3,4] from salmon, iridine[3,4,10] from rainbow-trout, and mugiline[11,12] from mullet, has been reported from German[1-7] and Japanese[8-12] laboratories. Nevertheless, it is still uncertain how the heterogeneity of protamines originates and what the biological activities of different molecules are. Thus, as the first step to resolve the problem, clupeine has been examined

* Presented at the 8th Annual Meeting of the Chemical Society of Japan held on April 1, 1955, in Tokyo.

1) A. Kossel and E. G. Schenk, *Z. physiol. Chem.*, **173**, 278 (1928).

2) K. Felix and K. Dirr, ibid., **184**, 111 (1927); K. Felix and A. Mager, ibid., **249**, 111 (1937); H. M. Rauen, W. Stamm and K. Felix, ibid., **291**, 275 (1952).

3) H. M. Rauen, W. Stamm and K. Felix, ibid., **292**, 101 (1953).

4) K. Felix, "The Chemical Structure of Proteins", a Ciba Foundation Symp., J. & A. Churchil Ltd., London (1953) p. 151.

5) K. Felix, *American Scientist*, **43**, 431 (1955); K. Felix, A. Krekels and W. Rick, *Trans. Faraday Soc.*, **53**, 252 (1957).

6) E. Waldschmidt-Leitz, F, Ziegler, A. Schaeffner and L. Weil, *Z. physiol. Chem.*, **197**, 219 (1931); E. Waldschmidt-Leitz and L. Pflanz, ibib., **292**, 150 (1953); E. Waldschmidt-Leitz and K. Gauss, ibid., **293**, 10 (1953); E. Waldshmidt-Leitz and R. Voh, ibid., **298**, 257 (1954).

7) K. E. Rasmussen, ibid., **224**, 97 (1934).

8) T. Ando, E. Abukumagawa, Y. Nagai and M. Yamasaki, *J. Biochem. (Japan)*, **44**, 191 (1957); T. Ando, M. Yamasaki, E. Abukumagawa, S. Ishii and Y. Nagai, ibid., **45**, 429 (1958).

9) T. Ando, S. Ishii, M. Yamasaki, K. Iwai, C. Hashimoto and F. Sawada, ibid., **44**, 275 (1957).

10) F. Sawada and T. Ando, The 31th Annual Meeting of the Japanese Biochem. Soc., Sapporo, July 14, 1958.

11) T. Ikoma, *J. Japanese Biochem. Soc.* (*Seikagaku*), **26**, 460 (1954).

12) S. Morisawa, Symp. on the Structure of Proteins, Fukuoka, Oct. 29, 1956.

for heterogeneity by means of Craig's countercurrent distribution (C. C. D.) method[13-15].

The usefulness of C.C.D., using a solvent system consisting of lauric acid in butanol and aqueous sodium acetate, for the fractionation of the methyl ester hydrochlorides of clupeine[3-5] and mugiline-β[11,12] has already been described. This solvent system, however, proved to be unsuitable for these protamine sulfates[3,11]. The sulfate is considered to represent more intact protein without any treatment of methyl esterification and to be suitable for the elucidation of the origin of the heterogeneity of clupeine. Thus, a course of study aiming to obtain desirable conditions for the fractionation of clupeine sulfate by means of C.C.D. is described in this paper.

Experimental

Preparation of Clupeine Sulfate[9]. — Dry powder** (50 g.) of the matured milts of herring (*Clupea pallasii*) obtained in 1951 (at Yoichi facing the Japan Sea, Hokkaido, Japan) was stirred with 0.2 N hydrochloric acid (600 ml.) under ice-cooling for 50 minutes, and clupeine was precipitated as picrate (yield 12.3 g.) by the addition of 0.125 M sodium picrate to the first extract. The clupeine picrate (5.29 g.) was then dissolved into 67% (wt./wt.) aqueous acetone, and converted in to the sulfate by adding sulfuric acid (to pH 2) and ethanol under cooling. The aqueous solution of clupeine sulfate reprecipitated once was passed through the Dowex-2 column (sulfate form) to remove the contaminating picric acid. Thus white glittering powder (yield 2.29 g.) of clupeine sulfate was obtained from the eluate after two reprecipitations.

Preparation of Clupeine *p*-Toluenesulfonate.—An aqueous acetone solution of clupeine picrate (253 mg. in 2.5 ml.) and an aqueous solution (6.8 ml.) of 4% *p*-toluenesulfonic acid (see below) were mixed. The liberated picric acid was removed by means of ether extraction (five times with 10 ml. each) and by means of treatment with Amberlite IRA-410 (*p*-toluenesulfonate form). The resultant solution (pH 2) was neutralized with Amberlite IR-4B (OH-form). White amorphous powder of clupeine *p*-toluenesulfonate was obtained by lyophilization (yield 99 mg.)***.

Solvents for the C.C.D.—*n*-Butanol, commercial grade; acetic, dichloroacetic, trichloroacetic and picric acid, commercial grade.

p-Toluenesulfonic acid—The commercial reagent was treated with charcoal and recrystallized from a hot solution in concentrated (1 : 1, by volume) hydrochloric acid, or by saturation of the aqueous solution with gaseous hydrogen chloride. The melting point was 104~105°C (cor.).

Principles of Method. — To the C.C.D. of proteins, only a few types of solvent systems, especially the so-called "butanol systems"[16] are applicable. The author tested, therefore, various systems consisting of *n*-butanol and aqueous solution containing some reagents such as hydrochloric, acetic, dichloroacetic, trichloroacetic, *p*-toluenesulfonic**** or picric acid, sodium *p*-toluenesulfonate and sodium chloride. In every case, the partition coefficients of clupeine in these systems were measured, and the system satisfying the conditions necessary for C. C. D.[14] —no irreversible effects on the solute and a linear partition isotherm***** with a partition coefficient not much shifted from unity—was searched for.

Determination of Partition Coefficient.—A mixture of 1 ml. of *n*-butanol and 1 ml. of an aqueous solution containing the known concentrations of a clupeine sample and a reagent or reagents (see above) were put into a test-tube (1×12 cm.) with a glass stopper, and left to stand at a constant temperature in an incubator for 30 minutes. Then the test-tube was vigorously shaken for about 30 seconds at room temperature, and allowed to stand again in an incubator for 10 minutes. After the phases separated, the amounts of clupeine in both of the phases were measured by the retention analysis using an acidic dye, ponceau 6RF[9]. The average value from three to six measurements was used. The ratio $K=C_1/C_2$, where C_1 and C_2 are the equilibrium concentration of the sample in the upper and the lower phases respectively, was defined as a partition coefficient.

Results and Discussion

Dependence of the Partition Coefficient upon Concentration of the Reagents in the System.—In the systems consisting of *n*-butanol and aqueous solutions of various concentrations of hydrochloric, acetic or picric acid, the *K*-values of clupeine sulfate were found to be almost zero. Therefore these systems were discarded.

In the case of the systems containing

13) L. C. Craig, *J. Biol. Chem.*, **155**, 519 (1944).
14) L. C. Craig, C. Golumbic, H. Mighton and E. Titus, ibid., **161**, 321 (1945).
15) J. R. Weisiger, "Organic Analysis", Vol. 2, Interscience Publisher, New York (1954).
** The preparation of the dry powder of the milts was performed by Dr. M. Yamasaki according to the Rasmussen's method[7].
*** An atempt to obtain clupeine *p*-toluenesulfonate by elution of clupeine adsorbed on Amberlite XE-64 (IRC-50) with aqueous *p*-toluenesulfonic acid was unsuccessful.
**** Dichloroacetic, trichloroacetic and *p*-toluenesulfonic acids are known to be good complexing agents for peptides or proteins[16,17].
16) F. Sawada, *Protein-Nucleic Acid-Enzyme*, (*Tampakushitsu-Kakusan-Koso*), **2**, 167 (1957).
17) L. C. Craig, *Anal. Chem.*, **28**, 723 (1956).
***** A plot of the concentration of solute in one phase in equilibrium with the concentration in the second one is called a partition isotherm. When a partion isotherm remains constant over a wide range of concentration, the isotherm is said to be linear (Ref. 15. p. 277).

dichloroacetic, trichloroacetic or *p*-toluenesulfonic acid, the *K*-values of clupeine sulfate at a definite concentration increased as the concentration of these acids increased (Fig. 1). Because of the low *K*-value for dichloroacetic acid and of the difficult solubility of the sample in trichloroacetic acid, only the system containing *p*-toluenesulfonic acid was found to be favorable for the distribution of clupeine.

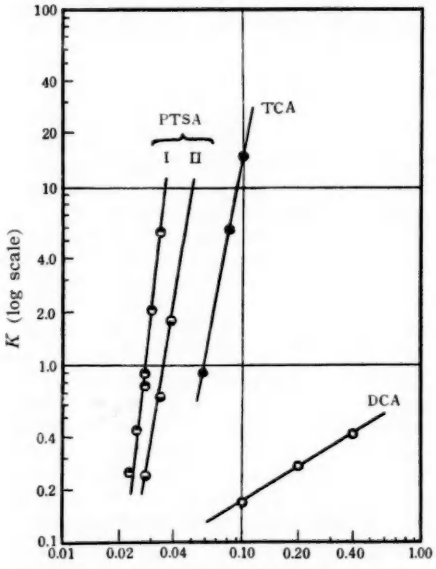

Fig. 1. Dependence of *K*-value of clupeine sulfate upon the concn. of acid in the system of *n*-butanol vs. aq. acid (18~23°C).

Symbol	Acid	Concn. of clupeine sulfate (%)
○—○	dichloroacetic	0.025
●—●	trichloroacetic	0.025
I ◑—◑	*p*-toluenesulfonic	0.02
II ◑—◑	*p*-toluenesulfonic	0.04

Dependence of the Partition Coefficient upon the Concentration of the Sample.— In the solvent system consisting of *n*-butanol and an aqueous *p*-toluenesulfonic acid at a definite concentration, the partition isotherm was not linear; in other words the *K*-value of clupeine sulfate decreased as its concentration increased (curve I in Fig. 2). The same relation was observed when either clupeine *p*-toluenesulfonate was taken for its sulfate (curve II in Fig. 2) or *p*-toluenesulfonic acid was replaced with its sodium salt (curve III in Fig. 2); only in the last case *n*-butanol in the system was replaced by *n*-butanol-*n*-propanol mixture (3 : 1, v./v.) from the viewpoint of miscibility.

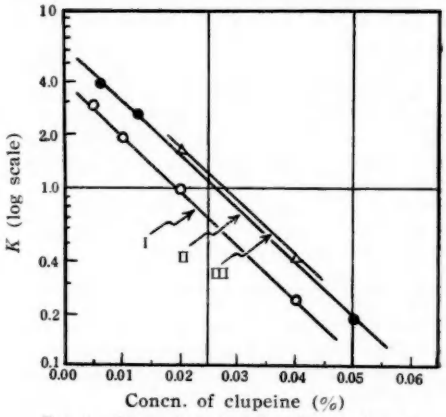

Fig. 2. Dependence of *K*-value of clupeine salt upon its concn. in the system of *n*-butanol* vs. *p*-toluenesulfonic acid or its Na salt.

Symbol	Concn. of the acid or the salt	Clupeine	Temp. (°C)
I ○—○	0.029 M acid	sulfate	20
II ●—●	0.020 M acid	*p*-toluenesulfonate	27
III △—△	0.021 M salt	sulfate	30

* In the case of III, *n*-butanol-*n*-propanol (3 : 1).

The non-linearity of an isotherm is generally observed in the partition of inorganic cations, and the favorable partition can be performed by the use of a solvent system containing a large excess of a complexing agent at a constant pH[18]. The same situation is expected in the case of clupeine which is a strongly basic protein.

Thus, the higher concentration of *p*-toluenesulfonic acid may bring a linear isotherm but with an undesirably large *K*-value and a very low pH. However, its salts, for example sodium *p*-toluenesulfonate, would have the same effect at neutral pH as the acid has, and the addition of sodium chloride in the system would make the *K*-value decrease because of its "salting-in" effect. Therefore, in the solvent system consisting of *n*-butanol and an aqueous solution containing a high and suitable concentration of both sodium *p*-toluenesulfonate and sodium chloride, a

18) E. Hecker, "Verteilungsverfahren im Laboratorium", Verlag Chemie, GMBH, Weinheim/Bergstr. (1955), pp. 18, 107.

linear isotherm with a suitable K-value would be obtained at a neutral pH range. In fact, these considerations were proved to be the case as shown in Fig. 3.

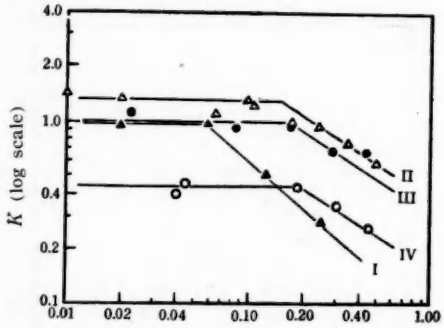

Concn. of clupeine sulfate (% in log scale)

Fig. 3. Dependence of K-value of clupeine sulfate upon its concn. in the system of n-butanol vs. aq. salts.

Symbol	Concn. of Na p-toluene-sulfonate	Concn. of NaCl	Temp. (°C)
I ▲—▲	ca. 0.07 M	0.20 M	23~24
II △—△	ca. 0.12 M	0.40 M	ca. 17
III ●—●	0.12 M	0.40 M	22~23
IV ○—○	0.12 M	0.48 M	22~23

The range of the clupeine concentration where the K-value remains constant becomes broader as the concentration of sodium p-toluenesulfonate increases (curves I and II, III or IV in Fig. 3). It seems that the constant K-value ranges depend only upon the concentration of sodium p-toluenesulfonate; temperature (curves II and III in Fig. 3) and concentration of sodium chloride (curves III and IV in Fig. 3) seem not to affect the constant ranges and the gradients of the curves.

Thus, the solvent system consisting of n-butanol and an equal volume of aqueous solution of 0.12 M sodium p-toluenesulfonate and 0.40 or 0.48 M sodium chloride (curve III or IV in Fig. 3) was found to possess at common temperature the linear isotherms with adequate K-values for clupeine sulfate, so far as its concentration was less than 0.2 per cent in the total volume of both phases. In ranges of the higher concentration of clupeine, the K-values suddenly decreased (see also Fig. 3).

Dependency of the Partition Coefficient upon Temperature. — The K-values of clupeine sulfate in the solvent system consisting of n-butanol and aqueous p-toluenesulfonic acid at 0°C and 40°C were equal (Table I). On the other hand, they decreased obviously in the system of n-butanol and an equeous solution containing sodium p-toluenesulfonate and sodium chloride as temperature increased (Table II). Therefore, we must do a C.C.D. procedure with the latter system at a constant temperature.

TABLE I

DEPENDENCE of K-VALUE OF CLUPEINE SULFATE (0.02%) UPON TEMP. IN THE SYSTEM OF n-BUTANOL VS. AQ. 0.029 M p-TOLUENESULFONIC ACID

Temp. (°C)	K-value
0	0.7_5
40	0.7_9

TABLE II

DEPENDENCE OF K-VALUE OF CLUPEINE SULFATE (0.022%) UPON TEMP. IN THE SYSTEM OF n-BUTANOL VS. AQ. 0.14 M Na p-TOLUENESULFONATE—0.40 M NaCl

Temp. (°C)	K-value
1	3.9_2
11~12	2.8_3
19~20	1.5_7
34~35	1.0_3

The solvent system described in the above, well satisfies the conditions necessary for C.C.D. procedure (see principles of the method). In such a system of neutral condition, a danger of secondary transformation of protamines would be minimized. In this system the K-value can be easily controlled by changing the concentration of the components. Moreover, the presence of sodium chloride increases the capacity of the system to dissolve the sample and reduces the time necessary for the separation of phases.

The usefulness of the present system was practically proved by a preliminary experiment of C.C.D., in which the heterogeneity of clupeine sulfate was evidently demonstrated[9], contrary to Rauen's result******,3). Recently, Scanes and Tozer[19] reported the fractionation of clupeine sulfate by C.C.D. technique, using a unique solvent system, n-propanol-3 M sodium acetate (3 : 2, by volume). The fractionation efficiency of their system seems to be nearly the same as ours.

In connection with the unique effect of p-toluenesulfonate anion in the solvent system, a strange phenomenon was pointed

****** In the Rauen's system, undesirably small K-values were obtained for the sulfates of clupine[3] and mugiline-β[11].

19) F. S. Scanes and B. T. Tozer, *Biochem. J.*, **63**, 565 (1956).

out by Pierce[20] in the case of C.C.D. of an ox pituitary growth hormone. In spite of the fact that the distribution pattern of the hormone protein agreed with the theoretical curve in the solvent system consisting of *sec*-butanol and 0.0044 M aqueous *p*-toluenesulfonic acid, some disagreement was found between the experimental and theoretical curves, when the acid concentration was 0.0022 M. This phenomenon might be explained by such non-linearity of the partition isotherm of the hormone as is shown above in clupeine, though Pierce denied its possibility in his paper.

Summary

The conditions and solvent system suitable for C.C.D. of clupeine sulfate, were systematically studied and the following results were obtained.

1. In the solvent system consisting of *n*-butanol and aqueous hydrochloric, acetic or picric acid, the partition coefficient (K) of clupeine sulfate was almost zero.
2. In the system consisting of *n*-butanol and aqueous dichloroacetic, trichloroacetic or *p*-toluenesulfonic acid, the K-value increased with the increase of the acid concentration at a constant solute concentration. In the last system, at a constant acid concentration, the K-value decreased with the increase of the solute concentration.
3. The system consisting of *n*-butanol and an equal volume of aqueous solution containing 0.12 M sodium *p*-toluenesulfonate and 0.40 or 0.48 M sodium chloride was found to satisfy all the conditions necessary for the C.C.D. of clupeine sulfate.

The author wishes to express his hearty thanks to Professor T. Ando for his guidance and encouragement throughout this work, as well as to Dr. I. Ishii for his helpful discussions and also to Dr. C. Hashimoto for her cooperation in the preparation of clupeine. The present work was supported in part by the Scientific Research Grant from the Ministry of Education given to Professor T. Ando.

Department of Biophysics and Biochemistry, Faculty of Science the University of Tokyo Hongo, Tokyo

20) J. G. Pierce, ibid., **57**, 16 (1954).

Crystal and Molecular Structure of 1-Oxa-azulan-2-one. I. X-ray Determination of Crystal Structure

By Yoshio SASADA

(Received August 18, 1958)

We investigated previously the crystal and molecular structures of sodium salt[1] and hydrochloride of tropolone[2,3] as a part of the serial structural studies of the compounds containing planar seven-membered carbon rings. We have extended our study to the related compounds of azulene. Azulene, a fused five- and seven-membered ring system, is a well-known representative of non-benzenic aromatic compounds. Since Hückel[4] explained the large dipole moment of this compound by molecular orbital treatment, many theoretical and experimental researches especially measurements of dipole moment and absorption spectra, on azulene and its derivatives have been made. These studies were reviewed by several authors[5]. However, there have appeared only a few investigations using diffraction methods which can determine the molecular structures in detail. Even for the mother substance, azulene, it was in 1956 that its structure was reported by Takeuchi and Pepinsky[6] and Robertson and Shearer[7] independently, but no accurate molecular dimension sufficient to discuss in comparison with the theoretical results has

1) Y. Sasada and I. Nitta, *Acta Cryst.*, **9**, 205 (1956).
2) Y. Sasada, K. Osaki and I. Nitta, ibid., **7**, 113 (1954).
3) Y. Sasada and I. Nitta, This Bulletin, **30**, 62 (1957).
4) E. Hückel, *Z. Physik.*, **70**, 204 (1931).
5) e. g., M. Gordon, *Chem. Rev.*, **50**, 127 (1952).
6) Y. Takeuchi and R. Pepinsky, *Science*, **124**, 126 (1956).
7) J. M. Robertson and H. M. M. Shearer, *Nature*, **172**, 885 (1956).

yet been reported. The other few papers on structures of azulene derivatives[8] deal only with crystal data or approximate structures.

Thus the accurate determination of these compounds by means of X-ray analyses will be desirable to the structural chemistry of non-benzenic aromatic compounds. Moreover, the accumulation of knowledge on the molecular orientation in the crystals so determined may contribute to the crystal chemistry of organic compounds, because, for example, azulene is isomer to naphthalene but the electron density distributions in the molecules are more or less different from each other.

Nozoe and his collaborators[9] have obtained, since several years ago, many related compounds of azulene from corresponding derivatives of tropolone, and they kindly supplied us with their valuable products. We have determined the crystallographic data of these compounds[10], some of which were further analysed[11,12]. The present account deals with the structure determination of 1-oxa-azulan-2-one, together with some remarks on the method of X-ray analysis.

Experimental

Crystals are obtained as very fine yellow needles elongated in the *c* axis direction.

Crystallographic and physical data obtained are as follows:

1-Oxa-azulan-2-one, $C_9H_6O_2$, m. p. 69~70°C; Orthorhombic; $a=21.45\pm0.08$, $b=8.28\pm0.04$, $c=3.96\pm0.02$ Å; Absent spectra, $(h00)$, $(0k0)$ and $(00l)$ when h, k and l are odd respectively; Space group, $P2_12_12_1-D_2^4$; Four molecules per unit cell; Volume of unit cell, 703 Å^3; Density (by floatation); 1.36 g. cm^{-3}; Density (calc.), 1.38 g. cm^{-3}; Linear absorption coefficient for Cu K_α radiation, $\mu=9.45$ cm^{-1}; Total number of electrons per unit cell, $F(000)=304$.

For the structure analysis, a complete set of relative intensities for $(hk0)$, $(hk1)$ and $(hk2)$ was obtained by the integrated Weissenberg procedure. The specimen used has the following maximum and minimum dimensions at right angles to the axis of rotation: 0.01×0.02 cm.

Intensities were estimated by visual comparison with a calibrated scale. The multiple-film technique was used to correlate strong and weak reflexions, ranging in relative intensities from 22000 to 1. Reflexions from only 128 planes were observed out of 232 possible $(hk0)$'s. The corrections for polarization and Lorentz factors were made in the usual way, and that for absorption was neglected.

Results and Discussion

Structure Determination. — Patterson functions[13] have been customarily used in order to obtain some clues to the structure determination problems. However, the two-dimensional Patterson method is generally powerless in the case of the crystals containing no heavy atoms.

For several years, proposals of the so-called direct methods of crystal analysis[14,15] have been made and some of them were applied with success to the actual structure determinations. However, these successful applications are only for the fortunate cases. Some empirical remarks on this point were made by Watase and Nitta[16]. The cause of the inapplicability is due to the fact that the limiting conditions for deriving these analytical forms, such as the non-negativity principle of electron density, are scarcely severe enough. As the actual situations are more complicated, analytical processes based on such rather simple conditions are not enough to solve the crystal structures containing more than, e. g. five independent atoms in the cell.

Therefore the applications of the systematic methods mentioned above may not be effective for the present case. Otherwise information given by individual intensity of each reflexion had to be used carefully as it is.

The very short period of the *c* axis suggests that the approximate crystal structure can be obtained by the use of the $(hk0)$ reflexions alone. The starting-point was very favorable; that is, the shape of the molecule was already known from the preceding studies of the related compounds. Moreover, the shortest axis of the unit cell strongly limited the inclination of the molecular plane to the (001) plane.

As the plane group of this projection is *pgg*, the structure factors are represented as follows:

For the reflexions with $h+k=2n$

$$F(hk0)=\sum_j f_j \cos 2\pi hx_j \cos 2\pi ky_j$$

and for the reflexions with $h+k=2n+1$

8) e. g., K. H. Jost, *Naturwiss.*, **43**, 224 (1956).
9) T. Nozoe, Festschrift Arthur Stoll (Birkhauser A.G.) Basel, p 746 (1957).
10) Y. Sasada, to be published.
11) C. Tamura, Y. Sasada and I. Nitta, to be published.
12) Y. Takaki, Y. Sasada and I. Nitta, to be published.
13) A. L. Patterson, *Z. Krist.*, **90**, 517 (1935).
14) D. Harker and J. S. Kasper, *Acta Cryst.*, **1**, 70 (1948).
15) J. Karle and H. Hauptmann, ibid., **3**, 181 (1950).
16) H. Watase and I. Nitta, This Bulletin, **31**, 714 (1958).

$$F(hk0) = -\sum_j f_j \sin 2\pi hx_j \sin 2\pi ky_j$$

The structure factor maps, graphical representations of the above formulae, were made for all reflexions in the region within $2\sin\theta = 1.2$, the maps being drawn in the scale of 4 cm. = 1 Å.

The planes with very strong or weak intensities in the region with small $2\sin\theta$ severely limit the allowable approximate regions of molecular position and orientation together with symmetry considerations. For example, the value of the unitary structure factor of (400) is 0.36 and that of (200) is very small. As shown in Fig. 1, these facts require that the molecule should be in the regions A or B

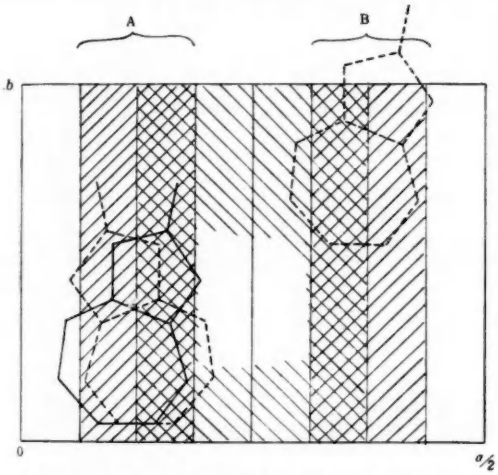

Fig. 1. Example of the determination of the allowable approximate regions using the structure factor maps. The areas shaded with lines obliqued right and left represent the negative regions in the structure factor maps of (400) and (200) respectively.

and the direction of the long axis of the molecule is nearly parallel to the *b* axis. From symmetry considerations, the molecule shown by the dotted line in the region B is equivalent crystallographically to that shown by the dotted line in the region A. Therefore, it was sufficient to apply the trial only to the region A.

The number of possible sets of atomic coordinates in this region which explains the intensities of lower order reflexions was reduced by elimination because of the requirements of the intensities of the higher order reflexions using the structure factor maps. After these successive procedures the structure has been obtained for which the agreement between the observed and the calculated structure factors is fairly good. (After the completion of this structure determination, it was found that the coordinates so obtained deviated from the final positions only by 0.2 Å or less.) Then ordinary Fourier and $(F_o - F_c)$ syntheses followed.

It is noted that the distinction of two structures shown by solid and dotted lines occurs only for the structure factors $(hk0)$ with odd h. In fact, the structure shown by the dotted line, which was concluded to be false from the detailed trial for $(hk0)$ with odd h, can also give a Fourier map pretty well to some extent. The detail on this point will be discussed elsewhere.

In the structure-factor calculation, the atomic scattering factors were taken from McWeeny[17], using for oxygen $\overline{f_o} = \frac{1}{3}(f_{\parallel} + 2f_{\perp})$ and for carbon the values for 'valence states'. The corrections were made only for isotropic B factors of individual atoms, though it was observed from the $(\rho_o - \rho_c)$ map that thermal motions of some atoms were anisotropic. The best B factors were: 6.0 for O_1, C_3, C_4, C_8, C_9 and C_{10}; 7.5 for O_2, C_2, C_5, C_6 and C_7.

The R index decreased to 0.134 including the contributions from hydrogen atoms placed radially at a distance of 1.0 Å from the carbon atoms.

TABLE I

ATOMIC COORDINATES (AT ROOM TEMPERATURE)

Atom	x/a	y/b	z/c
O_1	0.100	0.552	0.218
O_2	0.169	0.721	0.470
C_2	0.158	0.588	0.344
C_3	0.194	0.448	0.319
C_4	0.180	0.173	0.110
C_5	0.145	0.051	−0.034
C_6	0.084	0.052	−0.160
C_7	0.042	0.179	−0·168
C_8	0.050	0.335	−0.043
C_9	0.101	0.399	0.115
C_{10}	0.161	0.331	0.168

In Table I are listed the final atomic coordinates. Fig. 2 shows the comparison between observed and calculated structure factors and Fig. 3 the final Fourier projection of the electron density on the (001) plane.

Determination of z Coordinates.—As this crystal is a very fine needle in shape, the Weissenberg photographs about the a and b axes could not be taken. However, the

17) R. McWeeny, *Acta Cryst.*, **4**, 513 (1951).

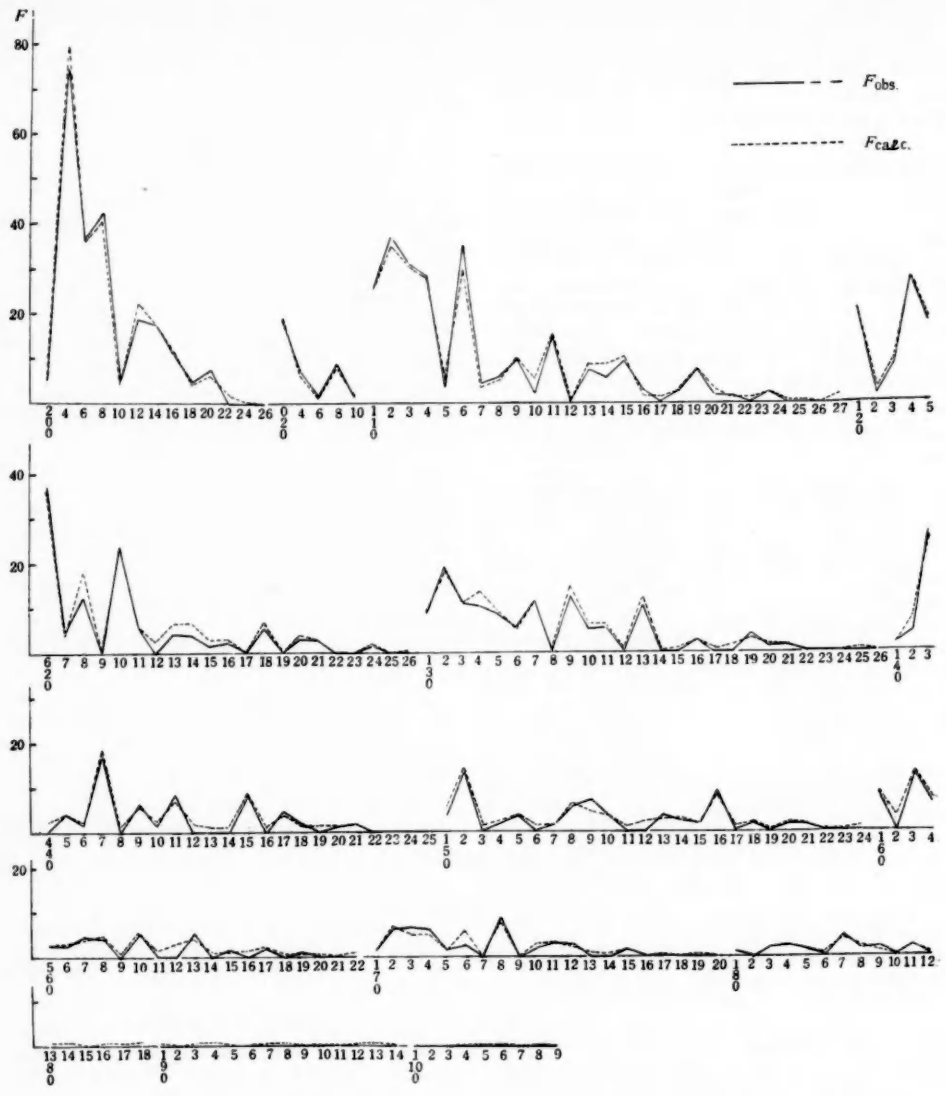

Fig. 2. Observed and calculated structure factors, $F(hk0)$.

very short period of the c axis does not require the full zonal reflexions about the a and b axes in order to estimate z coordinates. The data for $(0kl)$ and $(h0l)$ reflexions were taken from the equi-inclination Weissenberg photographs for the $(hk1)$ and $(hk2)$.

The process of the trial was very simple because the x and y parameters were already known. The coordinates so obtained were refined by the least squares method with suitable weights. For convenience, at the early two cycles, the four parameters, that is, z coordinate of the mass centre of the molecules, angles of the long and short axes of the molecule with the (001) plane and z coordinate of O_2, were corrected assuming the planarity of the fused system of five- and seven-membered rings. In the succeeding two cycles, the z coordinates of eleven atoms were shifted independently.

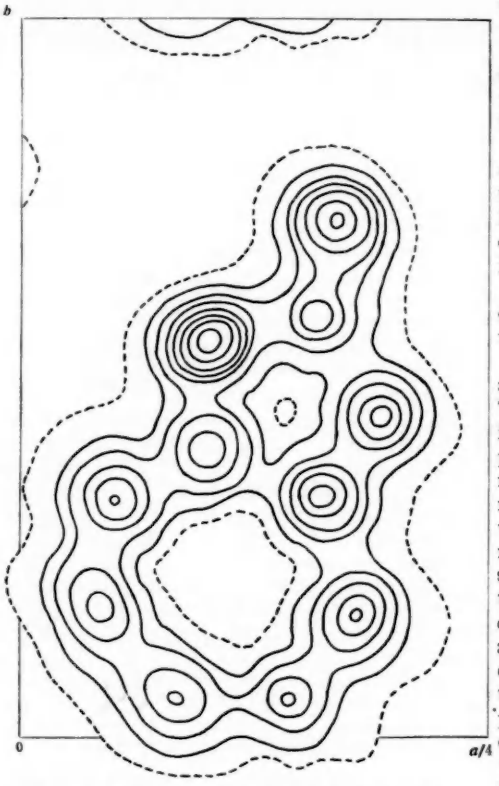

Fig. 3. The final Fourier projection of the electron density on (001). Contours at intervals of 1 e. Å^{-2}. Contour at 1 e. Å^{-2} is broken.

The final z coordinates are listed in Table I and the comparison between observed and calculated structure factors in Fig. 4.

Description of the Structure.—Fig. 5 shows the crystal structure projected on the (001) plane together with intra- and intermolecular distances.

The detailed discussions on the molecular structure are not significant, because the estimated standard deviations of bond lengths reach the values of about 0.04 Å owing to large thermal motions of atoms in the crystal.

There are no intermolecular distances deviating greatly from the sums of normal van der Waals radii.

As seen from Fig. 5, the molecular arrangement is somewhat characteristic. The seven-membered carbon ring, which is supposed to be the electrically positive part of the molecule, has as the first neighbors six five-membered rings, the negative parts, if we include the one within its own molecule. The five-membered ring is also surrounded by six seven-membered rings. Such characteristics of the molecular orientations are in contrast with those of azulene[6,7] and 2-amino azulene[12]. Mutual molecular orientations in these crystals are similar to those in naphthalene[18]. As the basic principles of the packing of molecules in organic crystals are yet to be explored, we shall only point out the parallel relation between molecular orientation and magnitudes of dipole moments of these substances. (According to Kurita and Kubo[19], the values of dipole moments are 5.64, 2.09 and 1.0 D for the present molecule, 2-amino azulene and azulene itself respectively.)

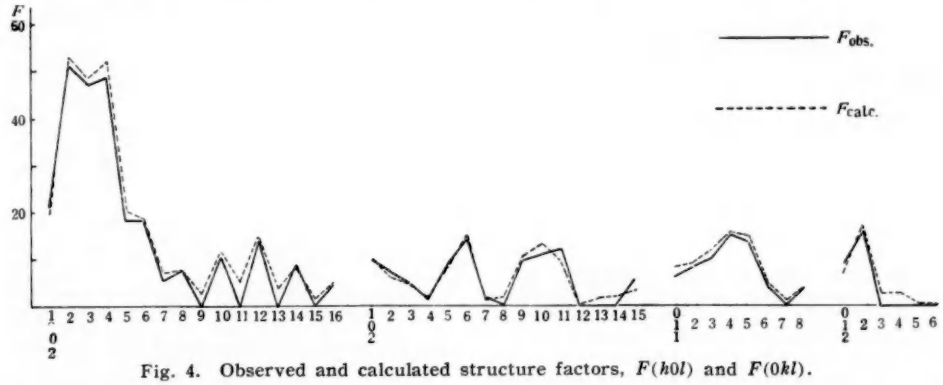

Fig. 4. Observed and calculated structure factors, $F(h0l)$ and $F(0kl)$.

18) S. C. Abrahams, J. M. Robertson and J. G. White, ibid., **2**, 238 (1949).

19) Y. Kurita and M. Kubo, to be published.

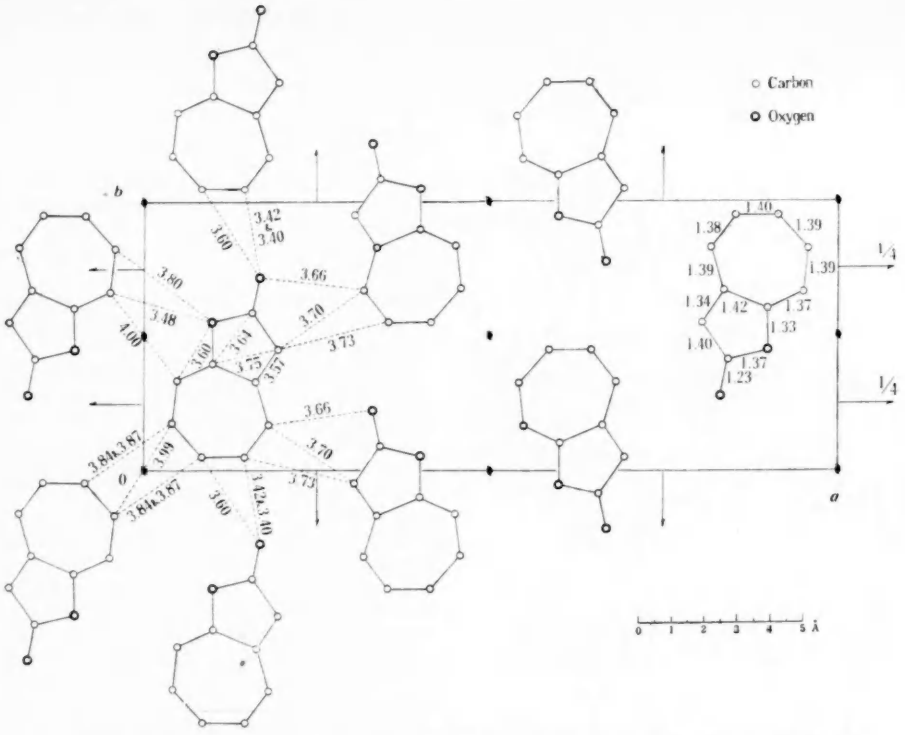

Fig. 5. Crystal structure projected on (001), together with intra- and intermolecular distances (Å).

Finally it was noticed that the *B* factor of each atom increases with increasing distance of an atom from the mass center of the molecule. This may correspond to the oscillational vibration of the molecule about its mass center.

Further discussion on these points will be given in the following paper which describes the refinement of the structure of this substance by low temperature technique.

The present author wishes to express his sincere thanks to Professor I. Nitta for his guidance and encouragement throughout this work. He is also indebted to Professor T. Nozoe for supplying the sample and also for continued interest.

Department of Chemistry
Faculty of Science
Osaka University
Kita-ku, Osaka

Crystal and Molecular Structure of 1-Oxa-azulan-2-one. II. A Refinement of the Structure by Low Temperature Technique

By Yoshio SASADA

(Received August 18, 1958)

As a part of the serial investigations of the compounds containing planar seven-membered carbon rings[1-5], the crystal structure of 1-oxa-azulan-2-one was reported in a preceding paper[6]. In that case the great thermal agitation at room temperature did not permit us to give the detailed determination of its crystal structure. The last Fourier projection indicated, moreover, considerably large anisotropic thermal vibrations of some atoms in the molecule. Therefore, it was highly desirable to carry out intensity measurement at low temperature in order to obtain the molecular dimensions with enough accuracy to discuss the molecular structure quantitatively.

Recently Cruickshank has published several papers[7,8] on the method dealing with molecular motions in crystals, which he applied to the cases of naphthalene[9,10] and anthracene[10-12] and compared the molecular vibrations obtained using X-ray data with those from infrared studies. Thus it will also be interesting to examine the thermal vibration of this polar molecule in order to make comparison with naphthalene and anthracene.

For these two main objects, the study of the crystal structure at low temperature was attempted and the present account deals with the analysis of this compound at $-110°C$.

Apparatus.—For several years, low temperature single crystal diffraction techniques have been adopted by several authors[13]. There are two main distinct procedures: one is the cold gas flow and the other the conduction method. The latter method has the advantage that good constancy of temperature is attained. However, for the present purpose, the former procedure is sufficient because fluctuation of temperature less than 5°C is allowable throughout the experiment.

The apparatus used for this work is shown in Fig. 1. This is a modification of the device described by J. H. Robertson. A large Dewar-vessel, 4 liters in volume, is fitted with a wooden cap in which there are holes for a large tube for filling, a level indicator, a vacuum jacketed nozzle and a pair of wires containing the heating element. Careful regulation of the current in this heating element allows sufficiently constant temperature to be maintained. The leakage of cold nitrogen gas, which make precise temperature control impossible, is avoided by the use of rubber packing.

The cold nitrogen stream is directed at the crystal on the goniometer head of a Weissenberg camera. A thermocouple fixed at the tip of the slit was placed between the tip of the nozzle and the crystal, the distance from the crystal being 3 mm. Difference between temperatures at this position and at the crystal was found to be less than 5°C at $-110°C$.

Special care was taken to prevent the frost from condensing on the crystal itself. For this purpose the cold nitrogen stream is surrounded by a supplementary stream of dry nitrogen gas of about 5°C. The velocity of the latter is controlled so as to reduce the frosting. When kept at $-110°C$, 0.7 litre of liquid nitrogen is necessary for one hour.

Experimental

Preliminary tests were made at 0°C, $-45°C$ and $-110°C$. The cell dimensions at these three temperatures show no sign of discontinuous change of considerable magnitude, the values being as follows: $a=21.4_5$, $b=8.28$, at 0°C; $a=21.3_7$, $b=8.28_5$, at $-45°C$; $a=21.2_6$, $b=8.28_2$Å, at $-110°C$. These values were obtained from the reflexions of (20, 0, 0) and (0, 8, 0) recorded on the same film respectively.

The intensity of each reflexion increases continuously with lowering temperature and the change of intensity is more significant with increasing angles. This corresponds to reduction of thermal motion without any phase transitions.

From these preliminary tests, it was expected that a satisfactory result for the present purpose could be obtained from an experiment at $-110°C$.

The final cell dimensions at $-110°C$ and space

1) Y. Sasada and I. Nitta, *Acta Cryst.*, **9**, 205 (1956).
2) Y. Sasada and I. Nitta, This Bulletin, **30**, 62 (1957).
3) K. Furukawa, Y. Sasada and T. Watanabé, to be published.
4) C. Tamura, Y. Sasada and I. Nitta, to be published.
5) Y. Takaki, Y. Sasada and I. Nitta, to be published.
6) Y. Sasada, This Bulletin, **32**, 165 (1959).
7) D. W. J. Cruickshank, *Acta Cryst.*, **9**, 754 (1956).
8) D. W. J. Cruickshank, ibid., **9**, 747 (1956).
9) D. W. J. Cruickshank, ibid., **10**, 504 (1957).
10) D. W. J. Cruickshank, ibid., **9**, 1005 (1956).
11) D. W. J. Cruickshank, ibid., **9**, 915 (1956).
12) D. W. J. Cruickshank, ibid., **10**, 470 (1957).
13) W. N. Lipscomb, *Norelco Rep.*, **4**, 54 (1957).

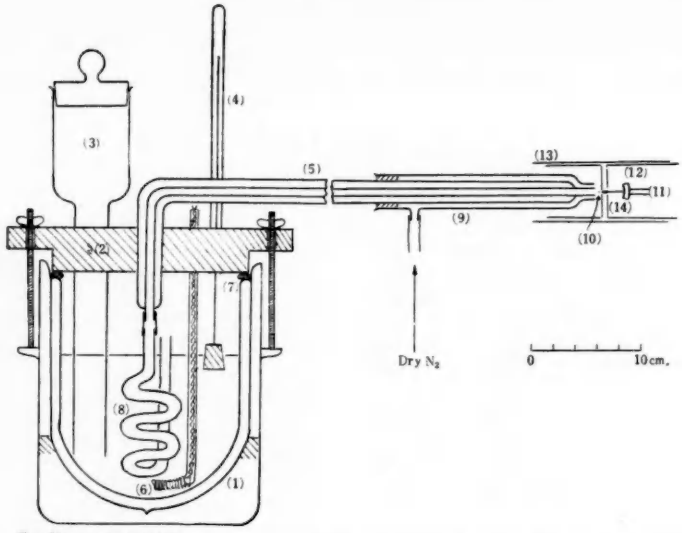

Fig. 1. Cooling apparatus.
(1) Dewar bottle. (2) Wooden cap. (3) Tube for filling. (4) Level indicator. (5) Vacuum jacketed nozzle. (6) Heating coil. (7) Rubber packing. (8) Copper tube. (9) Supplementary nozzle for dry nitrogen. (10) Thermocouple junction. (11) Goniometer head. (12) Screen. (13) Film pack. (14) Crystal.

group are: $a=21.26\pm0.06$, $b=8.28_5\pm0.04$, $c=3.91\pm0.03$Å and $P2_12_12_1$-D_2^4.

Using Cu K_α radiation, three complete sets of relative intensities for ($hk0$) were obtained by the Weissenberg procedure. Throughout the experiment temperature was kept within the range of ±5°C. The specimens used have the following maximum and minimum dimensions at right angle to the axis of rotation: crystal 1, 0.005×0.023; crystal 2, 0.004×0.018; crystal 3, 0.005×0.020 cm.

Intensities were estimated by visual comparison with a scale, which was prepared by counting the number of times of the repeating reflexion of the crystal 3. The multiple-film technique was used to correlate strong and weak reflexions, ranging in relative intensities from 25000 to 1. The corrections for polarization and Lorentz factors were made in the usual way. The effect due to the shape of the specimen was also allowed for.

The values of structure factors used in the following analysis are the weighted means of the values in the above mentioned three sets. Reflexions from 188 planes were observed out of 229 possible ($hk0$)'s.

Results

Refinement of the (001) Projection and Location of the Hydrogen Atoms. — The structure factors observed at -110°C almost agreed with those observed at room temperature, if the mean temperature factor of 4.0×10^{-16}cm^2 was applied to the former. This implies that the structure at low temperature remains essentially the same as that of room temperature so that the refinement can be made starting from the coordinates reported in the preceding paper[6].

Two successive Fourier and an (F_o-F_c) syntheses on the (001) plane were applied to correct the atomic coordinates. The corrections were estimated from the equation

$$\Delta r=(\mathrm{d}(\rho_o-\rho_c)/\mathrm{d}r)_{r=0}/2p\rho(0)$$

where $\rho(0)$ is the electron density at an atomic centre and p is a constant, whose value was deduced from the second Fourier map assuming the electron density near an atomic centre to be represented by the equation

$$\rho(r)=\rho(0)\ \exp(-pr^2)$$

In the structure-factor calculation, the atomic scattering factors were taken from McWeeny[14], using for oxygen $\overline{f}_o=\frac{1}{3}\times(f^{\parallel}+2f^{\perp})$, and for carbon the values for 'valence states'.

It was observed from the ($\rho_o-\rho_c$) map that the magnitudes of thermal motions of individual atoms are different from each other and some of them are considerably anisotropic. These thermal

14) R. McWeeny, *Acta Cryst.*, **4**, 513 (1951).

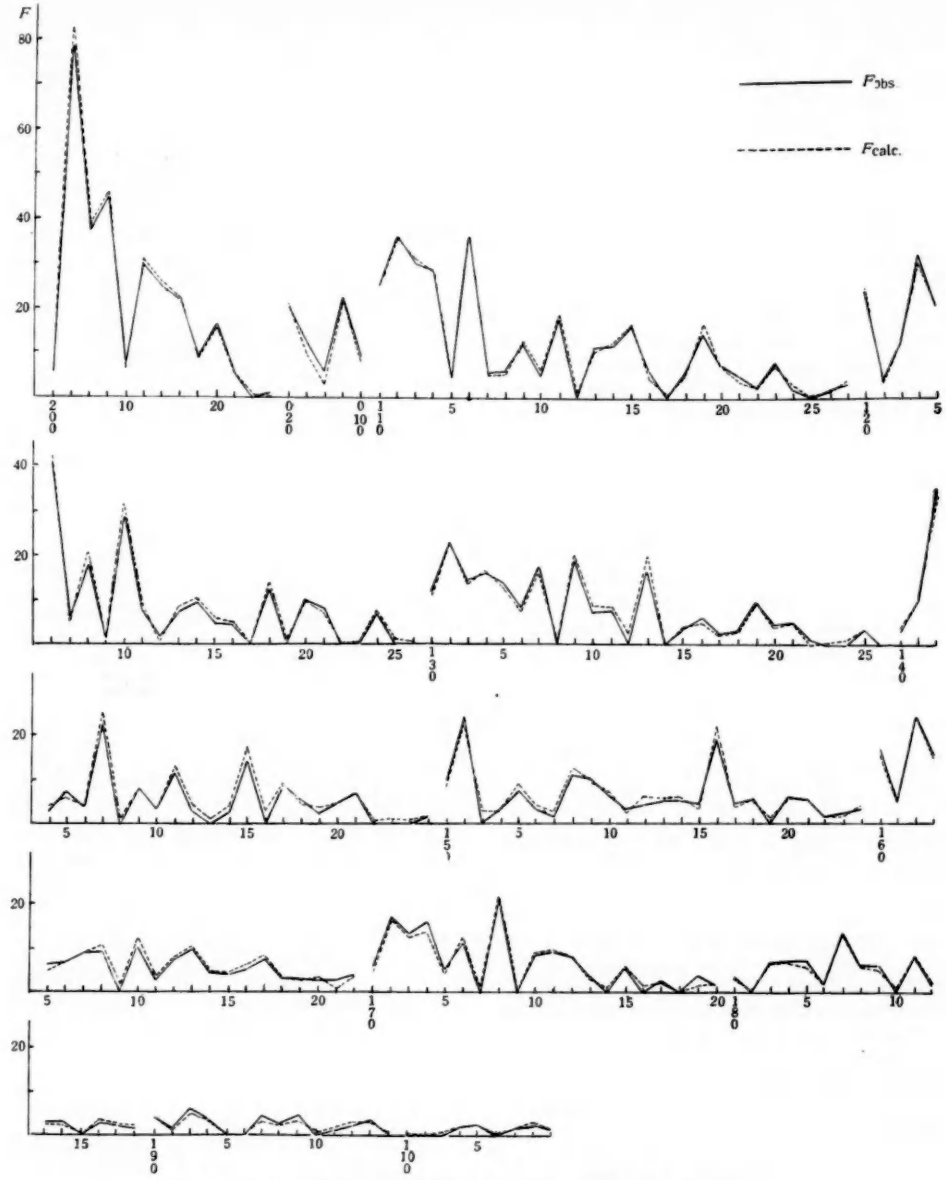

Fig. 2. Observed and calculated structure factors, $F(hk0)$.

factors for individual atoms and their anisotropy were obtained from the successive three (F_o-F_c) syntheses in the following way. The corrections for thermal factors were estimated from the equation[15]

$$\Delta B=\pi^2(\mathrm{d}^2(\rho_o-\rho_c)/\mathrm{d}r^2)_{r=0}/p^2\rho(0)$$

For the atoms vibrating anisotropically, the scattering factors of the form

$$f=f_0\exp[-\{\alpha+\beta\sin^2(\phi-\phi_b)\}(\sin\theta/\lambda)^2]$$

were employed[16,17], where α and β are

15) Y. Sasada, to be published.

16) E. W. Hughes, *J. Am. Chem. Soc.*, **63**, 1737 (1941).
17) W. Cochran, *Acta Cryst.*, **4**, 81 (1951).

constants, ψ_b is the angle between the direction of maximum vibration and the b axis, and $(2\sin\theta, \phi)$ are the polar coordinates of a point in the $(hk0)$ section of the reciprocal lattice, measured from the a^* axis. In the projection it should be noted that only two molecules are equivalent in dealing with the anisotropic vibrations.

Throughout these refinements F_c included the contributions from hydrogen atoms placed radially at a distance of 1.0 Å from the carbon atoms. In Table I are listed the final atomic coordinates and the final thermal parameters. The comparison between observed and calculated structure factors is shown in Fig. 2, where the R index becomes 0.097.

TABLE I
ATOMIC COORDINATES AND THERMAL FACTORS
(AT −110°C)

Atom	x/a	y/b	z/c	α	β	ψ_b
O_1	0.099_5	0.554	0.218	2.3	0.5	97°
O_2	0.168	0.722	0.470	2.6	1.3	87
C_2	0.157	0.589	0.344	2.8	0.5	90
C_3	0.194	0.451	0.319	2.8	0.5	85
C_4	0.180	0.169	0.110	2.3	0.5	95
C_5	0.145_5	0.050	−0.034	2.3	1.7	92
C_6	0.084_5	0.052	−0.160	2.6	1.4	83
C_7	0.042	0.175	−0.168	3.3	0	—
C_8	0.049	0.336	−0.043	2.8	0	—
C_9	0.100_5	0.398	0.115	2.2	0	—
C_{10}	0.162	0.329	0.168	2.2	0	—

Figs. 3 and 4 show the final Fourier projection on the (001) plane and the fifth $(\rho_o-\rho_c)$ map respectively. In the calculation of the latter, F_c's do not include the contributions from the hydrogen atoms. The significant peaks on this map are evidently due to the hydrogen atoms.

Coordinates and Molecular Dimensions. —The x and y coordinates obtained by the low temperature refinement hardly differ at all from those at room temperature. The z coordinates, the changes of which have scarcely any influence on the intra- and intermolecular distances due to the short c period, were expected to show no significant differences with those at room temperature. In fact, the change of the c period is of the same order as that of the a axis and a few oscillation photographs at low temperature did not show essential differences. Therefore the same z coordinates as those at room temperature are used in the following discussions. The final coordinates of the carbon and oxygen atoms are shown in Table I.

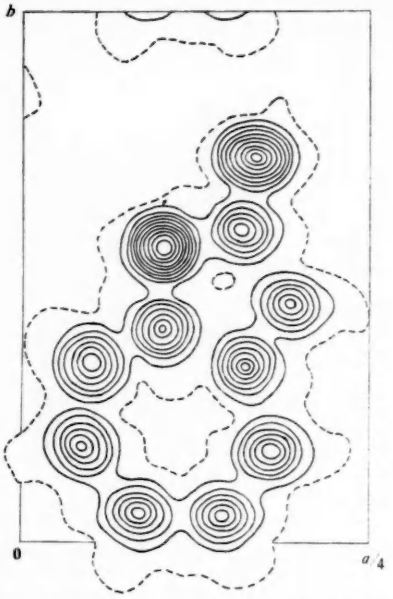

Fig. 3. The final Fourier projection of the electron density on (001). Contours at intervals of 1 e. Å^{-2}. Contour at 1 e. Å^{-2} is broken.

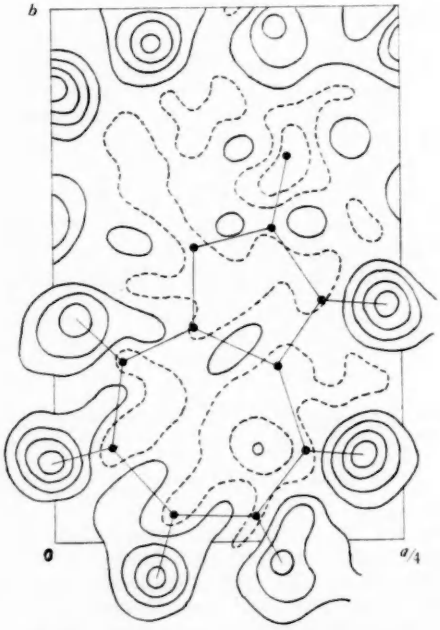

Fig. 4. The final $(\rho_o-\rho_c)$ projection on (001). Contours at intervals of 0.2 e. Å^{-2}. The zero and negative contours are broken.

By the use of least squares method the best plane through all carbon and oxygen atoms in the fused ring was determined to be

$$z = 0.3634x + 0.3192y - 1.4186$$

The perpendicular displacements of individual atoms from this mean plane are shown in Table II. The average displacement is 0.02$_1$ Å. The bond lengths and valency angles in the molecule are shown in Fig. 5 (a).

TABLE II
THE PERPENDICULAR DISPLACEMENT OF THE ATOMS FROM THE MEAN PLANE

Atom	Displacement (Å)
O_1	+0.033
O_2	+0.044
C_2	−0.007
C_3	−0.023
C_4	+0.010
C_5	+0.027
C_6	+0.002
C_7	−0.023
C_8	−0.015
C_9	+0.036
C_{10}	−0.042

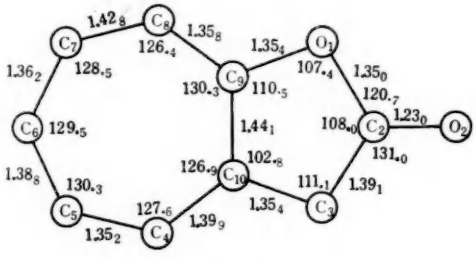

(a)

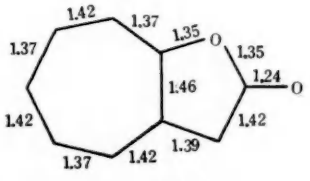

(b)

Fig. 5. (a) Observed bond lengths (Å) and bond angles (°). (b) Bond lengths calculated by Pauling's relation.

The estimated positions of hydrogen atoms from the fifth ($\rho_o - \rho_c$) map are given in Table III, the z coordinates being obtained by substituting the estimated x and y values in the equation of the mean plane of the molecule, although the assumed positions were used in the calculations of the ($hk0$) structure factors.

TABLE III
HYDROGEN COORDINATES AND BOND LENGTHS OF C—H

Atom	x(Å)	y(Å)	z(Å)
H_3	5.14	3.62	1.61
H_4	4.72	1.33	0.72
H_5	3.40	−0.31	−0.28
H_6	1.53	−0.58	−1.05
H_7	0.04	1.22	−1.02
H_8	0.36	3.46	−0.18

C_3—H_3=1.09, C_4—H_4=0.94, C_5—H_5=0.80,
C_6—H_6=1.13, C_7—H_7=0.95, C_8—H_8=0.91 Å

Estimation of Accuracy.—The standard deviations of the atomic coordinates, $\sigma(x)$ and $\sigma(y)$ were estimated by the method of Cruickshank[18-20] as follows: $\sigma(x)$ = 0.010−0.012; $\sigma(y)$ = 0.007−0.009 Å for carbon; $\sigma(x)$ = 0.007−0.008; $\sigma(y)$ = 0.005 Å for oxygen.

If the small error introduced by the uncertainty of the molecular orientation is ignored, the standard deviation of a bond length can be shown, in this case, to be

$$\sigma(b) = \sigma(d) \times b/d$$

where b is the length of the bond and d is its length in the projection on (001). From this equation the standard deviation of a C—C bond comes out to be about 0.018Å, and that of a C—O bond about 0.012 Å. The average standard deviation of bond angles was found to be 0.7°, and the standard deviation of electron density was 0.18 e. Å^{-2} for the (001) projection.

Discussion

Molecular Structure. — It is recognized clearly from Fig. 5 (a) that a larger and a

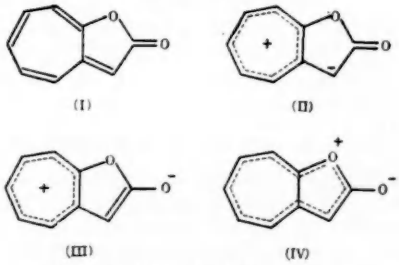

Fig. 6. Canonical formulae.

18) D. W. J. Cruickshank, ibid., **2**, 65 (1949).
19) D. W. J. Cruickshank, ibid., **7**, 519 (1954).
20) F. R. Ahmed and D. W. J. Cruickshank, ibid., **6**, 385 (1953).

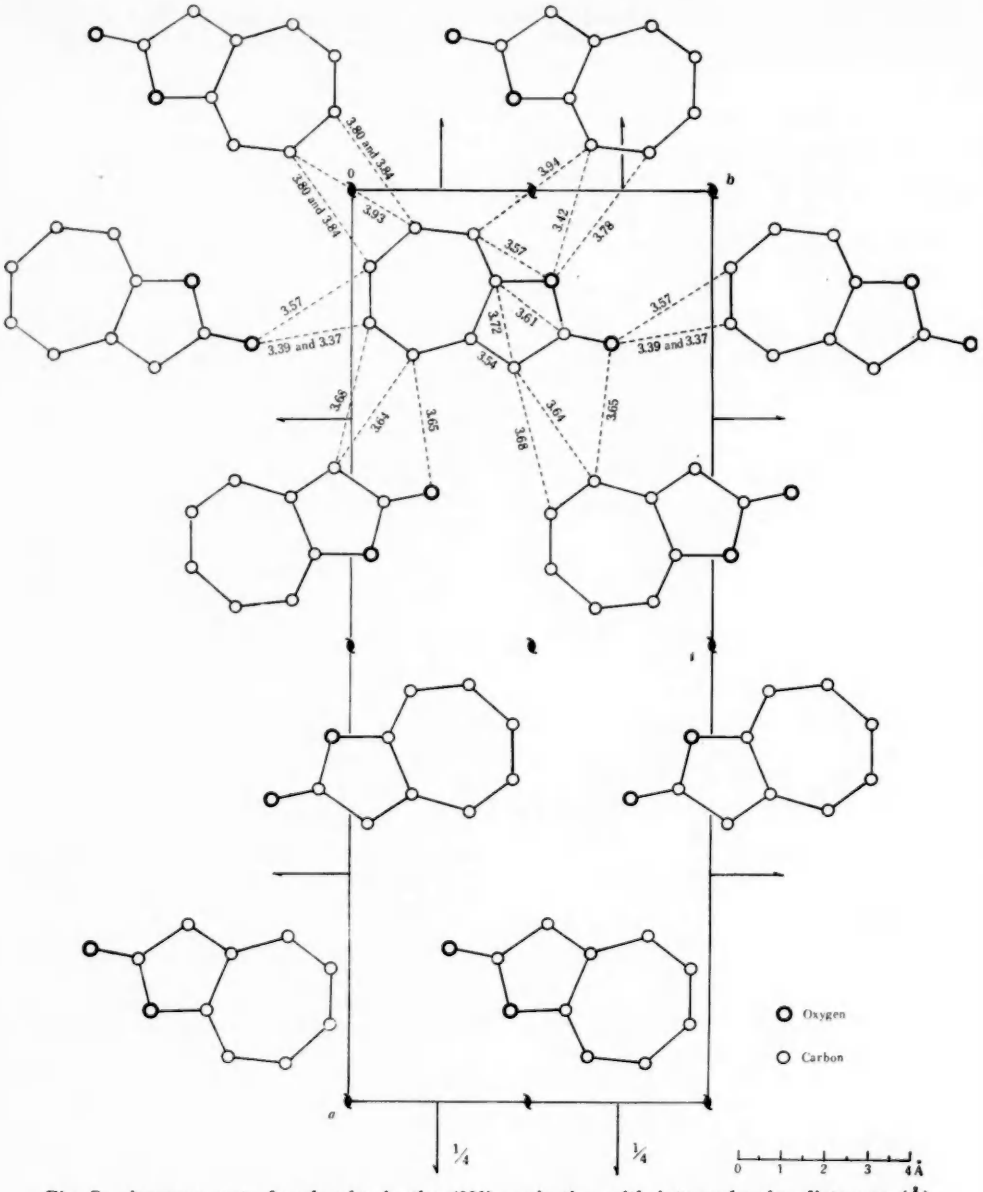

Fig. 7. Arrangement of molecules in the (001) projection with intermolecular distances (Å).

shorter C—C bonds are disposed alternately. The mean values for the larger and shorter C—C bonds are 1.40_9 and 1.35_7Å with estimated standard deviations of 0.01_0 Å respectively. The difference between these two values is highly significant, and this fact favors the conventional chemical formula I shown in Fig. 6.

However, the mean value of the larger C—C bonds and that of two C—O bonds in the five-membered ring (with standard deviation of 0.01_0 Å) are significantly different from their pure single bond lengths respectively. Thus, in order to interpret the bond distances more quantitatively, it becomes necessary to take into account the many resonance structures shown in Fig. 6.

In other words this molecule is not a simple γ-lactone but has the contributions from the structures similar to those in azulene and tropolone. As in the case of tropolone, the carbonyl oxygen is responsible for the drawing out of the ring electron and the lone pair electrons of the oxygen atom in 1-position supply the electron to carbonyl oxygen. The best agreement between measured and calculated bond lengths was obtained taking the following contributions: I, 34%; II (seven structures), each 3%; III (seven structures), each 3%; IV (two structures), each 12%, the relation[21]

$$R = R_1 - (R_1 - R_2)3x/(2x+1)$$

being used with $R_1 = 1.54$(C—C), $R_2 = 1.34$ Å (C=C), $R_1 = 1.42$ (C—O) and $R_2 = 1.20$ Å (C=O), (Fig. 5 (b)).

Considering the resonance structures given above, it seems that the seven-membered ring itself is somewhat positively charged. This is justified by the large dipole moment of this molecule[22] and by some chemical evidences[23], and also compatible with characteristic molecular arrangement in the crystal described in Part I of this series[6].

Molecular Arrangement. — The crystal structures projected on the (001) and (010)

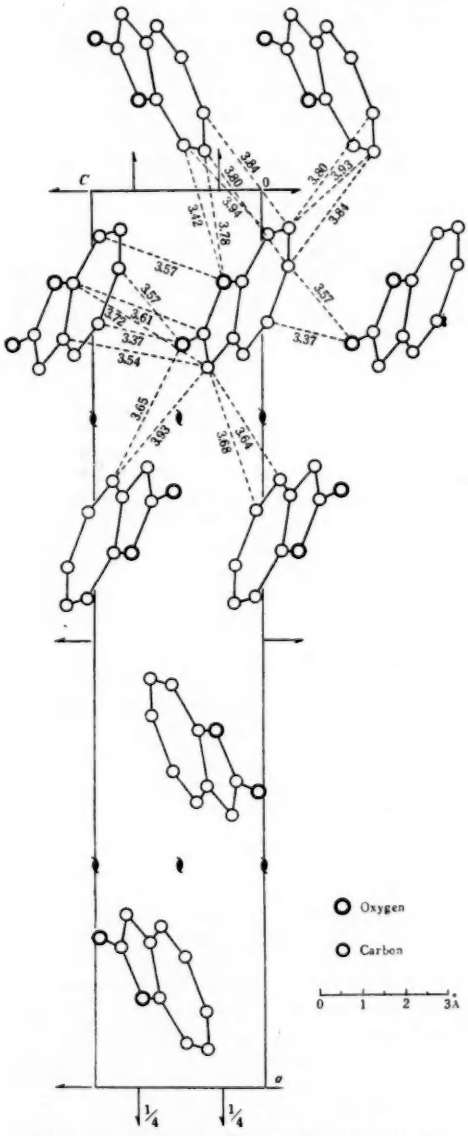

Fig. 8. Arrangement of molecules in the (010) projection with intermolecular distances (Å).

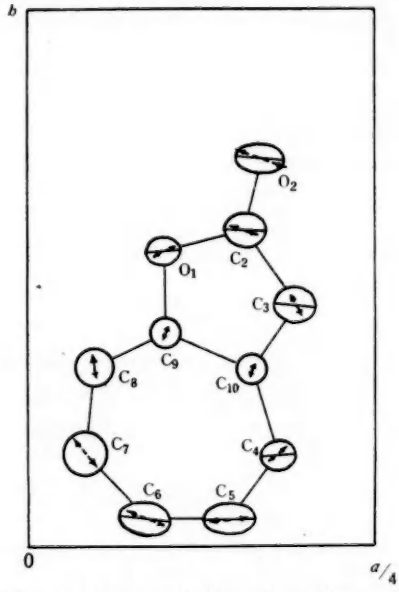

Fig. 9. Anisotropic thermal motions of individual atoms. Dimensions of solid circles and ellipses are proportional to the r. m. s. amplitudes estimated from B factors. The dotted arrows show the direction and relative magnitudes of the vibration of individual atoms due to the rigid-body angular oscillation of the molecule about its mass centre.

21) L. Pauling, "The Nature of the Chemical Bond", Ithaca, Cornell University Press, (1948).
22) Y. Kurita and M. Kubo, to be published.
23) S. Seto, *Sci. Rep. Tahoku Univ., Ser. I*, **37**, 367 (1953).

planes are shown in Figs. 7 and 8 respectively, together with the intermolecular distances. Intermolecular distances at a low temperature are shorter by about 0.03 Å than those at room temperature. Anisotropy of the change of the intermolecular distances, however, can not be detected owing to the greater standard deviations for them at room temperature.

Although an outline of the crystal structure is the same as that mentioned in Part I, the molecular arrangement can also be described as an assembly of the rods in which the molecules are joined together in a file by the interaction of dipoles in the same directions. The interaction between rods is less than that in the rod.

The thermal expansion coefficient along the *b* axis, which agrees approximately with the direction of the rod, is of negative sign, and those along the *a* and *c* axes are positive and of the same order as those in ordinary organic crystals[24]. This fact can be interpreted well from the point of view mentioned above, and will be further discussed in the following paragraph in connection with the anisotropic thermal vibrations.

Anisotropic Thermal Motion. — Fig. 9 shows the anisotropic thermal vibrations schematically. Dimensions of solid circles and ellipses are proportional to the r.m.s. amplitudes estimated from the *B* factors. These can be understood as the coupling of rigid-body libration of the molecule about its mass centre and the translational vibration whose amplitude along the *a* axis is greatest. The r. m. s. amplitudes of angular oscillation are about 3° and those of the translational vibration along the *a* and *b* axes 0.17 and 0.15 Å respectively. Contrary to the cases of naphthalene[9] and anthracene[11,12], the translational amplitude along the long axis of the molecule is smaller than that along the short axis. This is compatible with the characteristic arrangement of the polar molecules mentioned above.

The present author wishes to express his sincere thanks to Professor I. Nitta for his guidance and encouragement throughout this work. He is also indebted to Professor T. Nozoe for supplying the sample and for his continued interest and to Professor T. Watanabé for his kind advice particularly on the low temperature techniques.

Department of Chemistry, Faculty of Science, Osaka University
Kita-ku, Osaka

24) I. Woodward, *Acta Cryst.*, **11**, 441 (1958).

*The Roles of Prolyl Residue in Polypeptide Monolayers. I. On the Chain Configurations Deduced from Surface Pressure and Potential Measurements**

By Toshizo ISEMURA and Shoichi IKEDA

(Received August 25, 1958)

During the last decade, investigations on synthetic polypeptides as model substances of protein have made great progress. Their monolayer properties have also been studied and clarified by the present authors[1] and many other workers[2,3]. In these studies synthetic polypeptides with non-electrolytic or unionized electrolytic side chains are found to spread as condensed monolayers at the air-water interface. Many globular proteins also give condensed monolayers at the same interface. Generally, monolayers of high polymeric substances are of condensed type under the strong interaction between

* Surface Chemistry of Synthetic Protein Analogus VIII.

1) T. Isemura and K. Hamaguchi, This Bulletin, **26**, 425 (1953); **27**, 125. 339 (1954).
K. Hamaguchi and T. Isemura, ibid., **28**, 9 (1955).
T. Isemura, K. Hamaguchi and S. Ikeda, *J. Polymer Sci.*, **23**, 651 (1957).

2) D. F. Cheesman and J. T. Davies, *Adv. Protein Chem.*, **9**, 439 (1954).

3) C. H. Bamford, A. Elliott and W. E. Hanby, "Synthetic Polypeptides", Academic Press, New York (1956), p. 355-360.

constituent monomer units and of expanded type under the weak interaction.

Among amino acid residues constituting polypeptide chains in protein, prolyl residue is specific in respect to several properties: (1) it can not be incorporated into the β-configuration of a polypeptide chain because it has a pyrrolidine ring which makes a part of the main chain; (2) it reduces the degree of stertic rigidity because it is inhibited from rotating around some bonds involved; and (3) it can form no hydrogen bond with other carbonyl group because the nitrogen atom of keto-imido bond has no hydrogen atom to participate in the hydrogen bonding.

Synthetic polypeptides, the monolayers of which have so far been studied, contain no prolyl residue. It is of great importance to investigate how these properties of prolyl residue affect the behavior of monolayers of polypeptides and to correlate it with the chain configuration, the chain flexibility and the hydrogen bonding. These studies appear to be useful to interpret monolayer properties of gelatin and collagen.

In this connection, we have investigated the monolayers of synthetic polypetides composed of various proportions and arrangements of prolyl residues, that is, poly-DL-alanine, poly-L-prolyl-L-leucylglycine, copoly-1 : 1 : 1-(L-proline, L-leucine, DL-alanine) and poly-L-proline. Poly-L-hydroxyproline was also examined for comparison with poly-L-proline. In this paper, we will describe the results and some inferences derived from the measurements of surface pressure and potential.

Experimental

Materials.—Poly-DL-alanine is a sample prepared by Dr. Tani[4], the degree of polymerization of which was found to be about 300 by surface pressure measurement. It was spread from the solution in a mixed solvent, dichloroacetic acid-benzene (1 : 9 v/v). Poly-L-prolyl-L-leucylglycine is a sample synthesized by Dr. Sakakibara[5]. Its degree of polymerization was found to be 13 by end-group analysis and surface chemical method. Copoly-1 : 1 : 1-(L-proline, L-leucine, DL-alanine), poly-L-proline II[6] and poly-L-hydroxy-proline are gifts of Dr. Kurtz through Professor Noguchi. The degree of polymerization of copoly-1 : 1 : 1-(L-proline, L-leucine, DL-alanine) was found to be 129 by surface pressure measurement. Poly-L-prolyl-L-leucylglycine and copoly-1 : 1 : 1-(L-proline, L-leucine, DL-alanine) were spread from the solution in a mixed solvent, dichloroaceticacid-benzene (1:4 v/v). The spreading solvent for poly-L-proline II (D. P. 50) and poly-L-hydroxyproline (D. P. unknown) was 50% (v/v) isopropyl alcohol. Because of their hygroscopic nature, poly-L-prolyl-L-leucylglycine, poly-L-proline II and poly-L-hydroxyproline were dried for several hours at the boiling point of toluene in an Abderhalden's pistol, before weighing for preparing the spreading solutions. Poly-L-prolyl-L-leucylglycine contains one molecule of water of crystallization per periodic unit after such drying.

Distilled water was used as aqueous subphases, unless otherwise stated. The pH of subphases was adjusted by 0.01 N hydrochloric acid or by 0.01 M potassium carbonate, if necessary. To certify the minimum solubility of the sample into the aqueous phase, potassium chloride was often added, which was recrystallized from water after removing surface active impurities by using active charcoal as adsorbent and then baked.

Methods.—Surface pressure was measured by a surface balance of float type with a mica float and a double torque system. Its sensitivity was better than 0.01 dyne per cm. Surface potential was measured by the vibrating electrode method. The electrode was made of gold of 2 cm. in diameter. The signal picked up by the electrode was amplified by a three stage A. C. amplifier and detected by an oscilloscope. The potential was determined by the compensation method with a potentiometer. The trough was made of polymethyl methacrylate, the rim of which was coated by a thin paraffin layer to ensure a high contact angle.

All the measurements were carried out at room temperature, but the fluctuation of temperature never exceeded 1° during the experiments. The solution was spread by means of a micrometer syringe. Fifteen minutes after spreading, the compression of film was started. The films of all polypeptides other than poly-L-proline and poly-L-hydroxyproline showed no time effect.

Results

Surface pressure-area (Π-A) and surface potential-area (ΔV-A) curves of poly-DL-alanine, poly-L-prolyl-L-leucylglycine and copoly-1 : 1 : 1-(L-proline, L-leucine, DL-alanine) are shown in Figs. 1, 2, and 3, respectively. For comparison with poly-L-prolyl-L-leucylglycine, area of copoly-1 : 1 : 1-(L-proline, L-leucine, DL-alanine) in Fig. 3 was denoted in the unit of A^2 per three amino acid residues. In Fig. 4 the Π-A and ΔV-A curves of poly-L-proline together with the Π-A curve of poly-L-hydroxyproline both on 1 M potassium chloride are shown. The Π-A and ΔV-A curves of all these polypeptides other than the last

4) H. Tani and C. Ooizumi, Symposium on Synthetic Polypeptids, Osaka, Oct. 28, 1957.
5) H. Kitaoka, S. Sakakibara and H. Tani, This Bulletin, **31**, 802 (1958).
6) A. Berger, J. Kurtz and E. Katchalski, *J. Chem. Soc.*, **76**, 5552 (1954).

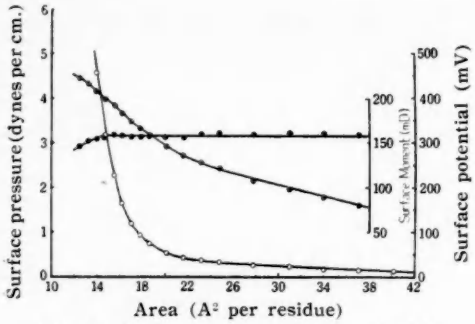

Fig. 1. Surface pressure (○), potential (⊕) and moment (●) *vs.* area curves of poly-DL-alanine at 18°C.

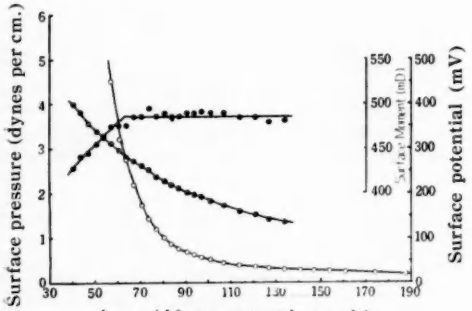

Fig. 2. Surface pressure (○), potential (⊕) and moment (●) *vs.* area curves of poly-L-prolyl-L-leucyglycine at 27°C.

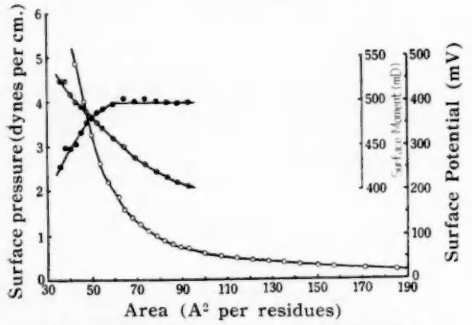

Fig. 3. Surface pressure (○), potential (⊕) and moment (●) *vs.* area curves of copoly-1 : 1 : 1-(L-proline, L-leucine, DL-alanine) at 16°C.

two were not affected by the addition of potassium chloride in the concentration of 0.1 M into the aqueous subphase. Therefore, they are considered to be spread completely as monomolecular films. The surface moment-area (μ-A) curves are also shown in these figures, which were calculated by the Helmholtz equation,

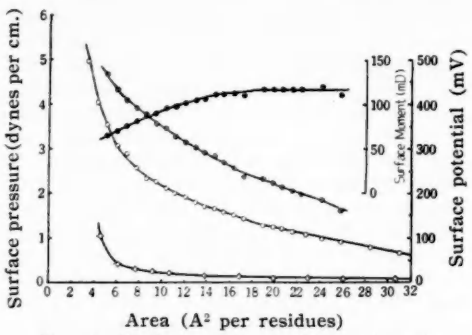

Fig. 4. Surface pressure (○), potential (⊕) and moment (●) *vs.* area curves of poly-L-proline and surface pressure-(◇) area curve of poly-L-hydroxyproline on 1 M potassium chloride at 29°C.

$$\Delta V = \frac{4\pi\mu}{A}$$

In the Π-A curve there appears an area, A_Π, where the surface compressibility

$$\delta = -\frac{1}{A}\frac{\partial A}{\partial \Pi}$$

is a minimum. This area corresponds to that occupied by a repeating unit in the close-packed monolayer. The surface moment is constant, namely, μ_c, over certain regions of area. When the monolayer is compressed, the surface moment begins to decrease at a certain definite area, A_μ. This area is that where the electric dipole of repeating unit begins to change its orientation. Since the dipole is considered to be contributed mainly by the carbonyl groups of peptide bonds in the polypeptides studied (except for poly-L-hydroxyproline), the values of surface moment are concerned with the orientation of carbonyl groups in the monolayer. All these characteristics are summarized in Table I.

TABLE I
MONOLAYER CHARACTERISTICS OF POLYPEPTIDES

Polypeptides	A_Π A² per repeating unit	A_μ A² per repeating unit	μ_c mD
Poly-DL-alanine	14.9	14.8	158
Poly-L-prolyl-L-leucyl-glycine	57	63	162×3
Copoly-1 : 1 : 1-(L-proline, L-leucine, DL-alanine)	46*	60*	166×3

* A² per three amino acid residues.

In spite of the marked difference in surface pressure among three polypeptides completely spread as monolayer, that is,

poly-DL-alanine, poly-L-prolyl-L-leucylglycine and copoly-1 : 1 : 1-(L-proline, L-leucine, DL-alanine), the values of surface moment were found to be nearly equal to one another, μ_c being about 160 mD per amino acid residue, as seen in Table I. This means that the orientation of the carbonyl groups of all these polypeptides are almost the same. Taking the electric moment of carbonyl group to be 360 mD, following Davies[7], it may be directed to 30° downwards to the aqueous surface.

Discussion

Chain Configuration in Polypeptide Films. — *a) Poly-DL-alanine.* — Poly-DL-alanine gives a monolayer of condensed type. Its Π-A and ΔV-A curves have already been reported by Glazer and Dogan[8], and its μ-A curve has been measured by Davies[7]. The Π-A curve in Fig. 1 shifts somewhat to larger area than that of Glazer and Dogan's, but the ΔV-A curve is in good agreement. The A_μ value found from the μ-A curve is much less than Davies'. The monolayer of poly-DL-alanine is much more condensed than some vinyl polymers with side-chains of the same order of length, such as polyvinyl acetate[9-12] and polyethyl acrylate[9]. This is attributed to the fact that the polypeptide chain is held together rigidly by the intrachain hydrogen bonds and is less flexible by the partial double bond nature of peptide bonds. The minor dependence of surface pressure on temperature also supports this view.

From the data in Table I, it appears probable that the β-configuration with the alternation of side-chains, methyl groups, up and down to the surface,

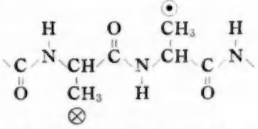

⊙ above the interface
⊗ below the interface

makes most parts of the chain, as Cumper and Alexander[13] and Davies[7,14] suggested from the surface viscosity and surface potential measurements, respectively.

b) Poly-L-prolyl-L-leucylglycine.—Recently, Leung and Marsh[15] determined the crystal structure of the tripeptide, L-leucyl-L-prolylglycine, which is similar to the repeating unit of poly-L-prolyl-L-leucylglycine. They found that all the peptide bonds are planar-*trans* and the tripeptide is in a highly extended configuration. Such a configuration appears to be probable also in this polypeptide. On the basis of these requirements and data in Table I, a possible configuration at the interface may be suggested as follows:

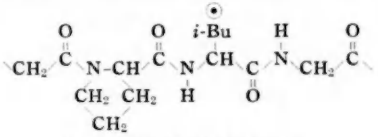

⊙ above the interface

in which the main chain assumes a β-configuration except for the glycyl-L-prolyl bond, and the side-chain of L-leucyl residue stands up out of the aqueous surface. While at the area larger than A_μ all pyrrolidine rings of L-prolyl residues lie flat on the aqueous surface, at the area less than A_μ some of them rise on the surface and at the area equal to A_{II} all of them rise and are closely packed.

c) Copoly-1 : 1 : 1-(L-proline, L-leucine, DL-alanine). — Although copoly-1 : 1 : 1-(L-proline, L-leucine, DL-alanine) has the same proline content as poly-L-prolyl-L-leucylglycine, the arrangements of prolyl and the other residues in the amino acid sequences might be different from each other. As seen in Table I, whereas the values of A_μ are equal for these two polypeptides, A_{II} for the former is much less than that of the latter. The former monolayer is more expanded. At the area larger than A_μ, their chain configurations appear to be similar to each other, and they should, however, be different at the area less than A_μ. The amino acid sequence in the former polypeptide cannot, therefore, be entirely periodic as in the latter. On the other hand, if it would contain any successive prolyl residues in some parts of the chain, no prolyl residues could always

7) J. T. Davies, *Biochim. Biophys. Acta*, **111**, 165 (1953).
8) J. Glazer and M. Z. Dogan, *Trans. Faraday Soc.*, **49**, 448 (1953).
9) D. J. Grisp, *J. Colloid Sci.*, **1**, 49 (1946).
10) G. C. Benson and R. L. McIntosh, ibid., **3**, 223 (1948).
11) T. Isemura, H. Hotta and T. Miwa, This Bulltetin, **26**, 389 (1953).
12) M. J. Shick, *J. Polymer Sci.*, **25**, 465 (1957).
13) C. W. N. Cumper and A. E. Alexander, *Trans. Faraday Soc.*, **46**, 235 (1950).
14) J. T. Davies, ibid., **49**, 949 (1953).
15) Y. C. Leung and R. F. Marsh, *Acta Cryst.*, **10**, 815 (1957); **11**, 17 (1958).

exist at the interface in an equivalent manner, orientating the pyrrolidine rings and carbonyl groups irregularly. Then the $A_{//}$ and μ_c values would be less than those observed. Thus the copolypeptide should contain the considerable amounts of L-prolyl-R-L-prolyl sequences, where R is either L-leucyl or DL-alanyl residue. Such parts of the chain will be folded by the steric hindrance and rigidity, submerging a part of the main chain into the aqueous subphase, instead of raising the pyrrolidine rings out of the surface, when the monolayer is compressed to the area less than A_{μ}. The other parts of the chain will remain the same as in poly-L-prolyl-L-leucylglycine. Hence, $A_{//}$ is much less than A_{μ}. It may, therefore, be considered that copoly-1 : 1 : 1-(L-proline, L-leucine, DL-alanine) is composed of a polypeptide with no successive but irregular arrangements of prolyl residues.

d) Poly-L-proline. — Poly-L-proline exists in two forms[16]. Poly-L-proline I is prepared by polymerization of N-carboxy-L-proline anhydride in pyridine and precipitated by adding ether to the reaction mixture. It is partly soluble in water and dextro-rotatory, $[\alpha]_D^{25} = +40°$. When it is dissolved in formic acid and precipitated by ether, it is transformed into poly-L-proline II, which is soluble in water and highly levo-rotatory, $[\alpha]_D^{25} = -540°$. But poly-L-proline I is regenerated when poly-L-proline II is dissolved into higher alcohols[17].

The poly-L-proline sample given to us was poly-L-proline II. However, at least, its most part is probably transformed into poly-L-proline I in the present spreading solution, that is, in 50% (v/v) isopropyl alcohol solution. The *II-A* curves of poly-L-proline on various aqueous subphases are shown in Fig. 5. It is unstable on salt-free subphases, and the higher the pH of the aqueous subphase, the more stable and the more expanded the film. The addition of potassium chloride into the water phase also aids the spreading of film. In any cases examined, films are of expanded type and pressure-soluble.

According to the study of X-ray diffraction by Cowan and McGavin[18], poly-L-proline II in the crystalline state exists in a left-handed helix with 3 residues per

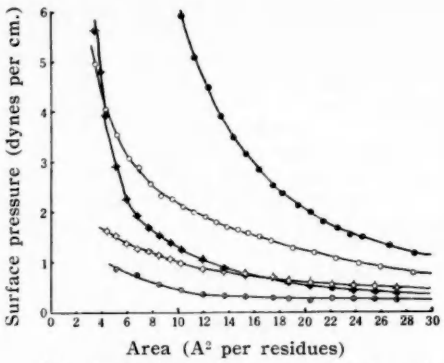

Fig. 5. Surface pressure-area curves of poly-L-proline on various aqueous subphases at 29°C: ⊖, 0.01 N HCl; ◇, H_2O; ○, 1 M KCl; ◆, 0.01 M K_2CO_3; ●, 0.01 M K_2CO_3; 1 M KCl.

turn, the keto-imido bonds being planar-*trans*. On the other hand, though no data on the structure of poly-L-proline I is available, Katchalski[17] inferred it to be a right-handed helix with *cis* bonds, and actually Crick and Rich[19] have deduced it to have approximately $3^1/_8$ residues per turn. Both structures have a high degree of steric rigidities, only permissible to the *cis-trans* transformation. Harrington and Sela[20] have demonstrated this for aqueous solutions. It will be found that no proline residues of poly-L-proline can always exist in an equivalent manner, when it is spread at the interface. Then no carbonyl groups can always orientate to the same direction, and the surface moment is, therefore, relatively low, owing to the intrachain cancellation of dipole moments. In fact, the values of μ_c did not exceed 120 mD in the cases of various subphases examined. The results obtained in the present investigation suggest that the *trans* peptide bonds in poly-L-proline dissolve into the aqueous subphase and the *cis* bonds remain on the surface, after being subjected to the *cis-trans* transformation, as soon as poly-L-proline I is spread. The lower the pH of subphase, the more feasible the transformation will be. The dependence of film behavior on the pH appears to have some correlation with the mutarotation of poly-L-proline I in formic acid, acetic acid or water. The addition of potassium chloride will support the *trans-cis* transformation, reducing the water

16) J. Kurtz, A. Berger and E. Katchalski, *Nature*, **178**, 1066 (1956).
17) E. Katchalski, Symposium on Synthetic Polypeptides, Osaka, Oct. 28, 1957.
18) P. M. Cowan and S. McGavin, *Nature*, **176**, 501 (1955).
19) F. H. C. Crick and A. Rich, cited in ref. (20).
20) W. F. Harrington and M. Sela, *Biochim. Biophys. Acta*, **27**, 24 (1958).

activity. The expanded nature of poly-L-proline films may be attributed to their being devoid of hydrogen bond, as shown later.

General Behavior of Polypeptide Monolayers.—From the *Π-A* curves in Figs. 1, 2, 3 and 4, it can be noticed that the polypeptide films change from the condensed type to the expanded type in the following order:

poly-DL-alanine;

poly-L-prolyl-L-leucylglycine;

copoly-1 : 1 : 1-(L-proline, L-leucine, DL-alanine);

poly-L-proline.

This order suggests that the higher the prolyl content, the more expanded the film, although the extent of the expansion of film depends also on the arrangement of prolyl residues in the polypeptide sequence. Even poly-DL-alanine, which has the shortest side-chain among polypeptides to be spread as monolayer, gives a very condensed film. The film of poly-L-proline is one of the most expanded.

To distinguish which factor of prolyl residue mentioned earlier is the most responsible for the expansion of film, the film of poly-L-hydroxyproline was studied which differs from poly-L-proline only in the presence of hydroxyl groups on pyrrolidine rings capable of hydrogen bonding. Its *Π-A* curve on 1 M potassium chloride solution is shown in Fig. 4. The film was unstable and spread incompletely even on such a concentrated salt solution. It is, however, of condensed type. Therefore, the expanded nature of poly-L-proline film may be attributed to the absence of hydrogen bond. The order of expansion of polypeptide films will mainly come from the fact that the prolyl residues involved reduce the number of hydrogen bonds in the film state. The hydrogen bonds in film hold the polypeptide chain together and make it rigid, and, conversely, their decrease in number will make the chain extended and flexible. Accordingly, it is believed that the chain flexibility caused by the reduced number of intrachain hydrogen bonds is generally more effective than the steric rigidity in the monolayer of polypeptide containing prolyl residues.

It is found from Table I that while the condensed poly-DL-alanine monolayer has equal values of $A_{//}$ and $A_{\perp}$, the expanded monolayer of the other two polypeptides has $A_{//}$ values less than $A_{\perp}$ values. Such a difference between monolayers of condensed and expanded type is extensively observed in other polymers so far reported. Since the condensation and expansion of monolayers of polymers are related to the intrachain interaction, this property depends on the chain configuration in monolayer. The condensed monolayer will collapse if it is compressed beyond the close-packed area, because the molecular chain is held together rigidly. In the expanded monolayer, however, the molecular chain can readily reorientate or fold itself on compression, as it is flexible. The difference in chain configuration or intrachain interaction is considered to be manifested in the monolayer property mentioned above.

Summary

To elucidate the roles of prolyl residue in polypeptide monolayers, the surface films of poly-DL-alanine, poly-L-prolyl-L-leucylglycine, copoly-1 : 1 : 1-(L-proline, L-leucine, DL-alanine), poly-L-proline and poly-L-hydroxyproline were studied by the surface pressure and potential measurements.

The area of minimum surface compressibility and the smallest area of constant surface moment were assigned to each of the first three polypeptides which were found to form monomolecular films. In the region of large area their surface moments were equal to one another and, therefore, the orientations of carbonyl groups might be the same. From these data their chain configurations at the interface were deduced. Poly-DL-alanine exists in the β-configuration and the other two have the similar configuration except for the bonds attached to prolyl residues. Based on the departure in surface pressure behavior of copoly-1 : 1 : 1-(L-proline, L-leucine, DL-alanine) from that of poly-L-prolyl-L-leucylglycine, the arrangement of prolyl residues in the sequence of the former polypeptides was discussed. In the poly-L-proline film it is likely that the parts of *cis* peptide bond form the film and the parts of *trans* bond dissolve into the aqueous subphase.

The polypeptide films were found to be more expanded as the prolyl content was higher, although the arrangement of prolyl residues also affected the expansion of film. From the comparison of poly-L-proline film with poly-L-hydroxyproline,

the evidence was obtained that the expansion of film comes from the decrease in number of hydrogen bonds because of the presence of prolyl residues. The condensation or expansion and its related properties of the film were interpreted in terms of the chain rigidity or flexibility and the intrachain interaction.

The authors are indebted to Dr. H. Tani and Dr. S. Sakakibara of the Faculty of Science, Osaka University, to Dr. J. Kurtz of the Weizmann Institute of Science in Israel and to Professor J. Noguchi of Kanazawa University for supplying the valuable samples. This work was partly supported by a grant given by the Ministry of Education, to which the authors' thanks are also due.

Institute of Scientific and Industrial Research, and Institute for Protein Research Osaka University, Osaka

---

The Electrolytic Reduction of Ketones at a Mercury Cathode.—Preparation of Organomercuric Compounds

By Toshio ARAI

(Received September 1, 1958)

Tafel[1] reported that on an electrolytic reduction, acetone might be reduced to isopropyl alcohol at a mercury cathode, and later he reported[2] that methyl ethyl ketone was reduced to diisobutyl mercury at a mercury cathode, and acetone to diisopropyl lead at a lead cathode. Haggerty[3] investigated the possibility of preparing diisobutyl mercury from acetone in a sulfuric acid solution at a mercury cathode. Dimenthyl mercury[4] was also obtained from menthone in a strong sulfuric acid electrolyte at a mercury cathode at a higher temperature.

It has been thought that on electrolytic reduction of ketones in a sulfuric acid solution at a mercury cathode, organomercury compounds are produced according to the following formula:

$$2\,\mathrm{R_2C{=}O} + 6\mathrm{H^+} + 6\mathrm{F} + \mathrm{Hg} \rightarrow \mathrm{R_2CH{-}Hg{-}CHR'_2} \qquad (1)$$

and when the organomercury compounds obtained are treated with mercuric halide in an alcoholic solution, organomercuric halides are prepared as follows:

$$\mathrm{R{-}CH_2{-}Hg{-}CH_2{-}R} + \mathrm{HgX_2} \rightarrow 2\mathrm{R{-}CH_2{-}HgX} \qquad (2)$$

It has been also recognized that when they are treated with hydrogen chloride gas in an alcoholic solution, organomercuric chloride and hydrocarbon are obtained:

$$\mathrm{R{-}CH_2{-}Hg{-}CH_2{-}R} + \mathrm{HCl} \rightarrow \mathrm{R{-}CH_2HgCl} + \mathrm{R{-}CH_3} \qquad (3)$$

The author has investigated electrolytic reduction of aryl alkyl ketones and cyclic ketones and prepared organomercury compounds from several ketones by using a diluted sulfuric acid solution at a mercury cathode at a higher temperature. Phenylacetone, acetylbenzoyl[5], cyclopentanone, cyclohexanone, and methylcyclohexanone were reduced to organomercury compounds, and their halides were prepared. These organomercury compounds were shown in Table II. The preparation of other ketones, namely, acetophenone, propiophenone, *p*-methylacetophenone, *p*-bromoacetophenone, benzoin, benzil, 1-acetonaphthone, and dibenzyl ketone were tried in this experiment in the same way, but mercury compounds were not obtained, and corresponding pinacol and alcohol were produced.

In general, it is thought that ketones which have carbonyl radical adjacent to phenyl radical are not reduced to mercury compounds.

1) J. Tafel, *Z. Elektrochem.*, **8**, 288 (1902).
2) J. Tafel, *Ber.*, **39**, 3626 (1906).
3) C. J. Haggerty, *Trans. Am. Electrochem. Soc.*, **56**, 421 (1929).
4) C. Schall and W. Kirst, *Z. Electrochem.*, **29**, 537 (1923).
5) T. Arai, unpublished.

Organomercury compounds were synthesized by many kinds of methods, and dicyclohexyl mercury and its halides were already obtained purely chemically[6,7], but other compounds obtained in this experiment, were not prepared by pure chemical methods. In this experiment the yield of organomercury compounds was not very good; this method, however, seems to be an easy and effective method of syntheses.

Experiment and Discussion

In most cases the cathodic solution consisting of 120 ml. of 5% sulfuric acid in which a ketone was suspended and alcohol was not used as electrolyte. A 5% solution of sulfuric acid served as an anodic solution and cylindrical lead was employed as anode. The anode was separated from the catholyte by means of porous pot. An electrical connection was made with the mercury at the bottom of a cathode by means of platinum wire sealed into a glass narrow tubing. Mercury was purified by washing with nitric acid. The electrolyte was first heated to 50° and during the electrolysis the catholyte was maintained at 50~55° by the reaction heat. The electrolytic chamber was kept upright and the cathodic solution was stirred vigorously. After the current was passed for a short time, a black turbidity appeared in the catholyte. It has been thought[3] that this turbidity seemed to be due to finely divided mercury.

As the electrolysis continued, the cathodic solution gradually cleared up. The amount of electric current passed was about one and a half of the theoretical one. After the electrolysis, a heavy viscous oil floated on the surface of the mercury. The catholyte was placed in a separate funnel, the oil was removed, the residue was extracted with ether, the ether extracts were evaporated under reduced pressure and a solid residue or a viscous oil was obtained. It was mercury compound and the yield of crude product was about 25~30% of the theoretical amount. As the compounds was unstable,

TABLE I

ELECTROLYTIC CONDITIONS

Cathode: Hg 15.2 cm^2; anode: Pb, cylindrical; anolyte: 5% H_2SO_4

Ketones	wt. (g.)	Elect. current amp.	Elect. current hours	Temp. °C	Catholyte	Products
Phenylacetone ($C_6H_5CH_2COCH_3$)	7	2	6	18°	5% H_2SO_4 120 ml.	Recovered
〃	10	2	6	20°	30% H_2SO_4 120 ml.	Hg Compd.
〃	10	3	4	55°	5% H_2SO_4 120 ml.	〃
〃	10	2	6	18°	6 N HCl 60 ml. + glac. HAc 60 ml.	〃
Cyclopentanone 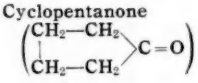	12	2	8.5	16°	5% H_2SO_4 120 ml.	〃
〃	15	3	5	50°	5% H_2SO_4 120 ml.	〃
〃	10	3	5	20°	6 N HCl 60 ml. + 50% H_2SO_4 60 ml.	〃
〃	10	3	5	21°	6 N HCl 60 ml. + glac. HAc 60 ml.	〃
Cyclohexanone 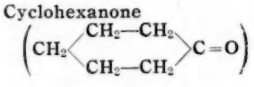	20	4	6	55°	5% H_2SO_4 120 ml.	〃
〃	50	4	15	55°	5% H_2SO_4 90 ml.	Pinacol and Hg Compd.
〃	12	3.5	5	16°	30% H_2SO_4 120 ml.	Hg Compd.
2-Methylcyclohexanone	10	3	4	55°	5% H_2SO_4 120 ml.	〃
3-Methylcyclohexanone	10	3	4	55°	5% H_2SO_4 120 ml.	〃
4-Methylcyclohexanone	10	3	4	55°	5% H_2SO_4 120 ml.	〃
Menthone 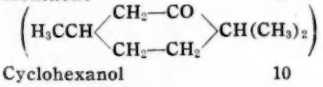	10	3	4	60°	50% H_2SO_4 120 ml.	Recovered
Cyclohexanol	10	6	8	60°	50% H_2SO_4 120 ml.	〃
Dibenzylketone ($C_6H_5CH_2COCH_2C_6H_5$)	8	6	6	60°	50% H_2SO_4 120 ml.	〃

6) G. Gruttner, *Ber.*, **47**, 1651 (1914).

7) O. Tiffeneau and O. Gannage, *Chem. Zentr.*, **1**, 766 (1921).

TABLE II

PROPERTIES OF ORGANOMERCURY COMPOUNDS

R—Hg—R (Group I)

R—	m.p. °C	Appearance	Solvent	Hg % Calcd.	Hg % Found	References
$C_6H_5CH_2CH(CH_3)$—	69～71°	needles	Et-OH	48.25	48.45	
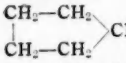	106～108°	needles	50% Et-OH	59.20	59.51	
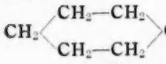	149～151°	needles	50% Et-OH	54.68	54.45	6,7
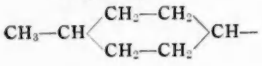	172～174°	needles	Et-OH	50.80	50.41	7

R—Hg—X (Group II)

$C_6H_5CH_2CH(CH_3)$—HgCl	80～81°	needles	Et-OH	56.47	56.49	
$C_6H_5CH_2CH(CH_3)$—HgBr	88°	needles	Et-OH	50.19	50.05	
$C_6H_5CH_2CH(CH_3)$—HgI	90°	needles→ pale yellow	Et-OH	44.91	44.71	
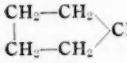	106～107°	needles	Et-OH	65.73	65.58	10
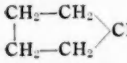	108～109°	leaflets	Et-OH	57.37	56.37	
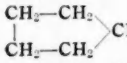	117～118°	needles→ pale yellow	Et-OH	50.57	50.40	
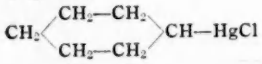	158°	needles	50% Me_2CO	62.84	61.90	7,9
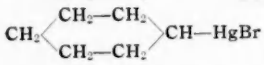	141～142°	leaflets	50% Me_2CO	55.16	54.79	6,9
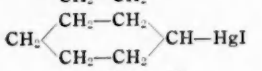	142～144°	needles→ pale yellow	Et-OH	48.85	48.75	7
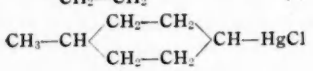	161～162°	plates	Et-OH	60.56	60.62	7
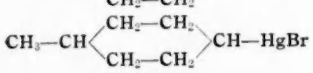	157°	leaflets	80% Et-OH	53.39	53.17	7
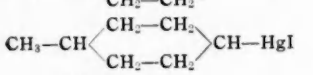	144°	plates	80% Et-OH	47.26	46.86	
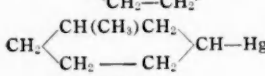	86～87°	needles	50% Et-OH	60.56	60.51	
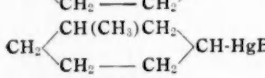	87～89°	plates	50% Et-OH	53.39	53.02	
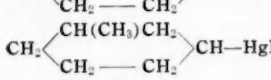	85～86°	plates	Et-OH	47.26	46.28	
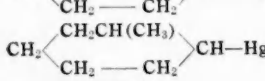	66～67°	needles	Et-OH	60.56	60.35	
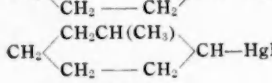	64～65°	leaflets	50% Et-OH	53.39	53.10	
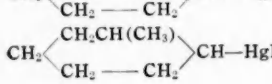	68～69°	plates	50% Et-OH	47.26	46.95	

crude product was dissolved in alcohol and the solution was used to prepare organomercuric halides. The product was crystallized from dilute alcohol, but some mercury compounds were difficult to crystallize.

The compound in the product was heated with alcoholic solutions of mercuric chloride, mercuric bromide, or mercuric iodide and white precipitates were formed as shown by Eq. 2. These substances were organomercuric halides; they were recrystallized from alcohol or acetone, and fine crystals were obtained. A quantitative yield was obtained.

The crude products were dissolved in alcohol and hydrogen chloride was passed into the solution and the hot reddish solution was cooled in an ice bath. Precipitates were produced as seen in Eq. 3; they were filtered and recrystallized from dilute alcohol containing charcoal. Fine crystals were obtained. It was organomercuric chloride and was identical with the compound obtained by treating the crude organomercury compound with mercuric chloride.

The analysis of mercury was carried out according to the convenient thiocyanate method recommended by Kharasch and Flenner (cited by Hillebrand and Lundell[8]) and good results were obtained.

The influence of various electrolytic conditions on the reduction of several ketones are shown in Table I. Phenyl acetone was not reduced to mercury compound in 5% sulfuric acid solution at a low temperature; it was recovered almost intact, and was not reduced to secondary alcohol or pinacol. It was mercurised in 30% sulfuric acid or in a mixture of glacial acetic acid and 18% hydrochloric acid solution at a low temperature; however, it was mercurised even in 5% sulfuric acid solution at a high temperature. Cyclohexanone behaves similarly to phenylacetone. Cyclopentanone was easily mercurised at a low temperature in various cathodic solution. By the use of 50 g. of cyclohexanone, in catholyte, pinacol[11] (dihydroxy-dicyclohexyl) was produced by about half the amount.

The ketones mentioned above were reduced to mercury compound even in a mild condition; however, in the case of menthone, it was reported[10] that menthone was reduced to dimenthyl mercury only in a strong sulfuric acid at 77~80° with a high current density and to methone or menthol in a weak sulfuric acid electrolyte at a mercury cathode.

Dibenzyl ketone, which was expected to be reduced to organomercury compound and tried in this experiment, was not reduced to mercury compound.

The formation of these mercury compounds is not a continuation of a secondary-alcohol formation because secondary alcohol was not reduced by electrolytic methods under various conditions; namely, cyclohexanol was reduced under the same conditions as above mentioned, but it was recovered almost as it was.

Dialkyl mercuries are volatile liquids and miscible with organic solvents, practically insoluble in water, decompose on standing at room temperature and are sensitive to light. Diaryl mercuries are solid and stable. The mercury compounds obtained in this experiment were also solid and soluble in ether and hot alcohol, but less soluble in cold alcohol and insoluble in water. Dicyclohexyl mercury was unstable and changed its color from white to gray slowly in several hours after recrystallization. It was reported[6] that dicyclohexyl mercury was unstable and decomposed to black oil after 25 hours in a vacuum desiccator over phosphrous pentoxide. Dicyclopentyl mercury was stable as compared with the former, but both compounds turned from gray to black in a few days and at last they decomposed to yellow liquid and black residue. These compounds, above mentioned, were very unstable in the pure and dried state, but comparatively stable in sulfuric acid, ether, and alcohol. Dicycloalkyl mercury has a strong specific odor like camphor and diisopropylmercury like aromatic hydrocarbon.

It was reported[7] that di-4-methylcyclohexyl mercury was a liquid, but this compound is a crystal and di-3-methyl, and di-2-methylcyclohexyl mercury might be solid; however, they were not obtained crystalline in this experiment and it seems that they have a lower melting point compared with the melting point of its halides, and di-4-methylcyclohexyl mercury and its halide have a high melting point owing to its symmetric structure.

Organomercuric halides are exceedingly stable, and are fine crystals with sharp melting points without odor; they are soluble in pyridine, hot alcohol, and acetone, less soluble in alcohol and insoluble in water. Iodides are white crystals, but their color changes to yellow on standing very slowly.

8) W. F. Hillebrand and G. E. F. Lundell, "Applied Inorganic Analysis," John Wiley & Sons, New York, (1953).
9) E. L. Hill, *J. Am. Chem. Soc.*, **50**, 167 (1928).
10) N. Turkiewitz and St. Pilat, *Ber.*, **71**, 284 (1938).
11) 1,1-dihydroxydicyclohexyl, m. p. 129~130°, plates.

The author expresses his sincere thanks to Professor Buhei Sakurai for his kind guidance and encouragement throughout this experiment.

Department of Chemistry, Faculty of Liberal Arts and Science
Shinshu University
Matsumoto

Syntheses of Pyrimidine Derivatives. XVII. On the Reaction Mechanism of Some Pyrimidine Syntheses

By Akira TAKAMIZAWA, Kanji TOKUYAMA and Kazuo TORI

(Received September 3, 1958)

Some interesting reactions have been presented in the previous papers[1-4] dealing with the syntheses of pyrimidine derivatives from 3-alkoxypropionitriles and acetamidine. These reactions can be divided into two types according to their reaction behavior, which are represented by A and B. In the case of reaction A, 2-methyl-4-amino-5-ethoxymethylpyrimidine (II) can be obtained directly by the reaction of 2-methoxymethylene-3-ethoxypropionitrile (I) with acetamidine.

On the other hand, in the case of the reaction of 2-methoxyethoxymethyl-3-ethoxypropionitrile (III) (derived from I) with acetamidine in alcohol, an intermediate IV′ can be detected spectrophotometrically in the reaction mixture (λ_{max} = 275 mμ), without being successfully isolated. Being heated with another one mole of acetamidine, the intermediate IV′ is converted into 2,7-dimethyl-5,6-dihydropyrimido(4,5-d)pyrimidine (V), hydrolysis of which produces 2-methyl-4-amino-5-acetaminomethylpyrimidine (VI), but treatment of IV′ with hydrogen chloride results in II (Reaction B). In view of these facts, the structure of IV′ has reasonably been supposed as 2-acetamidinomethylene-3-ethoxypropionitrile (IV). Besides the above-mentioned facts, it has been shown[5,6] that 2-methyl-4-hydroxy-5-ethoxymethylpyrimidine (VII) could be obtained by the reaction of ethyl 2-methoxymethylene-3-ethoxypropionate (VIII) or ethyl 2-methoxyethoxymethyl-3-ethoxypropionate (IX) with acetamidine in ethanol. One of the important purposes of the present investigations is to identify IV′ with IV, and to present the most reasonable mechanism of these reactions. Another purpose is to check and see if the mechanism of analogous reactions can be explained in a similar manner.

Identification of the Intermediate IV′.— In order to compare the structure of the intermediate IV′ with that of IV, the

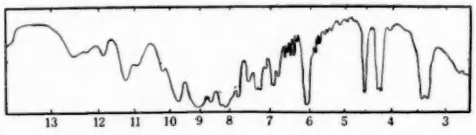

Fig. 1. Infrared absorption spectrum of 2-ethoxymethylene-3-ethoxypropionitrile (X) in nujol. 4.51 μ (conj. C≡N), 6.08 μ (—C=C—), 8.17 μ (=C—O—C). (Perkin-Elmer Model 12C IR spectrometer).

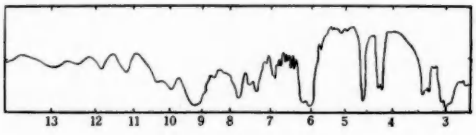

Fig. 2. Infrared absorption spectrum of 2-aminomethylene-3-ethoxypropionitrile (XI) in nujol. 2.85 μ, 2.95 μ (NH_2), 4.56 μ (conj. C≡N), 6.05 μ (—C=C—), 6.19 μ (δ NH_2). (Perkin-Elmer Model 12C IR spectrometer).

1) M. Tomita, S. Uyeo, A. Takamizawa and R. Maeda, *J. Pharm. Soc. Japan*, (*Yakugaku Zasshi*), **74**, 742 (1954); A. Takamizawa and R. Maeda, ibid., **74**, 746 (1954); A. Takamizawa, ibid., 748, 759 (1954).
2) A. Takamizawa, K. Ikawa and M. Narisada, ibid., **78**, 832, 637, 643 (1958).
3) A. Takamizawa, K. Ikawa and K. Tori, ibid., **78**, 649 (1958).
4) A. Takamizawa, S. Hayashi and K. Tori, ibid., **78**, 1166 (1958).
5) A. Takamizawa, ibid., **74**, 752, 756 (1954).
6) A. Takamizawa, K. Tokuyama and H. Satoh, ibid., **79**, (1959), in press.

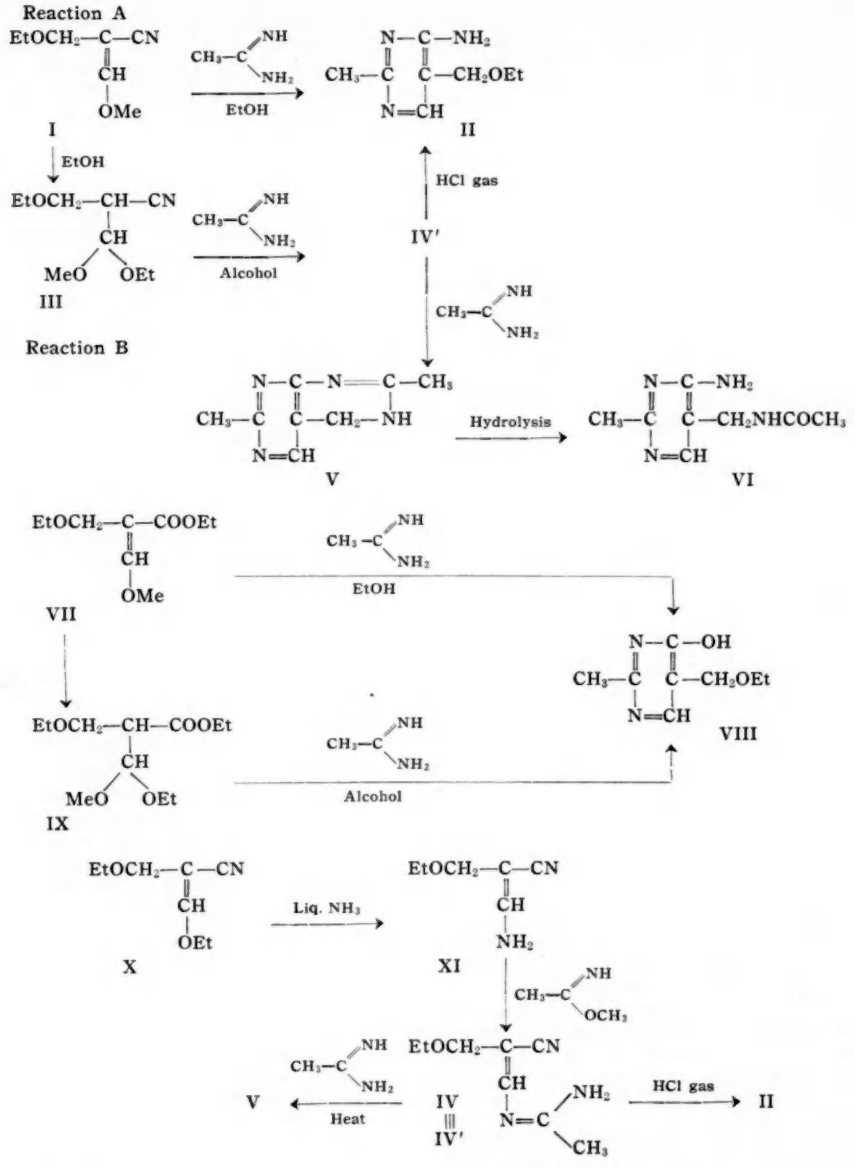

synthesis of the latter from 2-aminomethylene-3-ethoxypropionitrile (XI) and acetiminomethyl ester was undertaken. 2-Ethoxymethylene-3-ethoxypropionitrile (X) was dissolved in liquid ammonia, and after this solution was kept for a long time at room temperature, XI was obtained as a dark brown viscous liquid. The infrared spectra of this product and X were measured. From the results given in Figs. 1 and 2, it is clear that the absorption band due to —C=C—O— group of initial substance X disappears and that of an amino group newly appears. XI thus obtained being unstable, it easily liberated ammonia on heating. Furthermore, its picrate, hydrochloride, etc. could not be derived because of its weak basicity, and the expected derivatives could not be formed by the reactions of XI with acetic

anhydride, methyl iodide and 2,4-dinitrobromobenzene, but acetamide, ammonium iodide and 2,4-dinitroaniline were obtained, respectively.

It is quite natural to expect that IV can be prepared by the reaction of XI with acetiminomethyl ester. The reaction process was traced spectrophotometrically. The result given in Fig. 3 shows that the product has an absorption band (λ_{max}= 275 mμ) identical with that of the intermediate IV′ in the reaction B. The reaction mixture was converted into II by adding hydrochloric acid under cooling and into V by treating with acetamidine under heating. From the above facts, it seems conclusive that the intermediate IV′ is identical with IV.

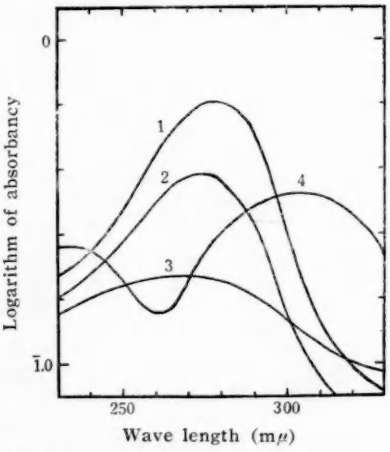

Fig. 3. Changes of ultraviolet absorption spectra of the reaction mixture, XI and acetiminomethyl ester. Curve (1), XI: (2), after 12 hr. at room temperature (IV was formed): (3) after treating IV (curve (2)) with hydrochloric acid gas: (4) after treating IV (curve (2)) with acetamidine. (Beckman DU spectrophotometer).

Reaction Mechanism of Pyrimidine Syntheses.—Thus it is easily inferred that there are two reaction processes for pyrimidine syntheses: namely, the first (reaction B) is the reaction of III with acetamidine whose characteristic is to produce the intermediate IV which is converted into V by heating with acetamidine, and the second (reaction A) is that of I with acetamidine in which II is formed directly without passing through any detectable intermediate.

On the basis of all the present data, the mechanisms of these two reactions may be surmised as below. In the first step of reaction A, the Michael type addition of acetamidine to I may conceivably occur. Then, the resulting intermediate XII may be immediately converted into II, since C^6 in $C^5=C^6=N^7H$ group in XII is positively charged to some extent owing to the polarity of C=N bond and N^1 in the acetamidino group has of course some amount of negative charge and therefore C^6 and N^1 can easily be bonded[7].

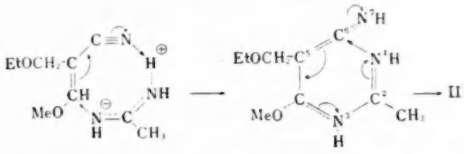

In the case of reaction B, however, the intermediate IV is derived from III by the replacement reaction. The N^1 atom in IV has probably a somewhat positive charge since the electron attracting effect of the $C^2=N^3$ bond and of the nitrile group is considerably large[8]. Moreover, the great dipole moment of $C^6\equiv N^7$ bond (3.5 D) suggests that the C^6 atom is charged positively to a large extent. Therefore, the bond formation between C^6 and N^1 may be very difficult. In addition to this, the intermediate IV can be stabilized by the resonance of the ordinary structure with polar structures where non-bonding electrons in the NH_2 group migrate to C=N and C≡N groups. These are the reasons why IV is fairly stable in the solution and can be detected spectrophotometrically. By heating the solution, the prototropy may occur continually to form the structure XIII, because of the strong electron attracting effect of the nitrile group. Then, another acetamidine molecule may be added to XIII, resulting in XIV which is finally converted into V eliminating an ammonia molecule[9].

However, by treating IV with a reagent such as hydrochloric acid, the nitrile group

7) In the structure XII, C^6 and N^7 have respectively about 16% positive and negative charges because of the difference in the electronegativity values between C^6 and N^7 of C=NH group. The above value can be evaluated by the aid of the bond moment of C=N. (0.9 D; C. P. Smyth, "Dielectric Behavior and Structure", McGraw Hill, New York, (1955), p. 245).

8) N^1 has a positive charge because of the strong electron attracting power of $C^2=N^3$ bond and of nitrile group affecting through the conjugated system of IV, although N^1 seems to charge negeatively due to the difference of electronegativity between C^2 and N^1 of C^2-N^1H_2 group, the moment of which is only 0.22 D.

9) Further investigation seems to be required for the final conclusion on these reaction mechanisms.

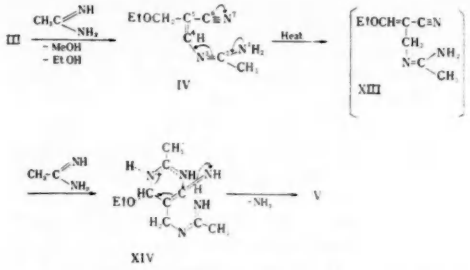

in it may be broken. Thereby the strong electron attracting effect of this group probably decreases and IV is conceivably converted into II[10] through a course similar to that of reaction A mentioned above.

In short, the important difference between these two reactions is that intermediate IV in reaction B has a nitrile group with strong electron attracting power and an amino group with electron donating property at both ends of its conjugated system and between these two groups resonance is possible, whereas the intermediate XII in the reaction A has no longer such a resonating system, since its nitrile group is converted into imino type.

It is quite natural from the above consideration that ethyl 2-methoxymethylene-3-ethoxypropionate (VII) gives 2-methyl-4-hydroxy-5-ethoxymethylpyrimidine (VIII) by the reaction with acetamidine[5,6] in the same manner as in the reaction A.

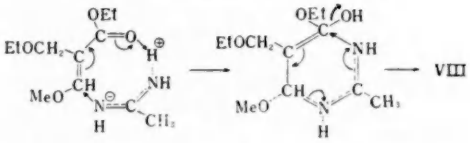

The situation is the same for the reaction of ethyl 2-aminomethylene-3-ethoxypropionate (XV) and acetiminomethyl ester. In this case, VIII was also obtained directly[11]. Now let us consider the reaction of ethyl 2-methoxyethoxymethyl-3-ethoxypropionate (IX) with acetamidine. In the course of this reaction, the intermediate like IV could not be observed spectrophotometrically but the reaction product VIII was obtained directly[5,6]. At the first glance, this fact looks strange because in the intermediate of this reaction, the stabilization due to resonance between the electron attracting (COOEt) and donating (NH_2) groups may be expected. However, this fact may probably be explained by taking account of the small electron attracting power of the carbethoxyl group compared with that of the nitrile group[12]. Further mention on this point will be made below.

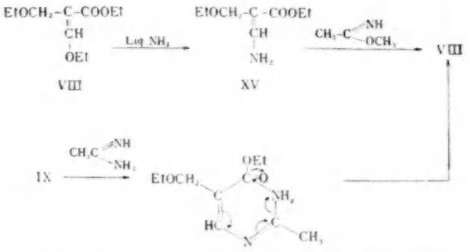

According to these two reaction mechanisms for pyrimidine syntheses, it is possible to explain consistently some analogous reactions indicated in the literatures, which have been re-investigated in our laboratory.

The reactions of ethoxymethylenemalondinitrile (XVI) (reaction C) and ethyl ethoxymethylenecyanoacetate (XVII) (reaction D) with acetamidine give 2-methyl-4-amino-5-cyanopyrimidine (XVIII) (reaction C) and 2-methyl-4-hydroxy-5-cyanopyrimidine (XIX) with 2-methyl-4-amino-5-carbethoxypyrimidine (XX) (reaction D), respectively. On the other hand, aminomethylenemalondinitrile (XXI) (reaction E) and ethyl aminomethylenecyanoacetate (XXII) (reaction F) are converted by the reaction with acetiminomethyl ester into acetamidinomethylenemalondinitrile (XXIII) and ethyl acetamidinomethylenecyanoacetate (XXIV), respectively[13-15], yielding the corresponding pyrimidines only by treating with alkali. It is probably that in the cases of the reaction C and D, the intermediates, XXV and XXVI, are led to the corresponding pyrimidines directly in a way similar to that of reaction A, since their nitrile groups disappear, whereas in the cases of the reactions E and F the

10) 2-Methyl-5-carbethoxy-3,4-dihydropyrimidine is also obtained. In this case, it must be considered that the nitrile group is converted into an iminoester group.

11) A. Takamizawa and K. Tokuyama, *J. Pharm. Soc. Japan*, (*Yakugaku Zasshi*), **79**, (1959), in pretss.

12) This is inferred from the fact that the σ vlaue (Hammett's substituent constant) for the nitrile group is apparently larger than that for the carboxyl group.

13) A. R. Todd and F. Bergel, *J. Chem. Soc.*, **1937**, 364.

14) T. Matsukawa, *J. Pharm. Soc. Japan* (*Yakugaku Zasshi*), **62**, 417 (1942).

15) Y. Sawa and T. Tsuji, This work was read at the Kinki Congress of Pharmaceutical Society of Japan, Osaka, 1955.

intermediates, XXVII and XXVIII, have still their nitrile groups and therefore do not react further without treating with alkali. That is to say, this mechanism is similar to that of reaction B.

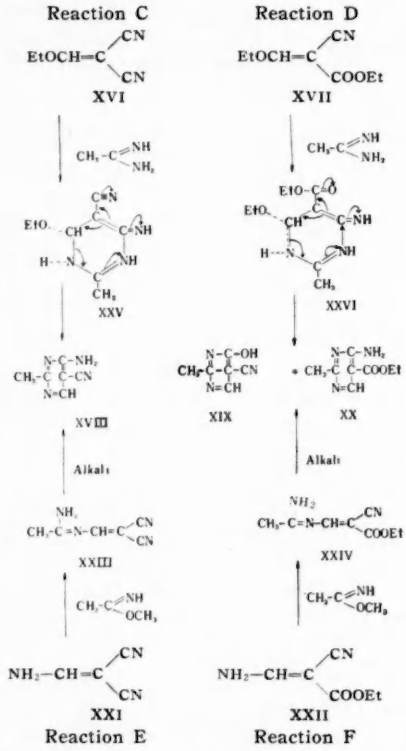

According to Todd[13], the intermediate XXVI was obtainable in the course of the reaction D, but this assertion has been refuted by Sawa and Tsuji[15], who reported that XXVI could not be obtained under the experimental conditions they employed. This result seems to be consistent with the above consideration that the intermediate like XXVI is too unstable to be detected. Moreover, Sykes et al.[16] have reported that XXVII′ was obtained by the reaction of XVII with two moles of acetamidine, but their result is not convincing. It contradicts the present authors' opinion. Inspecting more completely their data on the melting point and elemental analysis, we are led to the conclusion that the compound obtained by Sykes et al. is acetamidinate XXVII[15] of XIX.

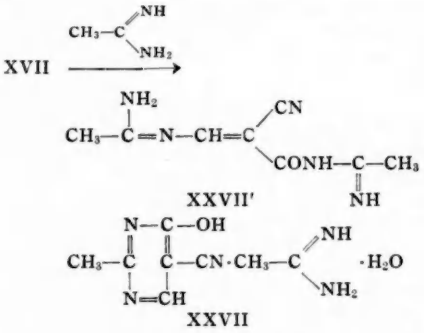

As mentioned above, the electron attracting effect of one carbethoxy group is weaker than that of a nitrile group, but the following fact indicates that two carbethoxy groups roughly correspond to one nitrile group in their electron attracting power. While 2-methyl-4-hydroxy-5-carbethoxypyrimidine (XXIX) was obtained at once by the reaction of diethyl ethoxymethylenemalonate(XXVIII) with acetamidine, diethyl aminomethylenemalonate (XXX) was converted with acetiminomethyl ester into diethyl acetamidinomethylenemalonate (XXXI), which gave XXIX on treatment with alkali.

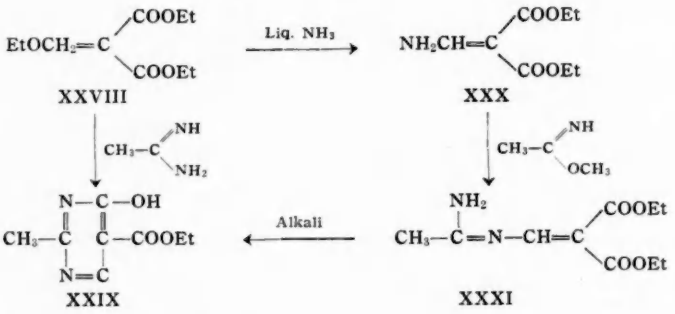

16) P. Nesbitt and P. Sykes, *J. Chem. Soc.*, **1954**, 3057.

Experimental

2-Aminomethylene-3-ethoxypropionitrile (XI).—A solution of 2-ethoxymethylene-3-ethoxypropionitrile (X) (5.0 g.) dissolved completely in liquid ammonia (20 cc.) was left at room temperature for 45 days. After removal of the liquid ammonia and the alcohol produced under reduced pressure, a dark brown liquid (3.8 g.) was obtained. $n_D^{20.5}$, 1.4759.

Anal. Found: C, 56.62; H, 7.64; N, 22.21; $-OC_2H_5$, 34.66. Calcd. for $C_6H_{10}N_2O$: C, 57.11; H, 7.99; N, 22.21; $-OC_2H_5$, 35.71%.

Reaction of 2-aminomethylene-3-ethoxypropionitrile (XI) with acetiminomethyl ester.—To an ice-cold solution of sodium (0.3 g.) in absolute methanol (50 cc.), was added acetiminomethyl ester hydrochloride (1.5 g.); the mixture was shaken for few minutes and quickly filtered from precipitated sodium chloride. To the cooled filtrate was added 2-aminomethylene-3-ethoxypropionitrile (XI) (1.3 g.) in portions with shaking. After being allowed to stand overnight at room temperature, (i) dry hydrochloric acid was vigorously passed into the solution during three hours at 10~15°C, and the solution was again allowed to stand overnight. After removal of methanol in a vacuum, the residue was neutralized with sodium carbonate, washed with ethyl acetate, made strongly alkaline with sodium hydroxide and extracted with benzene. The benzene layer was dried over sodium sulfate and purified by passing through an alumina column. After evaporation of the solvent, 2-methyl-4-amino-5-ethoxymethylpyrimidine (II) was given; it was crystallized from ethanol in colorless rods, m. p. 89~90°C. Yield, 10 mg., (5.86%). Picrate, m. p. 189~190°C.

Anal. Found: C, 42.44; H, 4.18; N, 21.57. Calcd. for $C_{14}H_{16}N_6O_8$ (as picrate): C, 42.42; H, 4.44; N, 21.21%.

(ii) A mixture of absolute methanol (20 cc.), sodium (0.3 g.) and acetamidine hydrochloride (1.4 g.) was added. After being boiled for three hours, the precipitated sodium chloride was filtered off and the solvent was removed. To the residue was added 10% aqueous solution of sodium hydroxide; the mixture was heated on a water-bath for one hour. After cooling, colorless crystals separated on salting out with 50% aqueous solution of sodium hydroxide. Recrystallization from water gave 2-methyl-4-amino-5-acetaminomethylpyrimidine (VI) of colorless prisms (1.0 g.), m. p. 204~206°C. Picrate was yellow needles, m. p. 200°C.

Anal. Found: N, 23.98. Calcd. for $C_{14}H_{15}N_7O_8$ (as picrate): N, 23.96%.

Reaction of diethyl aminomethylenemalonate (XXX) with acetiminomethyl ester.—To an ice-cold solution of sodium (0.6 g.) in absolute ethanol (50 cc.), was added acetiminomethyl ester hydrochloride (3.2 g.); the mixture was shaken for a few minutes and quickly filtered from precipitated sodium chloride. To the cooled filtrate was added diethyl aminomethylenemalonate (XXX) (3.7 g.) in portions with shaking. After being allowed to stand overnight at room temperature, the solvent was removed in a vacuum. The residue, m. p. ca. 190°C, decomposed by recrystallization. This may be diethyl acetamidinomethylenemalonate (XXXI).

The above product was heated on a water-bath for 15 minutes with an ethanolic sodium ethoxide (0.2 g.; 50 cc.). The yellow solution was cooled, acidified with acetic acid, and concentrated in vacuo to about half the original volume. On standing, 2-methyl-4-hydroxy-5-carbethoxypyrimidine (XXIX) separated; it crystallized from acetone in colorless needles, m. p. 190°C. Yield, 0.1 g.

Anal. Found: N, 15.11. Calcd. for $C_8H_{10}N_2O$: N, 15.38%.

Summary

The mechanism of the reactions of 2-alkoxymethylene-3-alkoxypropionitrile and 2-dialkoxymethyl-3-alkoxypropionitrile with acetamidine was studied. The results show that these two nitriles react with acetamidine in completely different manners. In the case of the reaction of 2-alkoxymethylene-3-alkoxypropionitrile with acetamidine, the final product (2-methyl-4-amino-5-alkoxymethylpyrimidine) can be obtained directly, while in the case of the reaction of the other nitrile with acetamidine, the intermediate with the absorption maximum at 275 mμ can be detected spectrophotometrically. This intermediate could be identified with 2-acetamidinomethylene-3-alkoxypropionitrile. The difference in the mechanism between these two reactions might be explained by taking into consideration the fact that the intermediate in the latter case can be stabilized by the resonance among the usual structure and the polar structures in which non-bonding electrons on the nitrogen atom of the amino group migrate into C≡N or C=N group.

We wish to acknowledge our indebtedness to Professors M. Tomita, University of Kyoto, and S. Uyeo, University of Osaka, and Dr. K. Takeda, Director of our laboratory, for their kind guidance and encouragement and we are also indebted to Assistant Professor S. Nagakura, the University of Tokyo, for his helpful discussion. We are grateful to Messrs. K. Kubota, M. Narisada and H. Miyazaki for the measurements of infrared and ultraviolet spectra and to Messrs. T. Iyeki and K. Miyahara and Misses H. Nakai and K. Numoto for the elemental analyses.

Shionogi Research Laboratory
Shionogi & Co., Ltd.
Imafuku, Amagasaki

Electron Diffraction Investigation on the Molecular Structure of 1,1,2-Trifluoro-1,2,2-trichloroethane

By Machio IWASAKI

(Received August 5, 1958)

In previous publications[1-3] it has been reported that the energy difference between *trans* and *gauche* isomer for 1,2-difluoro-1,1,2,2-tetrachloroethane is 0~500 cal./mol., and that for 1,1,2,2-tetrafluoro-1,2-dichloroethane is 440±110 cal./mol. In order to compare these results with the data for the well-known series of chlorinated ethanes[4] (CH_2Cl-CH_2Cl, $CHCl_2$-CH_2Cl and $CHCl_2CHCl_2$), it is desirable to elucidate the molecular structure of 1,1,2-trifluoro-1,2,2-trichloroethane. However, the problem of rotational isomerism in this molecule has not yet been studied except when an earlier study was made by Glockler and Sage[5]. Based solely on the number of observed Raman lines, they concluded that two isomers were present, but no attempt was made at the determination of the energy difference between the two isomers.

This report presents the results of studies on the molecular structure of CF_2Cl-$CFCl_2$ carried out by the sector-microphotometer method of electron diffraction mainly to find the effect of fluorine substitution on the energy difference between the two isomers. An attempt was also made at the determination of the equilibrium angle of the stable configuration.

Experimental

The sample was prepared by S. Nagase in this laboratory from hexachloroethane, which was fluorinated with antimony trifluoride under superatmospheric pressures in the presence of antimony pentachloride as a catalyst[6]. The product distilled at 47.8°C. The purity of this sample was tested with an infrared absorption spectrum and there were no absorptions due to impurities.

The diffraction patterns were taken at a room temperature of about 20°C using an apparatus[7] having an r^3-sector, which was rapidly rotated during photographic exposure. The apparatus and the experimental procedures were the same as described in the previous paper[3]. Two nozzle-to-plate distances of 125 mm. and 285 mm. were used: the former was used for large angle scattering and the latter for small angle scattering, which was sensitive to the internal rotation. The wavelength of the electron beam was about 0.055Å. The extraneous scatterings were removed by a beam trap and the spreading of the sample was prevented by a trap cooled with liquid air.

The molecular intensity curve qI_m shown by the top curve in Fig. 5 was obtained by the method similar to that employed by Karle and his coworker[8], the index of resolution being about 1.0.

Analysis

Radial Distribution Curve.—The radial distribution (RD) curve was calculated by the following equation:

$$f(r) = \sum_{q=0}^{q_{max}} qI_m \exp(-aq^2) \sin(\pi qr/10) \qquad (1)$$

where I_m is the molecular scattering intensity. The artificial damping factor a was chosen so as $\exp(-aq^2) = 0.1$ at $q = 100$. $q = (40/\lambda)\sin(\theta/2)$, where θ is the angle of scattering and λ is the wavelength of the electron beam.

In the calculation of the RD curve, a theoretical intensity curve which was computed with constant coefficients for the assumed model was substituted in place of the observed intensity below $q = 6$. Furthermore, a correction for the effect of non-nuclear scatterings[9] was made. The RD curve shown in Fig. 2 was obtained after several steps of successive

1) M. Iwasaki, S. Nagase and R. Kojima, *J. Chem. Phys.*, **22**, 959 (1954).
2) M. Iwasaki, S. Nagase and R. Kojima, This Bulletin, **30**, 230 (1957).
3) M. Iwasaki, This Bulletin, **31**, 1071 (1958).
4) S. Mizushima, "Structure of Molecules and Internal Rotation", Academic Press, Inc., New York, N. Y., 1954.
5) G. Glockler and C. Sage, *J. Chem. Phys.*, **9**, 387 (1941).
6) R. Kojima, M. Iwasaki, S. Nagase and H. Baba, *Repts. Govt. Ind. Research Inst., Nagoya*, (*Nagoya Kogyo Gijutsu Shikenjo Hokoku*), **5**, 225 (1956).
7) Y. Morino, M. Kimura and M. Iwasaki, The Sixth Annual Meeting of the Chemical Society of Japan, April 1953.
8) J. Karle and I. L. Karle, *J. Chem. Phys.*, **18**, 957 (1950).
9) L. S. Bartell, L. O. Brockway and R. H. Schwedeman, ibid., **23**, 1854 (1955).

approximations based on Karle's criteria[8].

The RD curve has maxima at 1.34_5, 1.75_5, 2.0~3.7, 3.89_0, and 4.31_3Å. The first two peaks at 1.34_5 and 1.75_5Å are assigned to C—F and C—Cl bond distances, respectively. The unresolved peak at 2.0~3.7Å is due to the superposition of various non-bonded distances, that at 3.89_0Å to the *trans* F···Cl distance, and that at 4.31_3Å to the *trans* Cl···Cl distance.

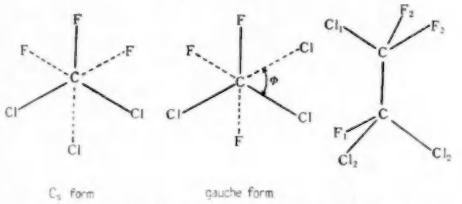

Fig. 1. Rotational isomers of CF_2Cl-$CFCl_2$.

Two configurations are conceivable for this molecule. One of them is a form having the C_s symmetry as shown in Fig. 1. This form will be called the C_s form. The other form having no symmetry is called the *gauche* form. Because the *trans* Cl···Cl distance is characteristic of the *gauche* form, the peak at 4.31_3Å evidently shows the existence of the *gauche* form. On the other hand, the *trans* F···Cl distance appears in both forms, but the number of this distance is three for the C_s form whereas it is one for the *gauche* form. Therefore, the ratio of the areas under these two peaks is expected to depend on whether there exists only the *gauche* form or whether two isomers exist. Because the area under the RD peak is approximately proportional to Z_iZ_j/r_{ij}, the ratio of the two forms, N_{C_s}/N_g, can be calculated from the areas of the two peaks mentioned above by means of the following formula:

$$\frac{N_{C_s}}{N_g} = \frac{Z_{Cl}r_{F\cdots Cl}A_{F\cdots Cl}}{3Z_Fr_{Cl\cdots Cl}A_{Cl\cdots Cl}} - \frac{1}{3} \qquad (2)$$

where Z_F and Z_{Cl} are, respectively, the atomic numbers of fluorine and chlorine, $A_{Cl\cdots Cl}$ and $A_{F\cdots Cl}$ are the areas of the peaks, and $r_{Cl\cdots Cl}$ and $r_{F\cdots Cl}$ are the *trans* Cl···Cl and the *trans* F···Cl distances. The ratio of the areas was hardly affected at all by the assumed value of the abundance ratio of the two isomers, because the correction for non-nuclear scatterings made it possible to use the observed values to such a small q value as 7. In this way, the amount of the *gauche* form was estimated as 80 per cent from the RD curve in applying Eq. 1. This value was further tested by the consideration of theoretical intensity curves described in the next section.

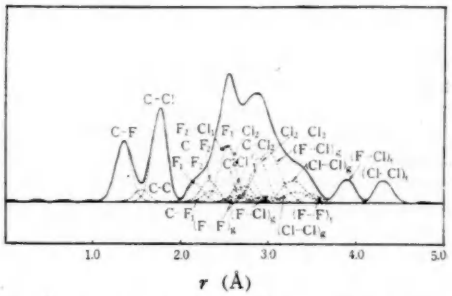

Fig. 2. Radial distribution curve for CF_2Cl-$CFCl_2$.

When the contributions from the C—F and C—Cl distances were subtracted from the composite peak ranging from 1.0 to 2.0Å, the remaining area forms a smooth curve having a maximum at 1.54_5Å which is attributable to the C—C bond distance. These three components of the first composite peak of the RD curve are illustrated in Fig. 2, and the areas under these peaks are in good agreement with the theoretical values shown in Table I.

According to the results of the previous reports[1-3] and many other papers about fluorochloromethane[10], the C—F and the C—Cl bond distances decrease with the number of fluorine atoms bonded with one and the same carbon atom. Therefore, the C—F and the C—Cl bond distances may probably be different for two halves of this molecule. In fact, the values of 1.38Å (C—F) and 1.76Å (C—Cl) in $CFCl_2$-$CFCl_2$, and those of 1.33_0Å (C—F) and 1.74_5Å (C—Cl) in CF_2Cl-CF_2Cl being assumed for the two halves of this molecule, the weighted mean values of the C—F and the C—Cl distances were 1.34₇ and 1.75_5Å, respectively; those values are in good agreement with the observed values of 1.34_5 and 1.75_5Å.

In analyzing the part of the RD curve from 2.0 to 3.7Å, an assumption was made that the bonded distances and the bond angles in two halves of the molecule were equal to those of $CFCl_2$-$CFCl_2$ and CF_2Cl-CF_2Cl, respectively. Furthermore, the

10) The C-F and the C-Cl distances in many organic fluorine compounds have been tabulated in the previous paper, ref. 2.

TABLE I
THE RESULT OF ANALYSIS OF THE RD CURVE
(THE DISTANCES ARE GIVEN IN Å UNITS)

		C—F	C—C	C—Cl	(F···Cl)$_t$	(Cl···Cl)$_t$
Distance		1.34_4	1.54_5	1.75_5	3.89_0	4.31_3
Mean amplitude.	obs.	0.055_5	0.041_7	0.054_0	0.063_8	0.069_5
	calc.	0.045	0.050	0.054	0.070	0.074
c_{ij}	obs.	0.259	0.055	0.514	0.307	0.335
	calc.	0.255	0.057	0.481	0.337	0.364

assumed values listed in Table II were used for the mean amplitudes. When contributions from distances that do not change with internal rotation were subtracted from the experimental RD curve, the remaining curve shown in Fig. 3 was

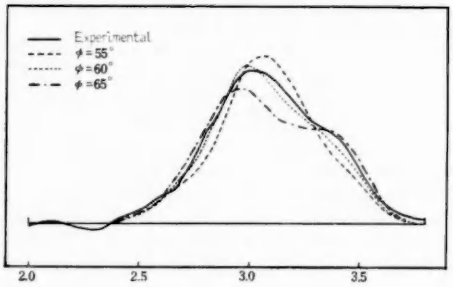

Fig. 3. Comparison between the experimental and the calculated RD curves which are attributable to the contributions from the distances that vary with the internal rotation.

TABLE II
MEAN AMPLITUDES USED IN THIS ANALYSIS
(IN Å)

Distance	Mean amplitude	Distance	Mean amplitude
C—F	0.045	(F···F)	0.114
C—C	0.050	(F···Cl)$_g$	0.120
C—Cl	0.054	(Cl···Cl)$_g$	0.125
F···F	0.056	(F···F)$_t$	0.061
C···F	0.059	(F···Cl)$_t$	0.070
F···Cl	0.065	(Cl···Cl)$_t$	0.074
C···Cl	0.073		
Cl···Cl	0.070		

obtained, the part from 2.4 to 3.7Å of this curve corresponding to the contribution from the *gauche* F···F, the *gauche* F···Cl, the *gauche* Cl···Cl, and the *trans* F···F distances, which change with the azimuthal angle of the *gauche* form and the relative amount of rotational isomers. The fact that the part of the remaining curve from 2.0 to 2.4Å which is attributable to the contribution from the distances that are independent of the internal rotation, is almost equal to zero reflects the correctness of the assumption about the bonded distances and bond angles. When the remaining curve thus obtained was compared with the theoretical one calculated for various azimuthal angles[11], ϕ, of the *gauche* form, the curve for $\phi=60°$ was found to be in good agreement with the observed one as shown in Fig. 3.

The mean amplitudes listed in Table I were obtained by fitting the RD peaks with Gaussian functions, no corrections being made for second order effects, such as a sample spread, multiple scatterings and the failure of Born approximation[12]. The observed mean amplitudes are in good agreement with those calculated by Morino et al.[13] from spectroscopic data.

Theoretical Intensity Curves. — The theoretical intensity curves were calculated using the following equation:

$$qI_m(q)=\sum_{i\neq j}\sum(c_{ij}/r_{ij}) \times \exp(-b_{ij}q^2)\sin(\pi q r_{ij}/10) \qquad (3)$$

where r_{ij} denotes the interatomic distance between i-th and j-th atoms, b_{ij} is the temperature factor, and

$$c_{ij}=Z_iZ_j/\sum_i(Z_i^2+Z_i) \qquad (4)$$

In the region of small q-values the effect of non-nuclear scattering was corrected for the experimental intensity and then the constant coefficient was used over the whole q region in calculating theoretical intensity curves. The summations of Eq. 3 were performed by use of punched cards and a Remington Rand Type-285 Model-2 Tabulating machine[14,15].

In determining the range of uncertainty of 13 structural parameters and 14 mean

11) The azimuthal angle of the *gauche* form is that for the two C-Cl bonds in the molecule.
12) R. Glauber and V. Schomaker, *Phys. Rev.*, **89**, 667 (1953); L. S. Bartell and L. O. Brockway, *Nature*, **171**, 978 (1953); J. A. Ibers and J. A. Hoerni, *Acta Cryst.*, **7**, 405 (1954).
13) Y. Morino, K. Kuchitsu, A. Takahashi and K. Maeda, *J. Chem. Phys.*, **21**, 1927 (1953).
14) Y. Morino and K. Kuchitsu, *X-Ray*, (*X-sen*), **8**, 37 (1954).
15) The calculation by use of punched cards was carried out by K. Kuchitsu of the University of Tokyo.

amplitudes, it was not feasible to exhaust the possible variations in all parameters. Therefore, all the parameters except the ratios, $\rho_{Cl}=C-Cl_2/C-Cl_1$ and $\rho_F=C-F_1/C-F_2$ the azimuthal angle of the *gauche* form, ϕ, and the fraction of the *gauche* form, N_g, were kept constant throughout the analysis. The mean amplitudes used were the same as those in the previous papers[2,3]. The majority of these values listed in Table II were taken from those calculated by Morino et al.[13] from spectroscopic data or obtained by Karle et al.[16,17] from electron diffraction experiments. The C—C distance and all the bond angles were assumed to be equal to those in $CFCl_2$–$CFCl_2$ and CF_2Cl–CF_2Cl, that is, C—C=1.54Å, $\angle CCCl_1=\angle CCCl_2=112°$, $\angle CCF_1=107°05'$, $\angle CCF_2=108°$, $\angle F_1CCl_2=107°30'$, $\angle F_2CCl_1=110°$, $\angle F_1CF_2=108°44'$ and $\angle Cl_1CCl_2=110°30'$. It was already shown in the RD analysis that this assumption was quite adequate.

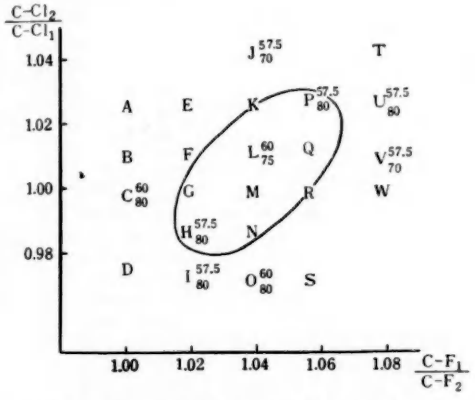

Fig. 4. Parameter chart. The positions of letters indicate the parameters of models for which intensity curves were computed. The values of the superscripts and the subscripts indicate the azimuthal angles and the amounts of the *gauche* form both of which were used in calculating the intensity curves reproduced in Fig. 5.

For each model indicated in a $\rho_{Cl}-\rho_F$ parameter chart (Fig. 4), parameters, ϕ and N_g, were further varied. The projection of the $\rho_{Cl}-\rho_F$ parameter chart on a $\phi-N_g$ plane is shown in Fig. 6. Some of the computed curves are reproduced in Fig. 5. The relative depth of the 5th and the 6th minimum, the position of the 3rd maximum and the 4th minimum and the feature of a shelf on the inner portion of the 4th maximum are very sensitive to small changes in the parameters. The models A–F, J and T in the parameter chart can be ruled out because the relative depth of the 5th and the 6th minimum contradicts with experiments, while the models, O, S, V and W, are unacceptable because the 6th minimum is too deep as compared with experiments. The model I can also be rejected because of the prominence of a shelf on the inner portion of the 4th maximum. The model U is unsatisfactory because the 7th and the 8th maximum are too faint. The models, G, H, L, M, N, P and Q, are regarded as acceptable fits, while the models, K and R, can be accepted as borderline fits. In Table III is given the comparison between the observed and the calculated intensity curve for the best model L. In Table IV

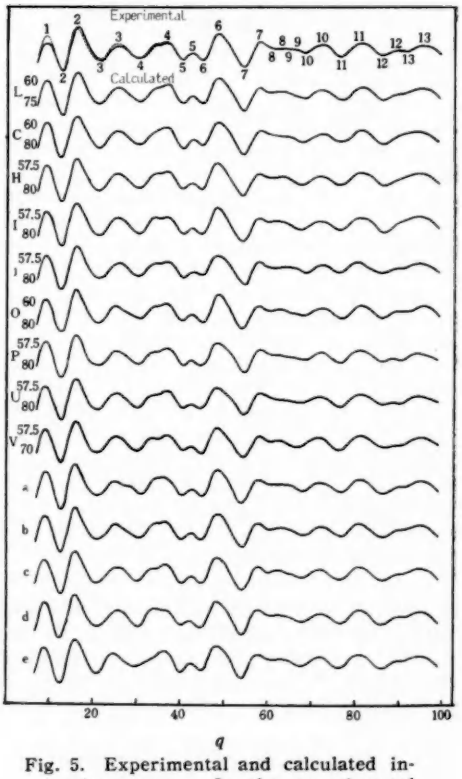

Fig. 5. Experimental and calculated intensity curves. In the experimental curve the dotted line indicates the correction for non-nuclear scatterings.

16) D. A. Swick, I. L. Karle and J. Karle, *J. Chem. Phys.*, **22**, 1242 (1954).
17) D. A. Swick and I. L. Karle, ibid., **23**, 1499 (1955).

TABLE III

COMPARISON BETWEEN EXPERIMENTAL AND THEORETICAL INTENSITY CURVES

Max.	Min.	Peak position			Peak height		
		q_o	q_c	q_c/q_o	I_o	I_c	I_o/I_c
1		9.0	9.0	1.000	+1.30	+1.24	1.048
	2	12.5	12.5	1.000	−1.90	−1.98	0.960
2		16.0	16.0	1.000	+2.05	+2.00	1.025
	3	21.0	21.0	1.000	−0.98	−0.90	1.089
3		25.2	25.2	1.000	+0.61	+0.58	1.052
	4	30.2	30.2	1.000	−0.73	−0.71	1.028
4		36.6	36.7	1.003	+0.80	+0.82	0.976
	5	40.2	40.2	1.000	−0.85	−0.86	0.988
5		42.5	42.5	1.000	−0.18	−0.20	0.900
	6	44.8	44.8	1.000	−1.00	−0.93	1.075
6		48.3	48.4	1.002	+1.62	+1.51	1.073
	7	54.3	54.2	0.998	−1.52	−1.57	0.968
7		58.0	57.8	0.997	+0.78	+0.67	1.164
	8	61.4	60.6	(0.987)	−0.15	−0.05	(3.000)
8		63.4	62.4	(0.984)	+0.24	+0.26	(0.923)
9		66.2	65.5	(0.989)	+0.07	−0.05	(——)
	10	68.5	68.2	0.996	−0.26	−0.42	0.619
10		72.1	72.2	1.001	+0.52	+0.37	1.405
	11	76.5	76.7	1.003	−0.52	−0.55	0.982
11		81.1	81.2	1.001	+0.60	+0.65	0.923
	12	86.2	86.2	1.000	−0.54	−0.65	0.831
12		89.5	89.5	1.000	−0.03	0.00	(——)
13		95.4	95.0	0.996	+0.45	+0.50	0.900
Average				1.000			1.005
Average deviation				0.001			0.096

TABLE IV

DISTANCES OBTAINED FROM q_c/q_o VALUES
(THE DISTANCES ARE GIVEN IN Å UNITS)

Acceptable models	Average q_c/q_o	Average deviation	C—F_1	C—F_2	C—Cl_1	C—Cl_2	C—C
L_{75}^{60}	1.000	0.001	1.38_0	1.33_0	1.74_5	1.76_0	1.54_0
N_{70}^{60}	0.999	0.003	1.37_9	1.32_9	1.76_8	1.74_3	1.53_8
$K_{80}^{57.5}$	1.001	0.003	1.38_1	1.33_1	1.72_6	1.77_1	1.54_1
$G_{80}^{57.5}$	0.999	0.002	1.36_3	1.33_9	1.75_4	1.75_4	1.53_9
$H_{80}^{57.5}$	0.999	0.003	1.36_2	1.33_7	1.76_8	1.74_6	1.53_8
$P_{80}^{57.5}$	1.000	0.003	1.39_5	1.32_0	1.72_5	1.77_0	1.54_0
Q_{75}^{60}	0.999	0.003	1.39_4	1.31_9	1.74_3	1.75_8	1.53_9
Most probable value			1.37_9	1.32_9	1.74_7	1.75_8	1.53_9

are listed the mean values of the q_c/q_o ratio for these acceptable models as well as the molecular parameters calculated therefrom. The accepted values of these parameters and the limits of errors are as follows:

C—F_1=1.37_9±0.02_1Å C—F_2=1.32_9±0.01_4Å

C—Cl_1=1.74_7±0.02_7Å C—Cl_2=1.75_8±0.02_0Å

With respect to the parameter N_g the models for N_g=100 per cent were all unsatisfactory because the positions of the 3rd maximum and the 4th minimum did not agree with experiments. This discrepancy could not be removed without taking into account the coexistence of the C_s form. Therefore, the existence of the C_s form is definitly concluded from the diffraction data. From the acceptable domains estimated for acceptable models

in the $\rho_F - \rho_{Cl}$ parameter chart, the limits of errors for the N_g and ϕ parameters were determined as follows:

$$N_g = 76 \pm 7 \text{ per cent } \phi = 59.5 \pm 3.5°$$

These values coincide with the results from the analysis of the RD curve.

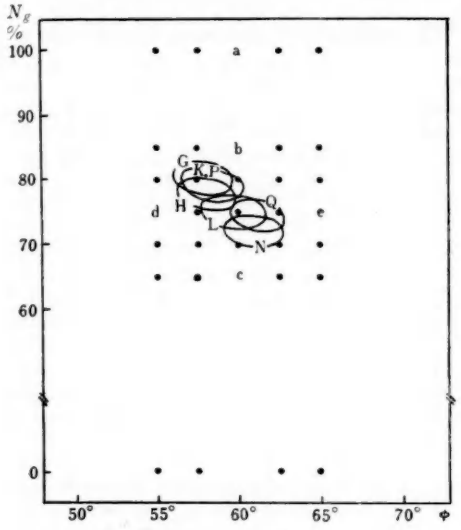

Fig. 6. Parameter chart for N_g and ϕ. The positions of the small letters and dots indicate the parameters of the models for which intensity curves were computed. The areas enclosed in the curved lines roughly indicate the acceptable regions for the models represented by the capital letters, which correspond to the positions in the $\rho_{Cl} - \rho_F$ parameter chart. The theoretical intensity curves corresponding to the positions indicated by the small letters are reproduced in Fig. 5.

Discussion of the Results

The shortening of the C—F bond distance found in $CF_2Cl—CF_2Cl$[3] is also revealed in this molecule. It is concluded that the C—F bond distance in a $-CF_2Cl$ group is different from that in a $-CFCl_2$ group. Moreover, the values of these distances are almost the same as those found in CF_2Cl-CF_2Cl and $CFCl_2-CFCl_2$. It implies that the structure of one half of the molecule scarcely affects the other half of the molecule. With respect to the C—Cl bond distances it appears that the similar difference in two halves of the molecule also exists, although great uncertainties of the data do not permit to draw a definite conclusion. From the analysis described in the preceding section, it was definitly concluded that there exist two rotational isomers, C_s and *gauche* forms for $CF_2Cl-CFCl_2$ molecules in the vapor state, the amount of the *gauche* form being 76±7 per cent. If the ratio of the vibrational and rotational partition functions for the C_s and the *gauche* form is assumed to be equal to unity, the energy difference, ΔE, between the isomers is calculated as 270±250 cal./mol. (the *gauche* form is more stable than the C_s form.) from diffraction data, in remarkable contrast to the value of 2900 cal./mol.[18,19] for $CH_2Cl-CHCl_2$. It appears that this lowering of energy difference arises mainly from the decrease in the difference of electrostatic interactions between the C_s and the *gauche* form due to the fluorine substitution, because the C—Cl bond moment is nearly equal to the C—F bond moment. The decrease in the difference of steric repulsion between the C_s and the *gauche* form, of course, should not be neglected, because the van der Waals' radius of a fluorine atom is larger than that of a hydrogen atom. However, the effect of the change in the steric interaction is less important for this lowering because it was reported[20] that the methyl substitution does not appreciably affect the energy differences in chlorinated ethanes.

In the case of 2-methylbutane, $CH_2(CH_3)-CH(CH_3)_2$, which has a similar skeletal structure to that of $CH_2Cl-CHCl_2$ but has a large difference in electrostatic interaction, the energy difference is reported by Sheppard and Szasz[21] to be almost zero. In this connection, it is interesting to mention that a large energy difference was not observed in a $CF_2Cl-CFCl_2$ molecule, in which the difference of electrostatic interactions decreases.

The azimuthal angle of the *gauche* form was determined to be 59.5° in contrast to the value of 70° in $CH_2Cl-CHCl_2$[22]. This change in the equilibrium position of the *gauche* form seems to have some relation to the lowering of the energy difference.

18) J. R. Thomas and W. D. Gwinn, *J. Am. Chem. Soc.*, **71**, 2785 (1949).
19) K. Kuratani and S. Mizushima, *J. Chem. Phys.* **22**, 1403 (1954).
20) I. Miyagawa, *J. Chem. Soc. Japan, Pure Chem. Sec.*, (*Nippon Kagaku Zassi*), **75**, 1162 (1954).
21) N. Sheppard and G. J. Szasz, *J. Chem. Phys.*, **18**, 145 (1950).
22) A. Turkevich and J. Y. Beach, *J. Am. Chem. Soc.*, **61**, 3127 (1939).

The result in this investigation is consistent with the conclusion reached by Mizushima, Morino and Shimanouchi[23] that the most important force in dterming stable configurations of rotational isomers is the steric repulsion and that the electrostatic force plays an important role in determining the energy difference between the rotational isomers because the steric repulsion may become of the same order of magnitude as the electrostatic force in the stable configurations.

Summary

The molecular structure of 1,1,2-trifluoro-1,2,2-trichloroethane was investigated by means of the sector-microphotometer method of electron diffraction. The existence of the two isomeric forms, C_s and *gauche* was ascertained and the amount of the *gauche* form was found to be 76±7 per cent at 20°C. This corresponds to the energy difference of 270±250 cal./mol., the *gauche* form being more stable than the C_s form. The interatomic distances were determined as follows: C—F_1=1.37$_9$±0.02$_1$Å, C—F_2=1.32$_9$±0.01$_4$Å, C—Cl_1=1.74$_7$±0.02$_7$Å, C—Cl_2=1.75$_8$±0.02$_0$Å and the equilibrium angle of the *gauche* form is 59.5±3.5°, where the C—C bond distance and the bond angles were assumed to be equal to the value of CF_2Cl–CF_2Cl and $CFCl_2$–$CFCl_2$ molecules, which have already been investigated by the present author.

The diffraction patterns and the microphotometer traces were taken by using apparatuses in Nagoya University. The author wishes to express his sincere gratitude to Professor M. Kubo, Professor R. Uyeda and Dr. Kimura for giving him facility to use the apparatuses and for their valuable advice. Thanks are also due to Dr. S. Shibata, Mr. H. Morimoto and Mr. K. Kimura of Nagoya University for their friendly assistance, and to Mr. K. Kuchitsu of the University of Tokyo for his help in calculating theoretical intensities by means of a punched card machine. Further, the author is much indebted to Professor Y. Morino of the University of Tokyo for his helpful criticism on this investigation.

Government Industrial Research Institute
Nagoya, Kita-ku, Nagoya

23) S. Mizushima, Y. Morino and T. Shimanouchi, *J. Phys. Chem.*, **56**, 324 (1952).

SHORT COMMUNICATIONS

Nuclear Magnetic Resonance Spectra of Dibromothiophene

By Shizuo Fujiwara, Mikio Katayama, Shôichi Hayashi, Hiroshi Shimizu and Shôji Nishimura*

(Received November 17, 1958)

An extensive investigation of nuclear magnetic resonance of substituted thiophenes was carried out recently by Hazato et al.[1], and the results of the measurements of the chemical shifts and of the indirect spin-spin coupling constants J for these molecules were reported. The observed values of the chemical shifts were found in good accord with the values expected from the electronic structures of the substituents, but the chemical shifts due to the difference in the substituent positions were not fully elucidated, since their measurements were not made of 2,3- or 3,4-disubstituted thiophene. We, thus, report here the results of the measurements of these compounds.

The apparatus used is the one constructed in this laboratory of the type of high resolution slow-sweep setup which is composed of oscillator, null-T bridge, pre-amplifier, Collins 51J4 receiver, Sanborn recorder, oscillograph, magnet and saw-tooth generator. The magnet has the same structure as the one previously described by Gutowsky[2]. The field strength of the magnet is about 6200 gauss in 4.8 cm. gap with 12.5 cm. pole face diameter.

The resonance was observed at 27.030 Mc. The disubstituted thiophene and cyclohexane were mixed equally in volume, and sealed in a capillary of about 1 mm. diameter. The shifts were measured as the separations between the spectra of the sample and of cyclohexane. The results are shown in Table I. As the two protons of 2,3-dibromothiophene are not chemically equivalent, multiple resonance lines should be observed. It was, however, unsuccessfull probably owing to the lack of the intensity.

Table 1
Chemical shifts of dibromothiophene

substance	shift from cyclohexane
2,5-dibromothiophene	140 cps
3,4-dibromothiophene	150
2,3-dibromothiophene	145

We see in Table I that the diamagnetic shieldings for the 3,4-protons in 2,5-dibromothiophene are larger than those for the 2,5-protons in 3,4-dibromothiophene. The shift of 2,3-dibromothiophene falls in the middle of the former two molecules. Our results presented here may be taken as the supplementary data for those of Hazato et al., and all the results will be used for the interpretations of the electronic nature of substituted thiophene.

Our thanks are due to Dr. Yonezô Morino of the University of Tokyo for his suggestion to make measurements on these compound.

University of Electro-Communications
Chofu, Tokyo

* Department of Chemical Engineering, University of Osaka Prefecture, Sakai, Osaka.

1) K. Takahashi, Y. Matsuki, T. Mashiko and G. Hazato. Lectured at the Annual Meeting of Chemical Society of Japan, Tokyo, April, 1958.

2) H. S. Gutowsky, L. H. Meyer and R. E. McClure: *Rev. Sci. Inst.*, **24**, 644 (1953).

Crystal Structure of Pyrazinamide

By Yoshito TAKAKI, Yoshio SASADA and Tokunosuké WATANABÉ

(Received December 9, 1958)

The crystal structure of pyrazinamide*, $C_5H_5N_3O$, (a new potential medicine for tuberculosis[1]) has been examined by X-ray analysis. The crystal data obtained were:

$a = 23.07$, $b = 6.72$, $c = 3.72$Å, $\beta = 100.8°$,

space group $P2_1/a$, four molecules per unit cell.

The analysis was carried on by two-dimensional procedures. By considering the molecular packings, all the atoms were roughly located in the projections onto (001) and (010). The atomic coordinates were refined by using structure factor maps and further by successive Fourier projections. At the present stage the discrepancy indices($R = \sum||F_o|-|F_c||/\sum|F_o|$) are 0.17 for ($hk0$) and 0.20 for ($h0l$).

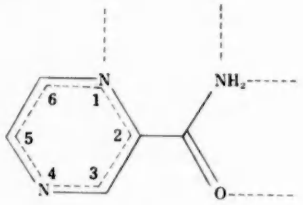

Fig. 1.

The molecule as shown in Fig. 1 is found to be approximately planar. Moreover the bond lengths C—C and C—N in the pyrazine ring show intermediate values between their single and double bonds. These suggest that there is a considerable amount of conjugation between the ring and the amide group.

Two amide groups are linked by a pair of NH—O hydrogen bonds forming a dimer molecule. These dimers are arranged in the direction (011), combining each other by NH—N'_1 hydrogen bonds. This structure explains the cleavage plane parallel to (100).

Further refinement is now going on by ($\rho_o - \rho_c$) and least squares methods. The details of this work will be shortly published.

Faculty of Science
Osaka University
Kita-ku, Osaka

* The sample used was supplied from Sankyo Co., Ltd.

1) S. Kushner et al., *J. Am. Chem. Soc.*, **74**, 3617 (1952).

*Dehydrogenation of the Degradation Products of Thujopsene**

By Hiroshi KOBAYASHI, Shizuo NAGAHAMA and Saburo AKIYOSHI

(Received November 4, 1958)

It has been reported[1] that thujopsene $C_{15}H_{24}$, (I) was oxidized with lead tetraacetate to a carbonyl compound $C_{15}H_{24}O$ having methyl cyclopentyl ketone structure, and that the ketone gave an alcohol $C_{13}H_{22}O$ (II), m.p. 78°, through the peracid oxidation followed by saponification. II was oxidized to the corresponding ketone III (pyroketone) which, when reduced with lithium aluminum hydride, gave the epimer of II, m.p. 133°.

Anal. Found. C, 80.30; H, 11.68. Calcd. for $C_{13}H_{22}O$: C, 80.35; H, 11.41%.

Both of the alcohols were shown to give α-methylnaphthalene by selenium dehydrogenation. The infrared spectrum was identical with synthetic α-methylnaphthalene. The m.p. of its picrate was 136~137°, undepressed upon admixture with the authentic sample.

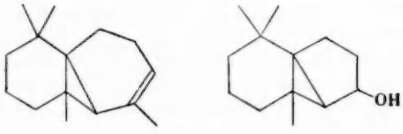

I II

Therefore, the carbon skeletons of both alcohols were considered to be shown by formula II, where the position of hydroxy group was determined by the following process. Through the Grignard

* Presented at the 2nd Symposium on Perfumery, Terpene and Essential Oil Chemistry held in Hiroshima, October 10, 1958.

1) S. Nagahama, H. Kobayashi and S. Akiyoshi, This Bulletin, in press.

reaction of III with methyl magnesium iodide a methyl group was introduced on the carbon atom of the carbonyl group of III and a corresponding alcohol IV, m.p. 63°, was obtained.

Anal. Found: C, 80.92; H, 11.76. Calcd. for $C_{14}H_{24}O$: C, 80.71; H, 11.61%.

Selenium dehydrogenation of IV gave 1,6-dimethylnaphthalene(picrate, m.p. 112°) which was identified by infrared spectrum.

Considering the above results together with the processes of degradation, the most probable structure of thujopsene is suggested to be formula I.

Department of Synthetic Chemistry
Faculty of Engineering
Kyushu University
Hakozaki, Fukuoka

The Reaction of Glycine Cobalt Complex with Acetaldehyde

By Yoshikazu Ikutani, Tôru Okuda, Mikio Sato and Shiro Akabori

(Received January 8, 1959)

Considerable progress in the chemical synthesis of threonine has recently been made by Sato, Okawa and Akabori by means of a Knoevenagel-type condensation of acetaldehyde with the active methylene groups of glycine copper complex[1]. As a continuation of their study we have investigated a similar type of reaction using acetaldehyde and glycine cobalt complex. The triglycino-cobalt was reported to occur in two isomeric forms, namely α- and β-form[2]. These two isomers can be obtained separately owing to the difference of their specific gravities.

A 0.02 g. portion of glycine cobalt complex was allowed to react with 0.1 cc. of acetaldehyde in the presence of 0.1 cc. of 6% aq. sodium carbonate as a condensing catalyst in a sealed tube. After suitable periods of time the total yields of products (threonine+allothreonine) and the ratios of threo- to allo-form in the products were determined by the dinitrofluorobenzene method[3] and a simplified ninhydrin method, respectively.

In general, the yields, especially when the β-form complex was used, were poor, while the threo/allo ratios obtained were much higher than those observed in the case of the copper complexes (threo/allo =1.8). The highest ratio was obtained when the condensation was carried out at 70°C for 2 hr. using the α-isomer. Under this condition the total yield (allo+threo) was 32%, (see Table I).

The poor yield may be due to remarkable stability of glycine cobalt complex, and the changes in the threo/allo ratios with reaction temperature and/or time (see Tebles I and II) suggest that the stabilities of cobalt threonine and cobalt

Table I
Influence of reaction temperature on the threo/allo ratio at a reaction time of 2hr.

Reaction Temp.	α-form			β-form		
	threo, %	allo, %	threo/allo	threo, %	allo, %	threo/allo
50°C	77	23	3.4	78	22	3.5
70°C	88	12	7.6	81	19	4.2
90°C	76	24	3.1	70	30	2.3

Table II
Influence of reaction time on the threo/allo ratio at 70°C

Reaction Time	α-form			β-form		
	threo, %	allo, %	threo/allo	threo, %	allo, %	threo/allo
1/2 hr.	78	22	3.5	74	26	2.9
1 hr.	82	18	4.5	75	25	3.0
2 hr.	88	12	7.6	81	19	4.2
4 hr.	85	15	5.6	78	22	3.5

1) M. Sato, K. Okawa and S. Akabori, This Bulletin, **30**, 937 (1957).
2) H. Ley and H. Winkler, *Ber.*, **42**, 3894 (1909).
3) J. C. Perrone, *Nature*, **167**, 513 (1951).

allothreonine complexes are different. Moreover, as can be seen in Tables I and II, the ratios obtained with the α-form appear to be slightly higher than those obtained with the β-form.

The effect of catalysts other than sodium carbonate was also examined and only potassium carbonate was effective. Disodiumhydrogenphosphate and sodium acetate were completely inactive. The detailed results on this reaction will be reported elsewhere.

Division of Organic Chemistry
Institute for Protein Research
Osaka University, Osaka